



**CLIMATE VULNERABILITY REDUCTION PROGRAM FOR BELIZE (BL-L1028).  
Component 1. Climate Risk Reduction in Tourism Sector – Flood Control**

---

**HAZARD AND RISK REDUCTION MODELING INCLUDING CLIMATE  
CHANGE SCENARIOS**

V. 1.0- 27 SEPTEMBER 2017



## INDEX:

<b>1. INTRODUCTION AND OBJECTIVES .....</b>	<b>1</b>
<b>2. DESCRIPTION OF BELIZE DOWNTOWN FLOOD REDUCTION SCHEME .....</b>	<b>6</b>
<b>3. DATA COLLECTION AND CLIMATE CHANGE ANALYSIS .....</b>	<b>16</b>
3.1. Socio-economic and vulnerability data of the study area.....	16
3.2. Hydro-climatic data.....	21
3.2.1. Meteorological stations and flow gauges.....	21
3.2.2. Waves and sea level .....	22
3.2.3. International Best Track Archive for Climate Stewardship (IBTrACS).....	23
3.3. Characterization of hydro-climatic variables in the study area .....	24
3.3.1. Modelling approach .....	24
3.3.2. Calculation of the IDF curves for the present climate .....	26
3.4. Climate change analysis and impact on the proposed system .....	30
3.4.1. Sea level Rise due to climate change in Belize .....	30
3.4.2. Hurricanes and Tropical Storms .....	31
3.4.3. IDF curves for Belize City under Climate Change .....	33
<b>4. HYDRAULIC MODELING AND DESIGN FEATURES .....</b>	<b>35</b>
4.1. Objectives and modelling approach .....	35
4.2. Dimensioning of the pumping scheme and associated works .....	35
4.2.1. Model implementation .....	35
4.2.2. Study cases .....	41
4.2.3. Results .....	42
4.3. Estimation of the probabilistic hazard: 2D hydraulic modeling .....	52
4.3.1. Digital elevation Model .....	52
4.3.2. Model description .....	56
4.3.3. Flood hazard maps. ....	56

<b>5. COST-BENEFIT ANALYSIS.....</b>	<b>61</b>
5.1. Vulnerability functions for economic and human losses. ....	61
5.2. Risk analysis and avoided losses .....	63
5.3. Land surplus and other benefits associated with the proposed works .....	65
5.4. Cost-benefit analysis of Belize Downtown flood reduction scheme.....	66
<b>6. REFERENCES .....</b>	<b>68</b>

## **ANNEX I: CLIMATE CHANGE ANALYSIS**

## **ANNEX II: HYDRAULIC MODELING RESULTS**



## LIST OF FIGURES:

Figure 1. Hurricane Earl flood map. Source: Baseline studies for Belize City (ESCI), 2016.....	1
Figure 2. Location of risk reduction actions for the different programs proposed in the baseline studies for Belize City, 2016. ....	3
Figure 3. Economic risk of building stock for 10-years RP in the present situation obtained in the baseline studies for Belize City, 2016. ....	4
Figure 4. Human risk for 10-years RP in the present situation obtained in the baseline studies for Belize City, 2016. ....	4
Figure 5. Conceptual framework for the estimation of the economic and human risks.....	5
Figure 6. Main components of the proposed system. ....	7
Figure 7. Examples of existing screw pumping stations. ....	8
Figure 8. Examples different types of gates technology. ....	9
Figure 9. Measurement sections carried out during the field campaigns.....	10
Figure 10. Severe siltation at the outfall to the sea of Collet Canal. ....	11
Figure 11. Longitudinal profiles of Collet (above) and East Canal (below) in the current situation, after dredging and in the final situation. ....	12
Figure 12. Left) Orange Street drainage system Type 1. Right) Drainage system Type 2. ....	13
Figure 13. Proposed drainage system in the pilot area during a 10-years return period storm. ....	14
Figure 14. Detail scheme of the connection between the roads and the canals. ....	14
Figure 15. Building quality distribution. ....	17
Figure 16. Population by building quality.....	17
Figure 17. Residential building stock by quality in the project area.....	19
Figure 18. Population density of the project area.....	20
Figure 19. Location map of the meteorological stations and flow gauges provided by the Belize Natural Meteorological Service.....	21
Figure 20. Daily time series of available rainfall and river flow.....	22
Figure 21. Above: Example of a sea estate propagation with different sea levels (0 m, left and 0.5 m right). Below: available time series of Hs, SS, AT and TWL at Belize City.....	23
Figure 22. Belize tropical cyclone climatology from the IBTrACS database. ....	24
Figure 23. Conceptual framework for the climate characterization used in in the baseline studies f Belize City (ESCI), 2016. ....	25
Figure 24. Rainfall, river flow and sea level distributions for different return periods obtained from the baseline studies in Belize City (ESCI), 2016.....	25
Figure 25. St John's College gauge Return periods (mm/day).....	27

Figure 26. St. John's College gauge (Observed data) Vs TRMM node. ....	28
Figure 27. Observed vs TRMM seasonality. ....	28
Figure 28. IDF curves in St. John's College meteorological station. Belize City. ....	29
Figure 29. IDF curves in Miami Beach station ID: 08-5658. NOAA. ....	29
Figure 30. Projections of mean sea level rise in meters relative to 1986-2005. Source: WGI AR5 Summary for Policymakers. ....	30
Figure 31. St. John's College gauge (Observed data) vs GCM series. ....	33
Figure 32. St. John's College gauge (Observed data) vs GCM average seasonality. ....	34
Figure 33. Canal drainage areas within the study area. ....	36
Figure 34. Conceptual scheme of the system implemented in the SWMM model. ....	37
Figure 35. Canal longitudinal profile for the current situation implemented in the SWMM model. ....	38
Figure 36. Canal longitudinal profile after debris removal implemented in the SWMM model. ....	38
Figure 37. Canal longitudinal profile after bottom regularization implemented in the SWMM model. ....	39
Figure 38. 1-hour design hyetographs for 10 years of return period. ....	40
Figure 39. Curve of the three base cases (Current, Debris removal and Case 0- bottom regularization) vs pump capacity. ....	42
Figure 40. Drainage system map in Current (base case) with a representation of links capacity and nodes flooding. ....	43
Figure 41. Canals longitudinal profiles in Current (base case) at the time of maximum flooding. ....	44
Figure 42. Drainage system map in Debris Removal (base case) with a representation of links capacity and nodes flooding. ....	45
Figure 43. Canals longitudinal profiles in the Debris Removal (base case) at the time of maximum flooding. ....	46
Figure 44. Drainage system map in Case 0- bottom regularization (base case) with a representation of links capacity and nodes flooding. ....	47
Figure 45. Canals longitudinal profiles in Case 0- bottom regularization (base case) at the time of maximum flooding. ....	48
Figure 46. Curve of rain distribution vs pump capacity. ....	49
Figure 47. Curve of rain duration vs pump capacity. ....	50
Figure 48. Curve of manning coefficient vs pump capacity. ....	51
Figure 49. Curve of curve number parameter vs pump capacity. ....	51
Figure 50. Pump capacity necessary for 1.5-hours and 2-hours event with different parameter values. ....	52
Figure 51. DEM with a spatial resolution of 2x2 m developed by Telespazio. ....	53
Figure 52. Telespazio DEM zoom. ....	53
Figure 53. Combined DEM (terrain and bathymetry) with a spatial resolution of 2x2 m. ....	54
Figure 54. British Admiralty Nautical Chart 522: Belize City and Approaches (scale 1:40.000). ....	55

Figure 55. Satellite-Derived Bathymetry Data at 15m resolution. ....	55
Figure 56. Bathymetry of the study area.....	56
Figure 57. Flood hazard map for the !0-year event, in the present situation, before the implementation of the proposed works.....	57
Figure 57. Flood hazard map for the !0-year event, after the implementation of the proposed works.....	58
Figure 59. Flood hazard map for the !00-year event in the present situation, before the implementation of the proposed works.....	59
Figure 60. Flood hazard map for the !00-year event, after the implementation of the proposed works.....	60
Figure 64. Damage function for type B buildings. ....	62
Figure 65. Damage function for type C buildings. ....	62
Figure 66. Evolution of the net current value over time for a discount rate of 12%.....	67

## LIST OF TABLES:

Table 1. Cross-sections geometry measurements obtained during the field campaigns.....	10
Table 2. Measurements summary table.....	12
Table 3. Buildings, population and total value of the buildings by building quality. Source: Natural disaster risk assessment study of Belize City, (IHCantabria and M&K, 2016). ....	16
Table 4. Characteristics of the provided meteorological stations.....	21
Table 5. Characteristics of the provided flow gauges. ....	21
Table 6. Observed and TRMM statistics.....	28
Table 7. Return periods (5, 10, 20, 50, 100 and 500 years) change in 2016-2035, 2046-2065 and 2081-2100 respect to 1986-2005 for the RCP 4.5 and RCP 8.5 scenarios. ....	34
Table 8. Precipitation (mm) for 10-years return period and different hyetograph durations. ....	40
Table 9. Simulation summary table for 10-years return period.....	41
Table 10. Simulation summary results for the three base cases for 10-years return period.....	42
Table 11. Nodes Flooding. Current (base case). ....	44
Table 12. Nodes Flooding. Debris Removal (base case). ....	46
Table 13. Nodes Flooding. Case 0- bottom regularization (base case). ....	48
Table 14. Simulation summary results for 10-years return period. ....	49
Table 15. Estimated economic damages and human losses for selected events and estimated annual losses (EAL) in alternative zero (present and future situation).....	63
Table 16. Estimated economic damages and human losses for selected events and estimated annual losses (EAL) in alternative one (present and future situation). ....	64
Table 17. Profitability indicators of the projected investments.....	66

## 1. INTRODUCTION AND OBJECTIVES

Belize City is highly prone to multiple flooding hazards, including storm surge, coastal flooding, riverine flooding and pluvial flooding, due to its location within the Caribbean basin and its flat and low topography. Furthermore, flood risks are expected to increase in the future due to climate change.

On August 3rd-4th 2016, the Country was hit by Hurricane Earl. With maximum wind speeds of 120 km/h, the storm made landfall in Belize City as a Category 1 hurricane and then moved westward across the country. Most areas affected received 20-30 cm of rain for a period of 5 to 8 hours. The wind and rain caused extensive damage to housing and infrastructure in Belize City, as well as to the country's two main industries: agriculture and tourism.

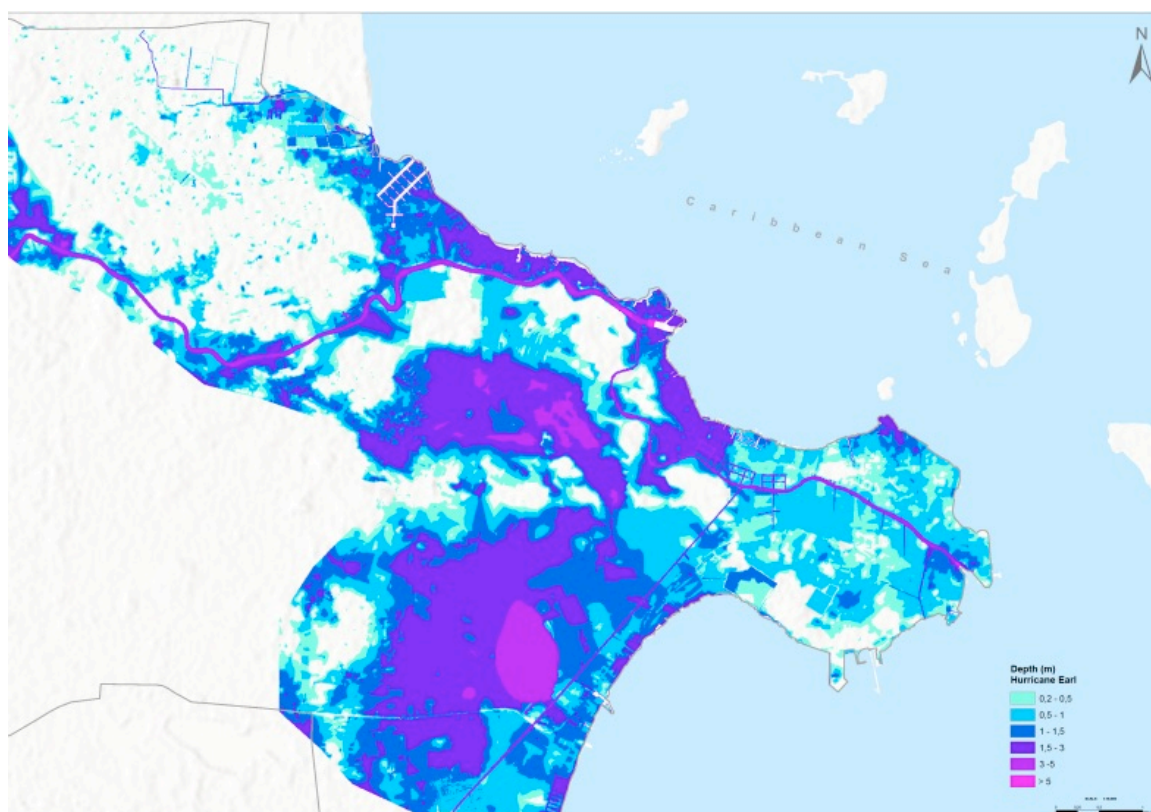


Figure 1. Hurricane Earl flood map. Source: Baseline studies for Belize City (ESCI), 2016.

Belize's National Emergency Management Organization (NEMO) was responsible for the immediate emergency response, in coordination with government authorities, including preliminary damage and needs assessments for the most urgent supplies and recovery work. However, in the medium to long term, there is a need for a nationally coordinated effort, in collaboration with relevant international agencies, to design a comprehensive strategy for climate and disaster risk resilient and sustainable reconstruction. The capacity of Belize City's Municipality to carry out this work on its own is very limited.

In this context, the Government of Belize (GOB) expressed his interest in IDB's Climate Vulnerability Reduction Loan Program, with the overall aims of:

- (i) Reducing the main climate-related vulnerabilities of the productive sector which includes the tourism and agriculture segments of the economy, especially in the areas affected by Hurricane

Earl—as identified in the Economic Commission for Latin America and the Caribbean (ECLAC's) damage assessment report—; and

- (ii) Building flood control measures in Belize City based on (a) the Bank-financed Flood Mitigation Infrastructure Program and (b) risk assessment studies recently completed under the Emerging and Sustainable Cities Program for Belize City.

The IDB and the GOB agreed on a strategy to reduce disaster and climate-related vulnerabilities in the productive sector and to improve flood control in Belize City that comprises two main components:

Component 1. Improving Climate and Disaster Risk Reduction Governance. This includes:

- (i) Making risk information accessible to technocrats, the private sector and general population;
- (ii) Increasing capacities for climate change adaptation planning with a focus on integrated water management, integrated coastal zone management and land use planning;
- (iii) Supporting the design of climate proof housing and tourism building codes, including nature-based solutions;
- (iv) Supporting the design of a climate risk financing strategy for the productive sector; and
- (v) Increasing damage assessment capacities, particularly in the agriculture and environment sectors.

Component 2. Climate risk reduction in sectors affected by Hurricane Earl. This includes:

- (i) Flood control in Belize City;
- (ii) Small-scale, nature-based shoreline stabilization measures in coastal areas of Caye Caulker that were most affected by Hurricane Earl for the purposes of risk reduction and climate change resiliency and
- (iii) Climate vulnerability reduction in agriculture.

As part of the pre-feasibility studies for Component 2 of the Climate Vulnerability Reduction Loan Program, the IDB hired IHCantabria to assist with the prioritization and subsequent detailed design of flood control works in Belize City. The contract advances the set of measures proposed in the baseline studies for Belize City, under the Emerging and Sustainable Cities Initiative (ESCI), in order to reduce the damages associated with flood events.

The definition of these interventions was based on a critical review of the available strategies of flood defense for cities built in flat low areas and the consideration of the effect of global climate change and, more precisely, of sea level rise on Belize's present strategy of flood defense.

There are two different strategies of flood defense in flat low areas, namely: to dredge large canals to increase the drainage capability of the city; or, alternatively, to increase the amount of water that can be stored in the canals, possibly increasing the available storage volume using pumping stations.

For a long time, and still at present, the flood defense of Belize City was based on the first model, and was entrusted to several large canals. The Collet Canal was the last "large canal" dredged in Belize City. A number of new canals have been built since then, but the ratio land/canal area has decreased dramatically. It is worth noting that the urbanised city area has increased from 140 ha in 1925 to 1,462 ha in 2015. Furthermore, in the last decades old canals like the Collet Canal have been transformed from a gently sloped canal to a straight deep concrete canal in order to generate parking lots for vehicles and many new small concrete canals have been buried or covered. Because of these processes, maintenance works are costly and the drainage capacity of these new small canals is low.



This situation is not likely to be reversed in the near future. Land is becoming more expensive and the drainage systems in new developments are being placed underground, usually under the sidewalks, with very low topographic slope. There are no new large canals planned and it is out of the question to build a large canal in the current situation of the city. Even with periodically dredged and well-maintained canals, the water levels in the sea and Haulover Creek usually exceed the ground levels, so that the water cannot flow outwards.

Consequently, and even more taking into account the expected sea level rise due to climate change, the only way to reduce flood hazards in Belize City in the forthcoming future is to move from a “canal-based” to a “polder-like” strategy for flood defence. Although the original concept of a polder refers to a trenched configuration, with the ground level permanently below the sea water level, in the case of Belize this situation would only occur temporarily, during extreme events.

In this context, the baseline studies for Belize City proposed four risk reduction management programs. The first 3 programs are related to the 3 types of flooding hazards (fluvial, pluvial and coastal) and the fourth program is a cross-cutting program related to the capacities to manage flood risks according to this new paradigm (Figure 2).

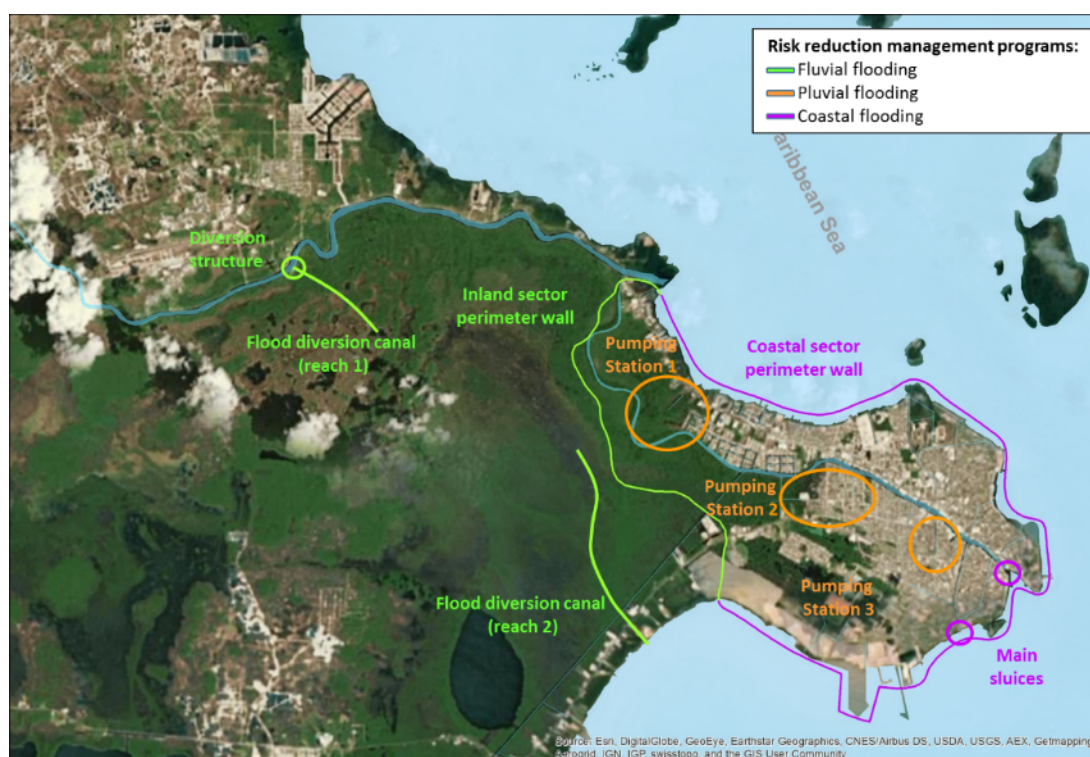


Figure 2. Location of risk reduction actions for the different programs proposed in the baseline studies for Belize City, 2016.

After the first mission of this project, that took place in May 2017, a review of the measures proposed in the baseline study of the ESCI was made. It was decided to prioritize a pumping station and associated works in Downtown Belize as a pilot project, with the idea of testing at a critical zone, Downtown Belize, the new polder-like strategy, including the possibility to expand it to other areas in the future, in case that the experience turns out to be satisfactory. The chosen location for the pumping station drainage area has been Belize Downtown between Collet and East Canal (approx. from Orange St. to Dean St.) because it is one of the most affected areas in the city. The area is flooded with more than one meter depths every 5-10 years obtaining great economic and human damages within the city (Figure 3 and Figure 4). This low-lying area floods frequently, because the drain system cannot evacuate the rainfall occurring for very low return periods. Besides, the water in the canals and

drains is stagnant for long periods (especially in the dry seasons), with consequent aesthetic and public health impacts.

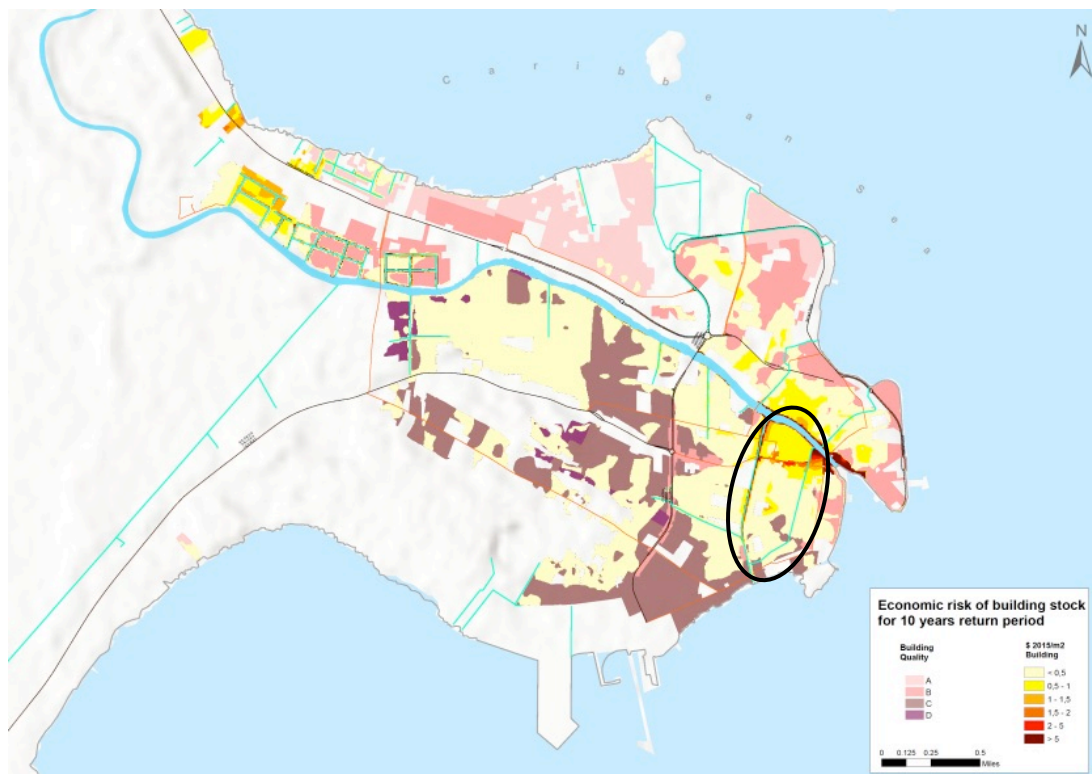


Figure 3. Economic risk of building stock for 10-years RP in the present situation obtained in the baseline studies for Belize City, 2016.

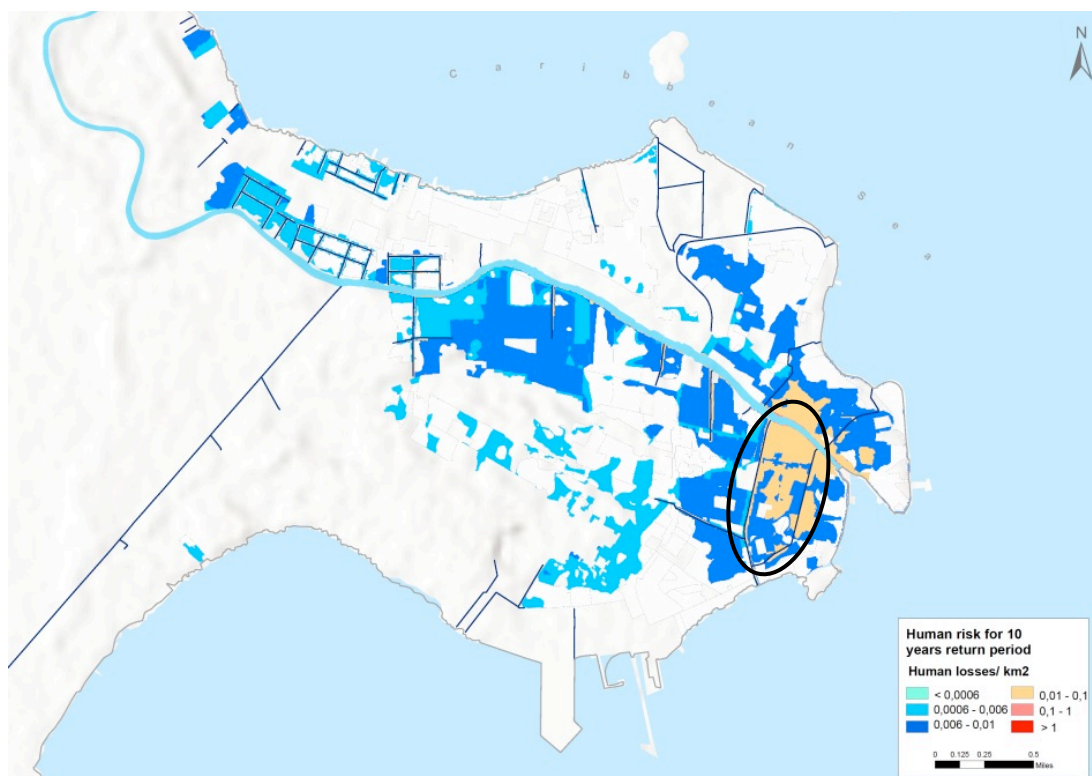


Figure 4. Human risk for 10-years RP in the present situation obtained in the baseline studies for Belize City, 2016.



This final report summarizes all the results of the consultancy, including:

- (i) The conceptual design of the flood reduction pilot project in Downtown Belize, including the dimensioning of the pumping scheme and associated works.
- (ii) A climate change analysis, focused on the potential modification of the extreme rainfall regime, and specifically the short-duration rainfalls, which are the most critical for the proposed system.
- (iii) The estimation of the economic and human risks in the area, comparing scenarios with and without flood mitigation works, and taking into account the climate change for the 2050 horizon.
- (iv) A cost-benefit analysis, based on different sources of information, including local surveys.

The design level for the proposed risk-reduction scheme has been 10-years of return period, and the numerical modeling has been carried out with the EPA Storm Water Management Model (SWMM) and Infoworks ICM.

For the estimation of the avoided losses for each scenario (present and 2050 horizon with climate change), the same methodology applied in the baseline study for Belize City has been used, adopting the scenario without measures as benchmark. Within this methodological framework, the probabilistic analysis of risks is based on the following conceptual elements:

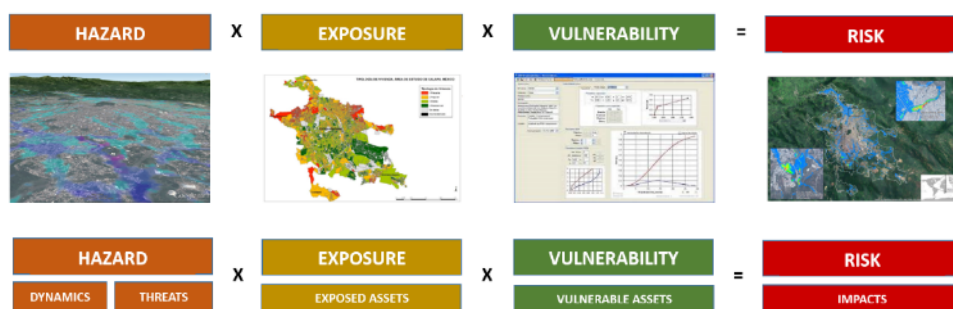


Figure 5. Conceptual framework for the estimation of the economic and human risks.

**Hazard or threat:** A dangerous phenomenon, substance, human activity or condition that may cause loss of life, injury or other health impacts, property damage, loss of livelihoods and services, social and economic disruption, or environmental damage (UN/ISDR, 2009). A hazard is characterised by its location, intensity, frequency, probability of occurrence and duration.

**Exposure:** People, property, systems, or other elements present in hazard zones that are thereby subject to potential losses. (UN/ISDR, 2009).

**Vulnerability:** The characteristics and circumstances of a community, system or asset that make it susceptible to the damaging effects of a hazard (UN/ISDR, 2009). Vulnerability is determined by physical, environmental, social, economic and administrative factors and processes. In probabilistic/quantitative risk assessments, the term vulnerability expresses the percentage of exposed elements that are likely to be lost due to a specific threat.

**Risk:** The combination of the probability of an event and its negative consequences.

In order to take into account the effects of climate change and future urban developments, the standard ESCI methodology has been applied. The methodology consists of the following steps, which will be explained in detail in the corresponding sections:

- Estimation of probabilistic hazard: A 2 D hydraulic analysis of the flood threat in the study area has been performed on the rainfall data for the return periods of 10, 20, 50, 100 and 500 years. The 2D analysis has been carried out through the application of the InfoWorks ICM model (Integrated Catchment Modeling) developed by Innovyze. Historical flood data has been used to calibrate and validate the results.
- Estimation of exposed value: Based on the data available, the value at risk of all the buildings that lie in the maximum flood extent area have been calculated.
- Structural vulnerability assessment: The physical vulnerability to flood events for each type of building stock in the study area has been assessed.
- Calculation of risk: Based on the information available and/or generated about the hazard, exposed value and structural vulnerability to flooding in the study area, the probabilistic flooding risk in the area in terms of physical (loss of physical stock) and human (loss of life) have been evaluated. This calculation shall include the maximum probable loss due to flooding with return periods of 10, 20, 50, 100 and 500 years and the expected annual loss.
- Calculation of risk for indirect damages: In addition to losses due to direct impacts to physical assets and loss of human life, indirect economic losses have been estimated.
- Finally based on the estimation of the avoided losses for the prioritized works, a cost-benefit analysis has been prepared following the IDB's requirements, valuing risk reduction costs plus the replacement of damaged assets in each scenario.

## 2. DESCRIPTION OF BELIZE DOWNTOWN FLOOD REDUCTION SCHEME

The proposed flood reduction scheme has the following main components (Figure 6):

- 1) Pumping station.
- 2) Closure gates.
- 3) Dredging and lining works.
- 4) Rehabilitation of street drains.
- 5) Real time operating system.

The proposed system's backbone is a pumping station that will drain the rainfall accumulated in each rainfall spell within the project area towards the sea. It will connect the low areas through a network of canals, being the main ones the Collet Canal and East Canal. The pumping facility, located on the coastline at the southern outlet of Collet Canal, is based on helicoidal (screw) pumps to raise the water to the sea. For the system to be

effective, it will also be necessary to isolate it from the surrounding water (Haulover Creek, West Canal and the sea, up to a certain level) with gates so that no water enters from the outside. Also, some dredging and reshaping of the main canals will be needed, together with the rehabilitation of street drains, so that they can supply their run off to canals connected with the pumping facility. Finally, the whole system will require a simple operational system, including procedures and sensors to actuate and maintain all its elements. A description of the main components of the system and its benefits is presented below.



Figure 6. Main components of the proposed system.



1) **PUMPING STATION.** A pumping station at the sea outlet of Collet Canal, with 3 or 4 screw pumps is required, with a total elevation head around 3-4 m. The choice of this type of pumps is due to its several advantages:

- Very long service life (20-40 years).
- High operational reliability.
- High efficiency (80-85%).
- Conveyance of solids and debris up to a certain size.
- Automatic discharge regulation, only dependent on water stage.
- No upstream raking system required.
- Low wear and tear.
- There is no need to place a deep collection sump upstream.



Figure 7. Examples of existing screw pumping stations.

2) **GATES.** 4 Gates are required, one at each of the main connections of the system with boundary canals or water bodies (Haulover Creek and the sea). They fulfill the function of isolating the system from the sea, the Haulover Creek and West Canal (see Figure 6):

- Gate 1: outlet of Collet Canal at the sea.
- Gate 2: confluence of Collet Canal with Haulover Creek.

- Gate 3: confluence of East Canal with Haulover Creek.
- Gate 4: confluence of Collet Canal with West Canal.

Some examples of available gate typologies are shown in Figure 8.



Figure 8. Examples different types of gates technology.

- 3) **DREDGING AND LINING WORKS.** These works will be carried out in Collet and East Canal within the project area (approx. 2.6 km). Currently both canals have a severe siltation that needs to be removed in order to increase the storage capacity and the hydraulic slope of the system.

The dredging volume in each canal has been estimated by Chemtec, based on the topographic survey of the canals (Figure 9 and Table 1). It has been found that it is necessary to dredge a sediment volume of around 7600 m<sup>3</sup> in Collet Canal and of 1800 m<sup>3</sup> in East Canal, giving a total volume of around 9400 m<sup>3</sup>.

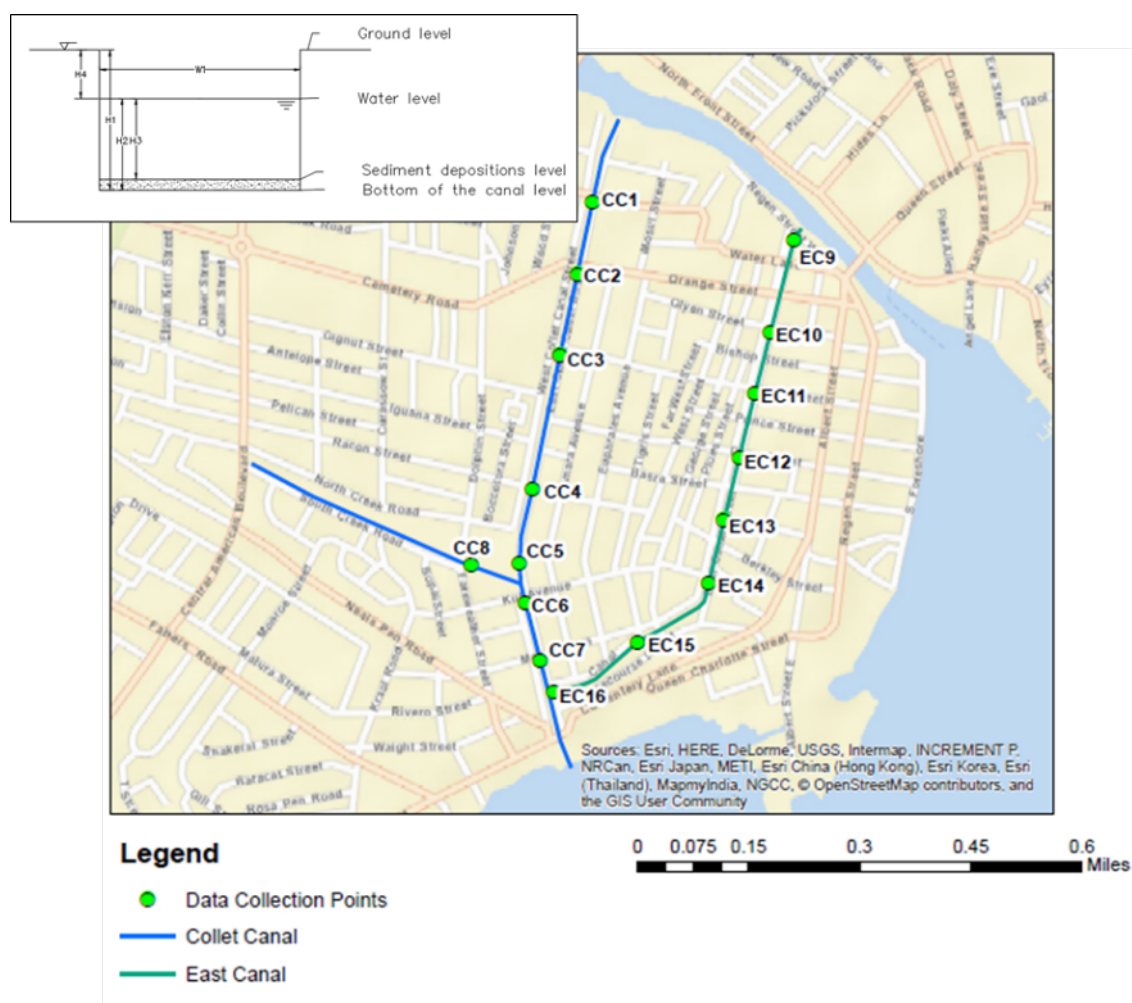


Figure 9. Measurement sections carried out during the field campaigns.

Collet Canal (CC)								
Point	Time	W1 - width of canal	H1 - Ground level to Canal bottom (H2 + H4)	H2 - Water level to Canal bottom	H3 - Water level to top of debris	H4 - Ground Level to water level	Description	Lined Cement Bottom/ Unlined Bottom
CC1	0.624	4.064	11:44	1.50	0.610	0.991	Vernon Street	LB
CC2	0.614	4.064	21:06	0.91	0.584	0.965	Orange Street	LB
CC3	0.610	4.013	18:03	0.74	0.483	1.016	King Street	LB
CC4	0.605	4.089	17:27	0.76	0.457	0.965	Allenby Street	LB
CC5	0.573	4.496	5:38	1.24	0.279	0.991	North of Kut Avenue Before Branch	LB
CC6	0.471	6.274	16:14	0.91	0.368	0.762	Kut Avenue	Unlined
CC7	0.467	5.817	14:24	0.89	0.432	0.711	Mex Avenue	Unlined
CC8	0.600	4.572	14:24	0.97	0.559	0.635	End of South Creek Road	LB
East Canal (EC)								
EC9	0.428	2.870	3:44	0.71	0.610	0.445	Street	LB
EC10	0.435	2.832	5:15	0.79	0.686	0.432	Church	LB
EC11	0.440	2.819	11:03	0.88	0.660	0.584	King Street	LB
EC12	0.442	2.858	15:37	1.17	0.648	0.483	Dean Street	LB
EC13	0.445	2.667	22:38	2.67	0.838	0.356	South of South Street	LB
EC14	0.449	2.870	3:12	1.78	1.067	0.356	Rocky Road	LB
EC15	0.453	2.794	14:24	1.19	0.356	0.406	West George Street	LB
EC16	0.460	2.692	3:25	0.69	0.102	0.457	Canal End - Before Meeting with Collet	Cement lining stops before bridge

Table 1. Cross-sections geometry measurements obtained during the field campaigns.



On the other hand, it is very important, in addition to the dredging of both canals, to reshape, deepen and line certain stretches of the canals, in order to connect their entire profile to the discharge point, avoiding low points and stagnant water, as far as possible. In this regard, a sector of around 400 m at the end of the Collet Canal and around 275 m at the end of the East Canal, both near the pumping station, have to be deepened and concrete lined, in order to increase the storage capacity and improve the working conditions of the system. As seen in Figure 10, the mouth of the Collet Canal is currently (June 2017) completely obstructed, providing little storage and conveyance capacity.



Figure 10. Severe siltation at the outfall to the sea of Collet Canal.

In Table 2, the post-processed information obtained from the field surveys, as provided by Chentec, is presented. This Table summarizes the main characteristics of the geometry in three different stages:

1. Current geometry: Invert level reference to the local mean sea level (LMSL), current depth and current debris height.
2. Sediment removal: Invert level and maximum depth after the cleaning of the canals.
3. Final geometry: Final invert level (reference to the local mean sea level) and dredge height from the clean canal bottom.
































		Current Canals				Debris removal		Final Canals		
Section	Max Width	Invert level	Depth	bris to remo	Invert level	Depth	Invert level	new fill/dredge (+/-)	Lined cement bottom	
CC1	4.06	-0.77	1.60	 0.89	-1.66	2.49	-1.66	 0.00	Lined	
CC2	4.06	-0.75	1.55	 0.33	-1.08	1.88	-1.08	 0.00	Lined	
CC3	4.01	-0.65	1.50	 0.25	-0.90	1.75	-0.90	 0.00	Lined	
CC4	4.09	-0.62	1.42	 0.30	-0.93	1.73	-0.93	 0.00	Lined	
CC5	4.50	-0.44	1.27	 0.97	-1.40	2.24	-1.40	 0.00	Lined	
CC6	6.27	-0.40	1.13	 0.55	-0.95	1.68	-1.50	 -0.55	Unlined	
CC7	5.82	-0.46	1.14	 0.46	-0.91	1.60	-1.50	 -0.59	Unlined	
CC8	4.57	-0.73	1.19	 0.41	-1.13	1.60			Lined	
EC9	2.87	-0.57	1.05	 0.10	-0.67	1.16	-0.67	 0.00	Lined	
EC10	2.83	-0.66	1.12	 0.10	-0.76	1.22	-0.76	 0.00	Lined	
EC11	2.82	-0.64	1.24	 0.22	-0.86	1.46	-0.86	 0.00	Lined	
EC12	2.86	-0.63	1.13	 0.52	-1.15	1.65	-1.15	 0.00	Lined	
EC13	2.67	-0.83	1.19	 0.75	-1.58	1.94	-1.58	 0.00	Lined	
EC14	2.87	-1.06	1.42	 0.71	-1.77	2.13	-1.77	 0.00	Lined	
EC15	2.79	-0.36	0.76	 0.84	-1.20	1.60	-1.50	 -0.30	Lined	
EC16	2.69	-0.12	0.56	 0.58	-0.70	1.14	-1.50	 -0.80	Unlined (bridge)	

Table 2. Measurements summary table.

Figure 11 shows the corresponding longitudinal profiles of the invert level for both canals, as present and after the proposed works (the final situation includes dredging and reshaping).

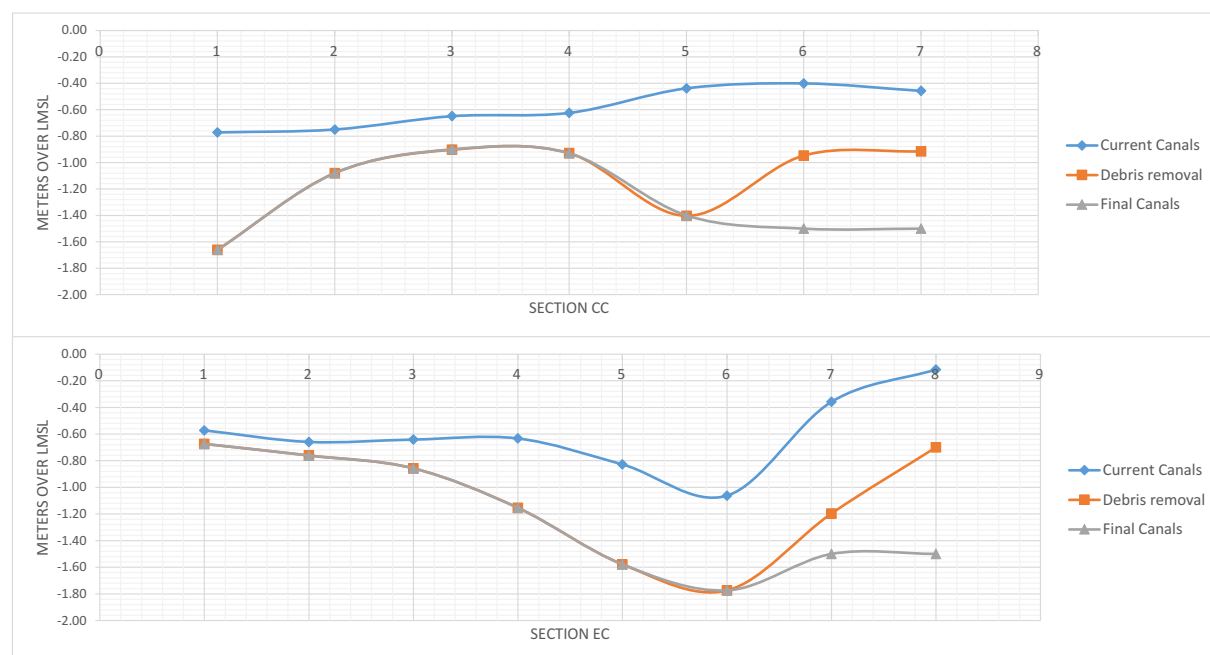


Figure 11. Longitudinal profiles of Collet (above) and East Canal (below) in the current situation, after dredging and in the final situation.

- 4) **REHABILITATION OF STREET DRAINS.** It is necessary to connect all the streets within the project area to the Collet and East Canal, so that the pump can evacuate this water as soon as possible during a flood event. Without these connections, the proposed system will be ineffective, since the canals will be emptied while the urban area can still be flooded.



Traditionally, urban drainage models are usually composed by a tree-shaped network of connected pipes that convey the street water by gravity. Optionally, and depending on the design criteria for the system, these infrastructures can include storm tanks, in order to increase the capacity of the systems during large events, minimizing environmental impacts associated with water spills.

At present, several drains can be found in Belize Downtown, as exemplified in Figure 12. In fact, there is a mesh of pipes and culverts connecting several streets with the canals, the Haulover Creek and the sea, but almost all of them are fully silted, obstructed or structurally damaged, so that the water is stagnant because it cannot flow inside them. Given the small dimensions of these street drains, their storage capacity is nearly negligible, and therefore all its functionality is linked to the conveyance capacity.

There are two types of drains in the study area:

1. Non-accessible drains, located below the pedestrian sidewalks, with rectangular gutters every 4-6 m; this scheme is the one followed in the main streets of Downtown area (see Figure 12, left). This solution is deficient from the point of view of operation (most of the drains are clogged) and maintenance; furthermore, it poses some threats to elder pedestrians. On the positive side, it has better looks and is more suited for vehicles than the one that follows.
2. Open culverts on the side/s of the road. This option is typical in smaller or secondary streets (Figure 12, right). Access to the buildings is enabled through numerous individual footbridges. This scheme is good from the point of view of functionality and maintenance (debris and silt removal), but performs poorly in terms of accessibility, traffic and aesthetics.



Figure 12. Left) Orange Street drainage system Type 1. Right) Drainage system Type 2.

These infrastructures can usually cope with the rainwater coming from common storm events, but its capacity is not enough when larger events happen, and especially at the peaks of maximum intensity of a particular storm. In addition to that, the seawater level can flood partially the two main canals and part of the conduits mesh, diminishing the capacity of the entire system. Furthermore, the maintenance level of the

system is poor, affecting directly to its capacity and aesthetic conditions. As a result, the current drainage system collapses several times during an average year, partly due to the boundary conditions imposed by the sea level, and partly because of the poor state of conservation of the system.

Given this situation, it is proposed to modify the drainage scheme of Belize Downtown, using the street area between the sidewalks as a wide, shallow culvert, where water can be both stored and conveyed directly to the canals. In order to achieve this functionality, it is important to guarantee the connectivity of the roads with the main canals, avoiding intermediate low points where water becomes stagnant. This solution also promotes the use of the store capacity of the roads, making possible to drain the rainwater quickly through the main canals, avoiding permanent flooding in the urban area, in case that it happens (therefore, not only flood intensity is reduced, but also flood duration in a very significant way). Specifically, it is proposed that the streets themselves can absorb the first 20 cm of flooding.

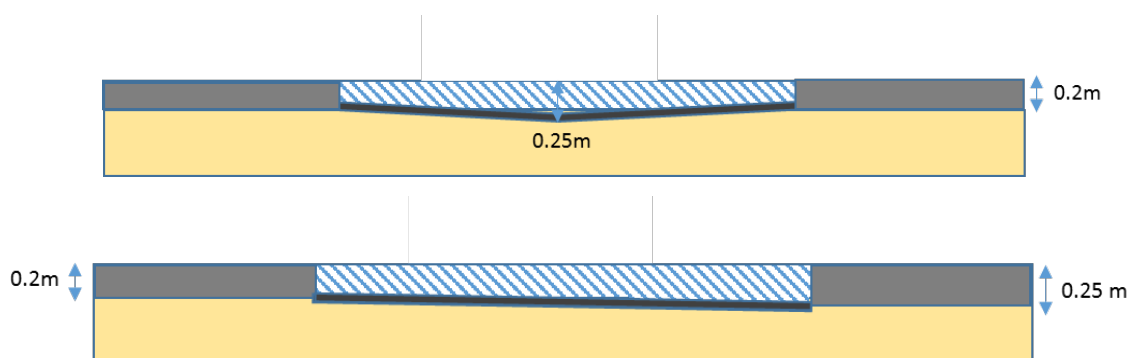


Figure 13. Proposed drainage system in the pilot area during a 10-years return period storm.

As shown in Figure 13, two different road sections are proposed, the first one for the main streets ( $\geq 6$  m width) with a slope ending in the center of the section and the second one for the secondary streets ( $< 6$  m width) with a continuous slope ending in one side.

For this solution to work properly, a key aspect is the connection of the streets with the canals. Figure 14 shows a sketch of the type of wide and open connection needed, in order to avoid that debris or local obstacles increase hydraulic losses.

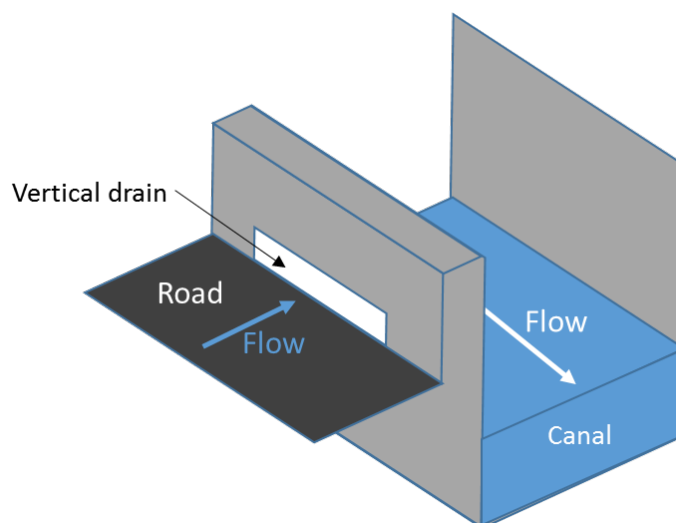


Figure 14. Detail scheme of the connection between the roads and the canals.

- 5) **REAL TIME OPERATING SYSTEM.** It will include the tools and procedures to operate the drainage scheme based on hydro-climatic data (sea level, river discharge and local rainfall). It will be designed later in the project, and will operate on simple rules, based on real time rainfall and sea level data.

Initially, it was included as a component of the project a protection wall about 1.5 m high (above mean sea level), placed along the right bank of Haulover Creek, between the outlets of Collet and East Canal (total length of 720 m). The function of this protection wall was to avoid the entrance of water from Haulover Creek into the project area. A more detailed inspection of such area showed that most of the border is already protected up to that height, and therefore the required wall is not strictly needed, or could eventually be built along some stretches at a later stage of the project.

The proposed flood reduction scheme will provide the following direct and indirect benefits:

**Direct benefits:**

- Flood reduction due to extreme local rainfall, by closing the gates and switching on the pumps.
- Flood reduction due to high river discharges and sea-level surge, only by closing the gates (there is no need to connect the pumps).
- Noticeable improvement of the water quality and sedimentation rates of Collet and East Canals during the dry period. This can be achieved by activating the system (pumping station and closure of Gate 1 at the sea) once per month for a few hours during the dry period, inducing flow velocities that would otherwise not happen by natural means. This procedure is advantageous from the point of view of the maintenance of the system, and will surely improve the urban environment (smells, visuals, insects, etc.).

**Indirect benefits:**

- Increase of urban land and property prices due to the improvement of flood conditions.
- Notable reduction of traffic and commerce interruption during the flood events.
- Improvement of public health conditions and risks of water-borne diseases.

### 3. DATA COLLECTION AND CLIMATE CHANGE ANALYSIS

The information included in this section is based on three main sources: (1) remote sensing and GIS-data analysis of data from previous studies; (2) field visits to the study area; and (3) climate analysis and climate change projections from the baseline studies for the ESCL in Belize City. Given the nature of the proposed flood reduction scheme, a more in-depth rainfall analysis is required, focused on the characterization of short-duration rainfall events. The extreme rainfall regime has also been projected into the future, considering several climate change scenarios.

#### 3.1. Socio-economic and vulnerability data of the study area

For the purpose of this section, the project area is defined as all the urban sectors that drain towards the East or Collet canals, including the blocks situated outside the perimeter defined by both canals. It is a consolidated urban zone located in Downtown of Belize City with a population of around 6600 inhabitants, in a total area of 65.3 ha, which yields an average population density of 95.6 inhab/ha. It is characterized by lower-middle residential classes (Table 3) with an urban morphology that varies from orderly to disorderly, and upper-middle class in mixed-use corridors along the main roads. The main use is the residential one, followed by mixed-uses.

There is one informal settlement inside the study area, with medium consolidation. The typology of the dwellings are single-family mainly. The elevation of the houses/dwellings are mainly ground floor and are characterized by resistant materials in walls (block) and weak roofs (sheet).

Building quality	Buildings	%	Population (2015)	%	Total Value (M US\$)	%
A	2	0.13	10.67	0.16	0.12	0.27
B	313	20.15	1260.44	19.13	17.66	39.94
C	1236	79.59	5307.4	80.56	26.44	59.79
D	2	0.13	9.89	0.15	0.0036	0.01
Total	1553	100.00	6588.41	100.00	44.22	100.00

Table 3. Buildings, population and total value of the buildings by building quality. Source: Natural disaster risk assessment study of Belize City, (IHCantabria and M&K, 2016).

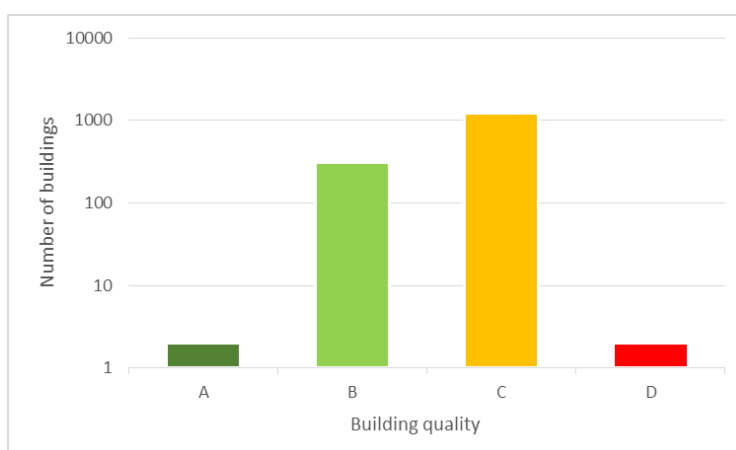


Figure 15. Building quality distribution.

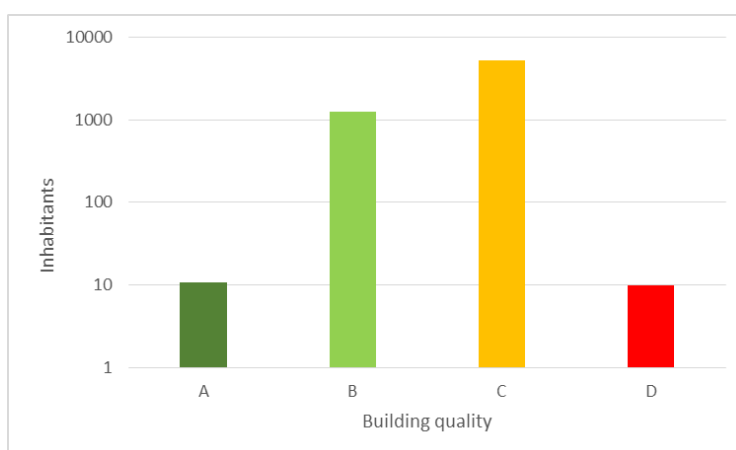


Figure 16. Population by building quality.

The main building quality is C followed by B. The following categories for the residential building quality apply:

**Category A (high constructive quality):**

- Buildings which have all basic infrastructure services: electric energy, potable water and drainage.
- Buildings with floor, roof and wall of resilient and high quality materials. Structure with good design and earthquake resilient.
- They can present single-family or multi-family typologies with a variable number of floors. Commercial, services or institutional buildings with high constructive quality are also included.

**Category B (middle quality building):**

- Buildings which have all basic infrastructure services: electric energy, potable water and drainage.
- Buildings built with permanent and resilient materials, and good quality finish.
- They can present single-family or multi-family typologies.

**Category C (low quality building):**

- Buildings which have all basic infrastructure services.

- Buildings built with basic construction materials (often auto-built) which correspond with simple designs and poor quality. They are built with resistant wall material (usually block) and sheet roof.
- They use to be single-family typologies with one or two floors.

Category D (very low quality building):

- They usually lack basic infrastructure services, especially in the case of informal settlements. This situation supposes an environmental pollution source which is important to have into account.
- These constructions are composed of fragile and waste materials on walls and roofs. They are auto-built.

The spatial distribution of the residential building stock by quality, and the population density, are presented in Figure 17 and Figure 18, respectively.



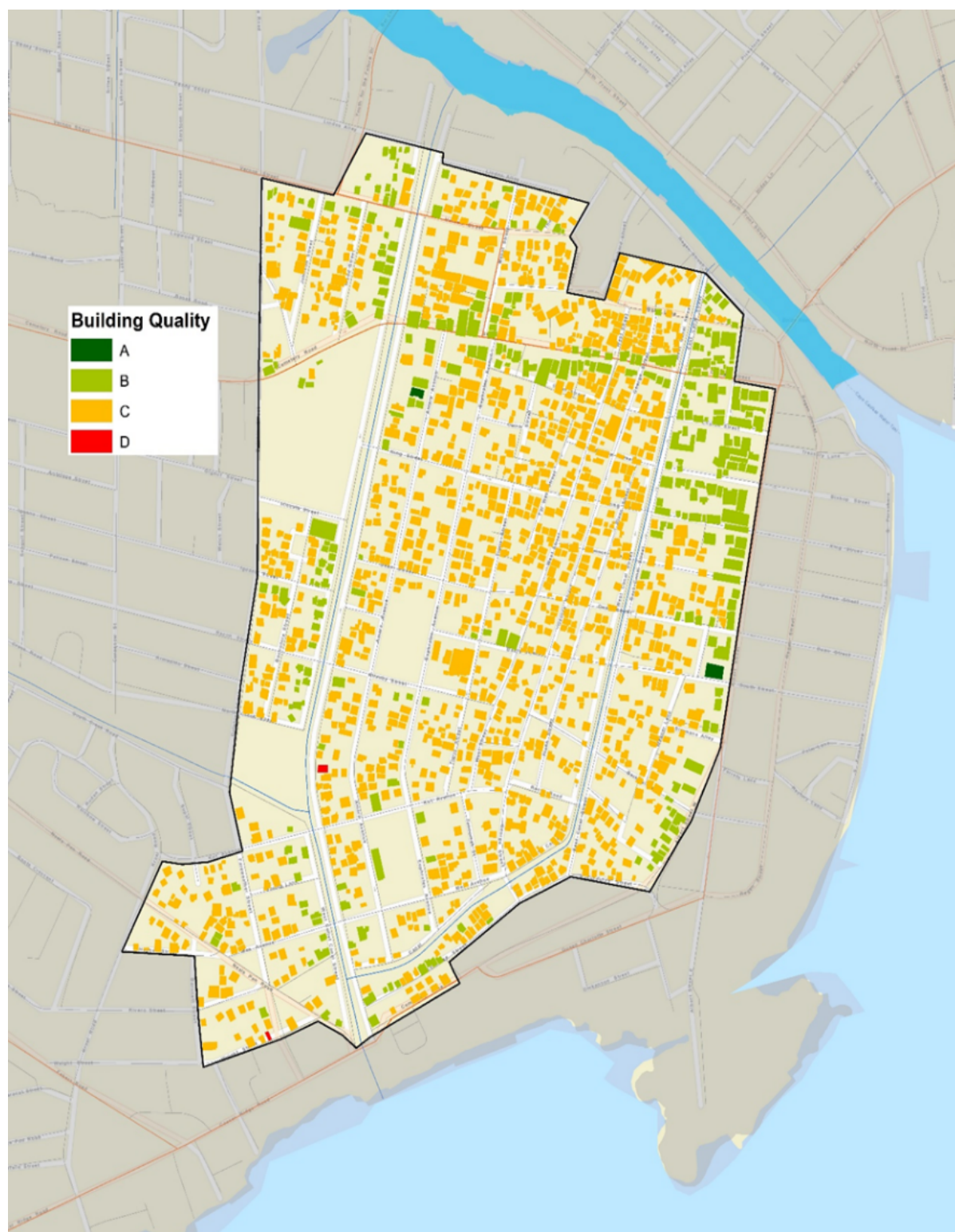


Figure 17. Residential building stock by quality in the project area.

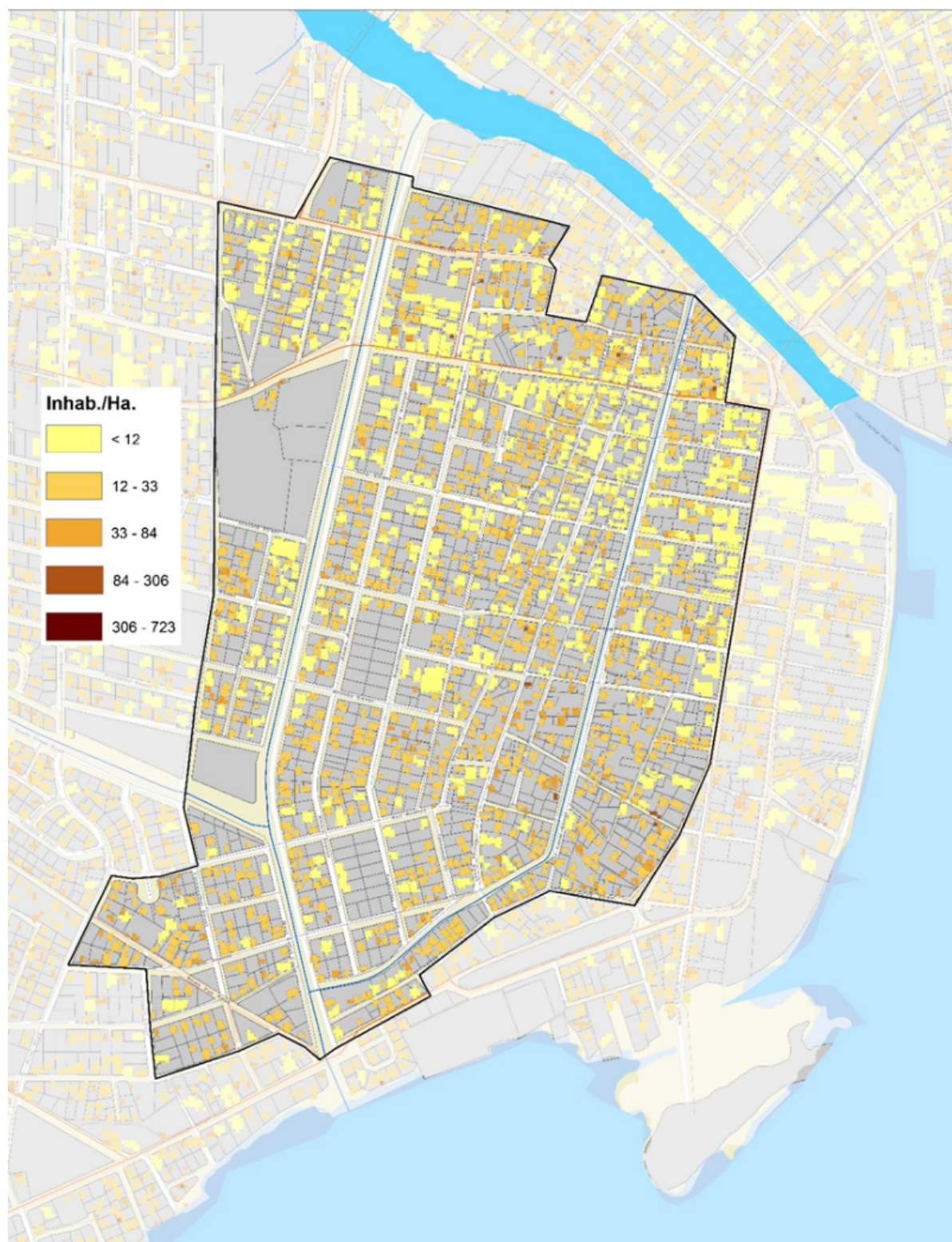


Figure 18. Population density of the project area.



## 3.2. Hydro-climatic data

### 3.2.1. Meteorological stations and flow gauges

Time series from meteorological stations and flow gauges have been provided by the Belize National Meteorological Service. There are five meteorological stations with rainfall data, from which only St John's College Station shows daily data, while in the remaining stations have monthly data. Regarding the flow gauging stations, there are four gauges with the average daily flow in  $m^3/s$ . The location of the stations and their main characteristics are shown in Figure 19, Table 4 and Table 5.

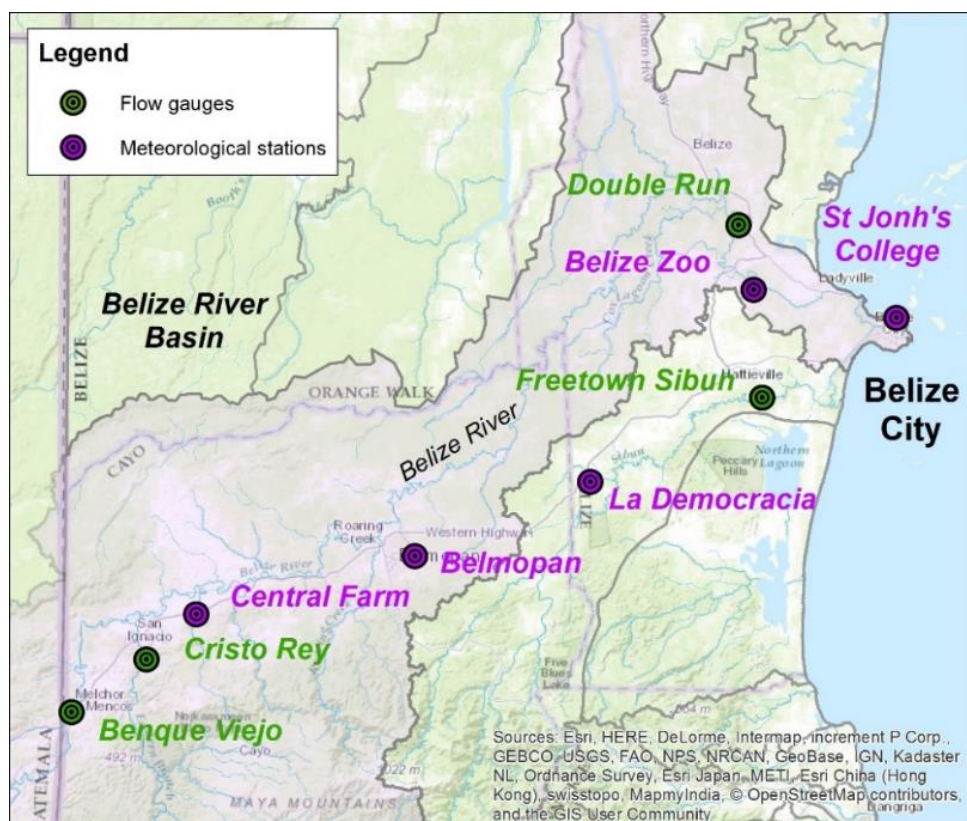


Figure 19. Location map of the meteorological stations and flow gauges provided by the Belize Natural Meteorological Service.

STATION	DISTRICT	PERIOD	LATITUDE	LONGITUDE
St John's College	Belize	1965-2010	17°31'	88°12'
Belize Zoo	Belize	1995-2014	17°22'	88°33'
La Democracia	Belize	1995-2014	17°20'	88°33'
Belmopan	Cayo	1995-2014	17°15'	88°46'

Table 4. Characteristics of the provided meteorological stations.

STATION	WATERCOURSE	PERIOD	LATITUDE	LONGITUDE
Double Run	Belize River	1981-2013	17°37'04"	88°22'54"
Freetown Sibun	Sibun River	1981-2013	17°25'39"	88°21'12"
Benque Viejo	Mopan River	1981-2013	17°04'26"	89°08'29"
Cristo Rey	Belize (Macal)	1981-2013	-	-

Table 5. Characteristics of the provided flow gauges.

In order to characterise the historical rainfalls over the city and the flow of the Belize river, the Saint John College rainfall-gauge and the Double Run flow-gauge have been selected and analysed for this study. The sensors provide daily accumulated rainfall in mm/day and flow in m<sup>3</sup>/s, covering from 1<sup>st</sup> January 1965 to 31<sup>st</sup> August 2010 and from 1<sup>st</sup> January 1981 to 12<sup>th</sup> December 2013, for rainfall and discharge, respectively. A partial representation of both time series is displayed in Figure 20.

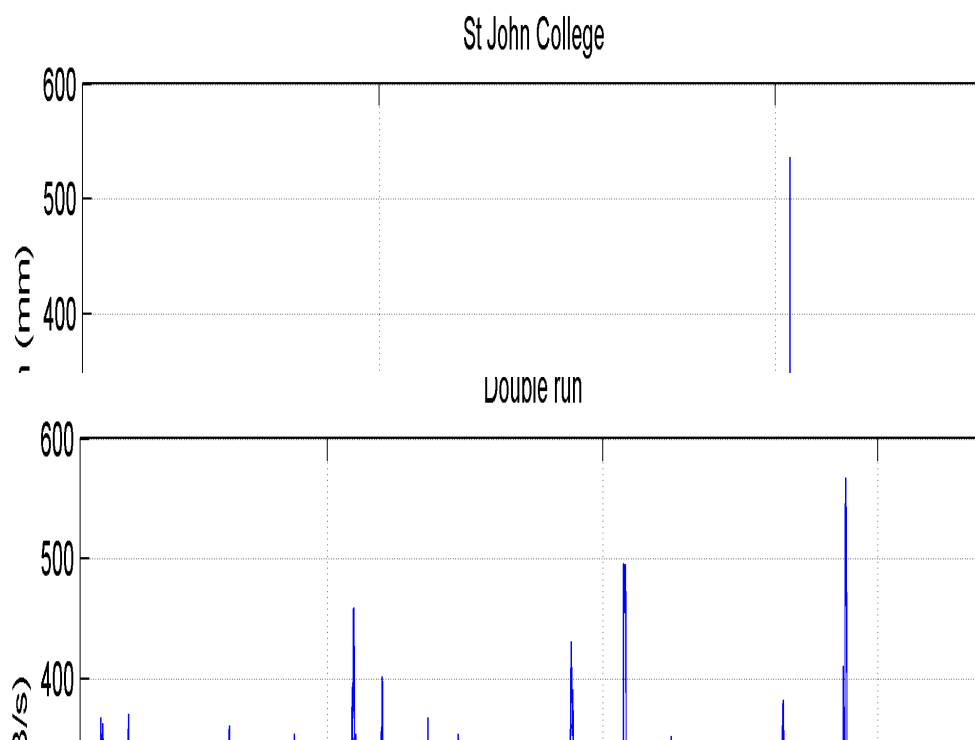


Figure 20. Daily time series of available rainfall and river flow.

Figure 20 reflects the tropical monsoon climate of Belize City, with warm and humid conditions throughout the course of the year. The city has a lengthy wet season that runs from June through to November and a short dry season covering the remaining three months.

### 3.2.2. Waves and sea level

Due to the absence of measured waves and long records of sea level data, it has been necessary to obtain this information from numerically simulated long-term series of these dynamics.

Waves, and meteorological tides have been obtained from GOW (Global Ocean Waves Reanalysis; Reguero et al., 2012) and GOS (Global Ocean Surges; Abascal et al., 2012) reanalyses, respectively. These hindcasts, developed by IHCantabria, have been extensively validated using available instrumental information. The astronomical tide has been extracted from the global model of ocean tides TPXO, developed by University of Oregon (Egbert and Erofeeva, 2002).

The presence of islands and barrier reefs produce dramatic modifications in the wave's energy that finally break over Belize's shoreline, reducing most of the wave run-up that could contribute to build up extreme water levels. For this reason, a hybrid methodology (dynamical-statistical) to transfer deep-water waves to the proximity of Belize City has been used, providing long-term series of shallow water wave parameters. This approach combines

the OLUCA model (developed in IH Cantabria) with statistical classification and interpolation techniques, in order to compute the most representative sea states. This sampling procedure is followed by an interpolation and final reconstruction of the complete time series.

Figure 21 shows two examples of a sea state propagation with different sea levels. With identical offshore wave conditions, two different sea levels are used in order to test the influence of the sea level rise, actual sea level (0 m, left) and future sea level (0.5 m, right). Despite of different baseline sea levels, only minor differences are observed in the vicinity of Belize, demonstrating the effectiveness of the barrier reefs in attenuating the wave energy, nowadays and in the future. Panel b in Figure 21 displays the available time series (1948-2008) of significant wave height (Hs), storm surge (SS), astronomical tide (AT) and total water level (TWL), excluding hurricane climate.

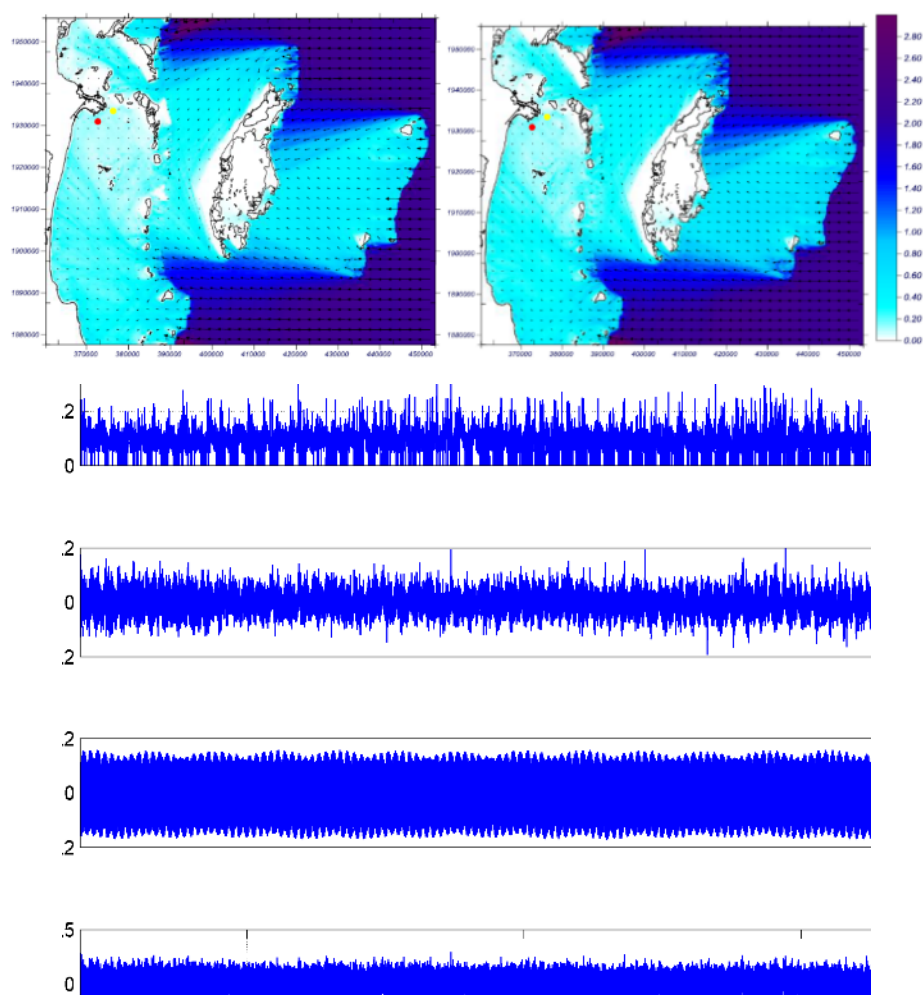


Figure 21. Above: Example of a sea estate propagation with different sea levels (0 m, left and 0.5 m right). Below: available time series of Hs, SS, AT and TWL at Belize City.

### 3.2.3. International Best Track Archive for Climate Stewardship (IBTrACS)

The characterisation of the current tropical cyclone climate requires a long-term database of historical cyclone tracks and intensities. In this study, the IBTrACS (International Best Track Archive for Climate Stewardship; Knapp et al., 2010) database has been used. This database contains 6-hourly information about hurricane centre

location (latitude and longitude in tenths of degrees) and intensity (maximum 1-minute surface wind speeds in knots and minimum central pressures in millibars) for all Tropical Storms and Cyclones observed from 1851 to date.

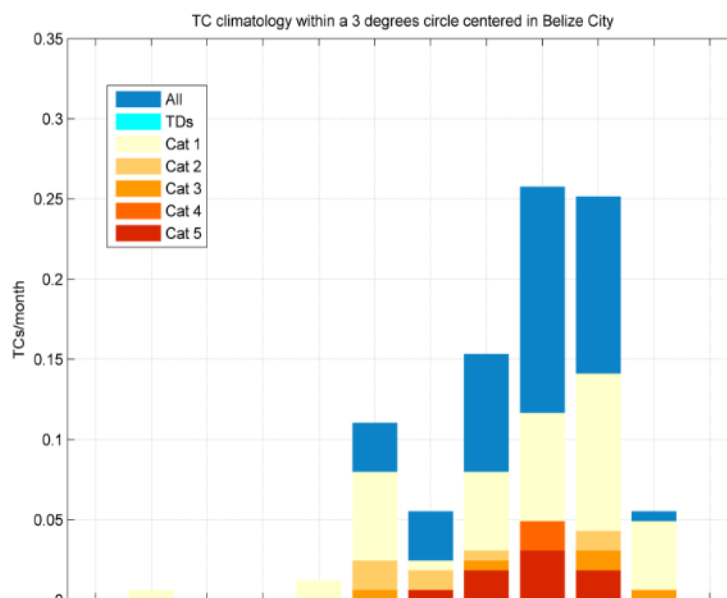


Figure 22. Belize tropical cyclone climatology from the IBTrACS database.

### 3.3. Characterization of hydro-climatic variables in the study area

#### 3.3.1. Modelling approach

As stated in the previous section, the primary drivers of urban floods in Belize City are the local rainfall over the city, the Belize River flow, the mouth of which is located north of the city (very close to the pilot area), and the sea level which governs the potential river runoff and may generate its own storm surge floods.

In the baseline studies for Belize City a novel methodology tackling at the same time coastal, fluvial and pluvial floods has been developed to conveniently deal with the three kinds of flood hazard types governing the flood risk in Belize City. A briefly summary of the methodology is presented below and the conceptual framework used is presented in Figure 23.

The methodology starts analysing the present climate, which in turn is split into **regular climate and hurricane climate**. The main dynamics defining the target hazards, here named met-ocean variables, are statistically analysed within the regular climate to define multivariate distributions that are able to generate plausible combinations of them producing various levels of flooding hazard.

On the other hand, based on the available historical information about tropical cyclone activity in the area, a Monte Carlo simulation is used to generate thousands of synthetic cyclones that are in statistical agreement with observations. Finally, the method integrates both climates into the same statistical distribution, thus providing the hazard (i.e. water depths over flooded areas) as a function of the time (i.e. return periods).

The method produces robust statistics to characterise wind, storm surge, rain and river runoff, considered as the main drivers of the hazards in Belize City. (For more detailed information see Annex I).

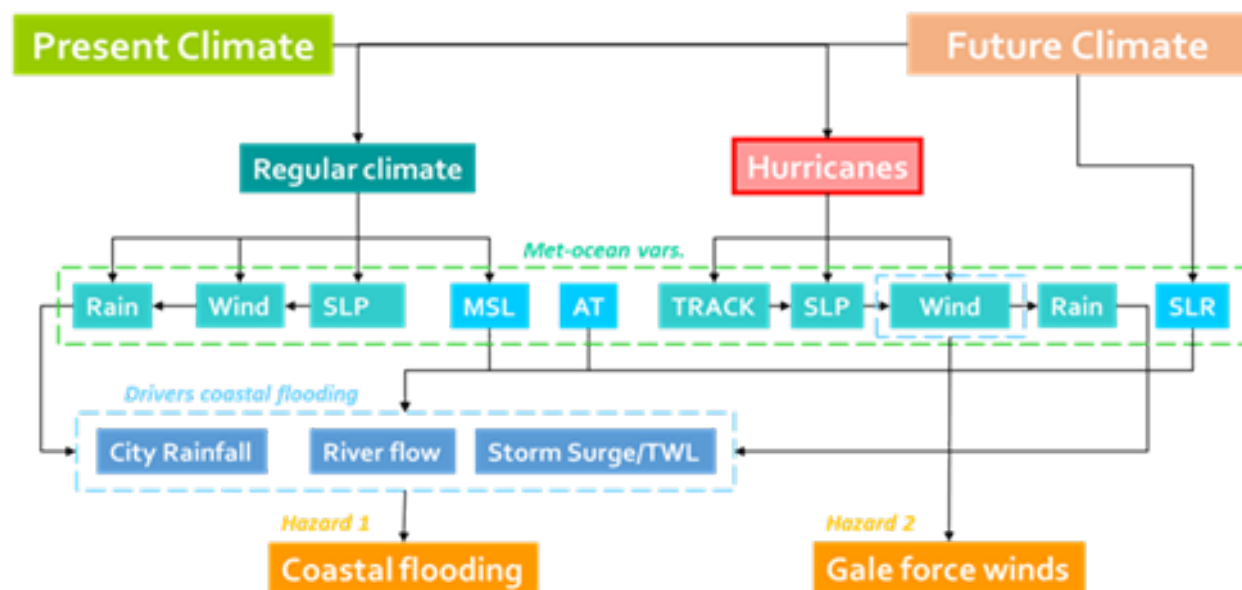


Figure 23. Conceptual framework for the climate characterization used in the baseline studies of Belize City (ESCI), 2016.

Figure 24 presents the three distributions obtained for the different return periods: One-day total rainfall (mm), Belize River flow ( $\text{m}^3/\text{s}$ ) and storm surge (TWL) (m).

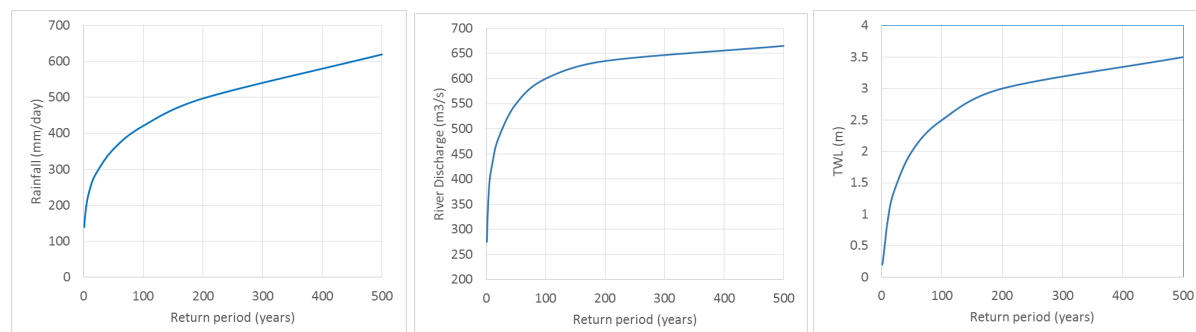


Figure 24. Rainfall, river flow and sea level distributions for different return periods obtained from the baseline studies in Belize City (ESCI), 2016.

In Belize Downtown floor reduction project, the intervention area is much smaller than the total study area in ESCI, and is exposed to specific hazards. For this reason, the general modelling approach used for the whole City must be adapted and revised, taking into account several facts.

Firstly, the project area is situated near the outlet of Haulover Creek (a branch of Belize River) to the sea. The sea is situated just 600 m downstream from the most upstream point of the project area, and in this configuration, it can be demonstrated (Annex II) that the river discharge has a negligible effect in the total water level occurring at the confluence of Collet Canal with Haulover Creek; the influence is even lower at the confluence of East Canal. For this reason, one of the three climatic sources used in the Baseline Study, the river discharge, can be omitted in this project, for practical purposes.

Regarding the effect of the sea, for events with a recurrence period lower than 20-years, the total sea level remains below 1.5 m above the mean level (Figure 24). Since the proposed project includes several gates to isolate the intervention zone from the exterior, at least up to that level (which is equivalent to less than 1 m above the ground level along the boundary of the project area), the sea level does not intervene either (although it will affect the estimated economic damages beyond the design level).

In consequence, the key design variable for this project are local showers of short duration, and the functionality of the system will be given by the total amount of rainfall that can be managed within a certain timespan, to be determined. While in the baseline studies for Belize City, the rainfall regime was characterized by the amount of total rainfall in one day, for this project a more detailed characterization of the extreme rainfall regime will be needed, in order to define the required capacity of the canals and pumps. The key variables for the proposed pumped scheme are:

- Critical duration of the design rainfall for the proposed system. It is the equivalent of the concentration time, in catchments dominated by topography-driven runoff, but in the proposed scheme the hydraulic slope is artificially induced by the pumps.
- Amount of precipitation in the total duration of the design spell, as given by the IDF curves.
- Distribution of the total rainfall over the spell. It does not need to be a constant intensity, a several possible hyetographs should be tested.
- Antecedent moisture content of the soil at the time of occurrence of the design spell. Depending on how saturated is the terrain, which basically depends on the timing of the spell within the longer storm, the total discharge flowing into the system will vary. The storage capacity of the land is given by a hydrological parameter called Curve Number (CN).

Therefore, the system must be designed to withstand the most unfavorable spell in the middle of a longer storm, and it is important to check the sensitivity of the system to the duration of the shower, the shape of the hyetograph and the antecedent humidity of the soil. These are the hydro-climatic variables that will determine the effectiveness of the proposed system. On these bases, the model will be run for different combinations of these variables.

For the hydraulic analysis and dimensioning of the different elements of the system (particularly the pumping capacity), the Storm Water Management Model (SWMM) by the US Environmental Agency (EPA) will be used. Apart from being the standard tool for the design of urban drainage systems worldwide, SWMM is a free an open source model, so that the system layout can be handed over to the Belizean Authorities and local consultants for future applications. To analyze situations beyond the design level, causing canal saturation and overflow, a proprietary 2-D model (InfoWorks Integrated Catchment Modeling) by Innovyze Inc. will be used to produce the spatial flood maps, which are needed to calculate the total damages for the different return periods. The whole set of damage results for the present and future situation (with the new drainage scheme) will eventually be used to estimate the profitability (cost-benefit analysis) of the proposed investments.

### 3.3.2. Calculation of the IDF curves for the present climate

The IDF curves represent the mathematical relationship between the average precipitation intensity for a particular rainfall spell, its duration and the frequency of observation. The correct statistical characterization of the rainfall, especially of short duration, is very important for the design of urban drainage systems, especially in small areas with short concentration times, as is the case in Belize Downtown.



The objective of this section is to calculate the Intensity Duration Frequency (IDF) curves for the city of Belize at a sub-daily time scale. However, due to lack of instrumental information on such time scales, it is necessary to apply statistical relationships to derive such information (Bell, F.C., 1969 and Libertino, A., 2016). In this context, satellite information from the Tropical Rainfall Measuring Mission database (TRMM 3B42) is used to derive relations between maximum daily rainfall and sub-daily rainfall depths (Ayman G. Awadallah, 2012).

The methodology starts by calculating the return periods of 5, 10, 20, 50, 100 and 500 years from the St. John's College gauge, the closet gauge to the city of Belize. St. John's College gauge is located at the coordinates LON, LAT [88°12'; 17°31'] and contains daily information from the period 1965-2010 with 17.5% of missing values. As can be seen in Figure 20, the station rarely exceeds 100 mm per day. In fact only 57 events have exceeded this intensity, and just 7 of these correspond to tropical cyclones or tropical depressions (Unnamed 1975-10-29, Unnamed 1979-10-11, Gert 1993-09-18, Unnamed 1994-09-26, Kyle 1996-10-11, Keith 2000-10-02 and Alex 2010-06-26). Very remarkable is the event that corresponds to the cyclone Keith-2000 with a rainfall depth of 536 mm/day on the date 2000-10-02. From a statistical point of view this event should be considered as an outlier, however, it is taken into account in the extreme analysis since other sources documented the intensity of the event.

The annual maximum values have been selected in order to calculate the return period values, provided that at least 90% of the data is available for each year; the Gumbel distributions is fitted then to the data. The confidence intervals are calculated using parametric bootstrap and the percentile interval method (Efron, B. and Tibshirani, R. 1987). Figure 25 shows the results of the extreme regime analysis. The orange dots correspond to the observed data while the continuous blue line corresponds to the result of the adjustment of the Gumbel function. The dashed lines show the confident intervals. In order to transform the daily rainfall values into 24-hr values the theoretical ratio of 1.13 is adopted (Hershfield, 1961).

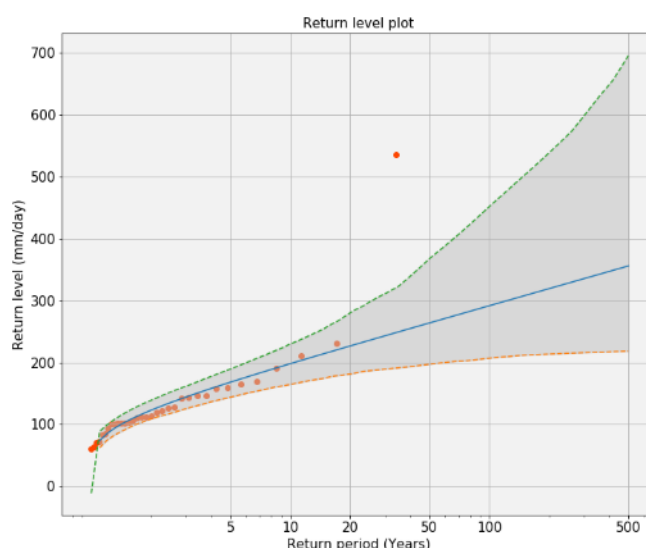


Figure 25. St John's College gauge Return periods (mm/day).

Once the return periods have been calculated, the closest TRMM node to that St. John's College gauge is selected to capture the ratios between the 24-hr and sub-daily rainfall return periods duration. The selected TRMM node has 3-hourly information from 1998 until today. As shown in Figure 26, which compares the instrumental information for the St. John's College gauge and the TRMM node, the latter correctly captures the basic statistics

such as mean, variance and rainy days (Table 6) as well as seasonality (Figure 27). However for higher order moments (Skewness), which represent the most extreme part of the distribution, there is great differences. That is why, in

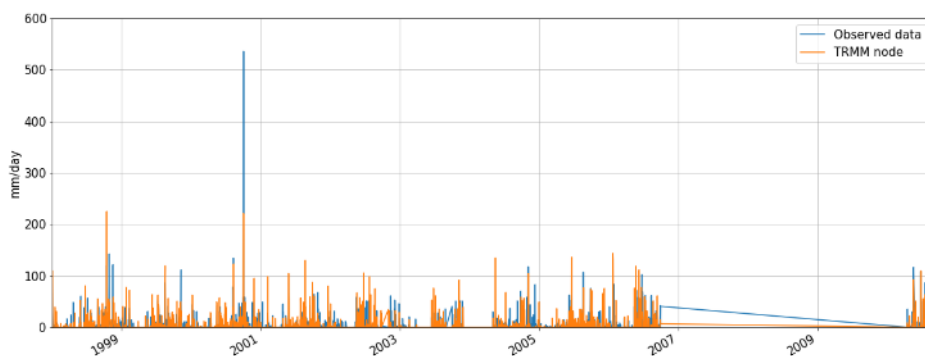


Figure 26. St. John's College gauge (Observed data) Vs TRMM node.

	Average daily rainfall (mm/day)	Variance	Skewness	Rainy days (Yearly)
<b>Observed data</b>	4.96	267	60605	130
<b>TRMM node</b>	5.11	243	21432	115

Table 6. Observed and TRMM statistics.

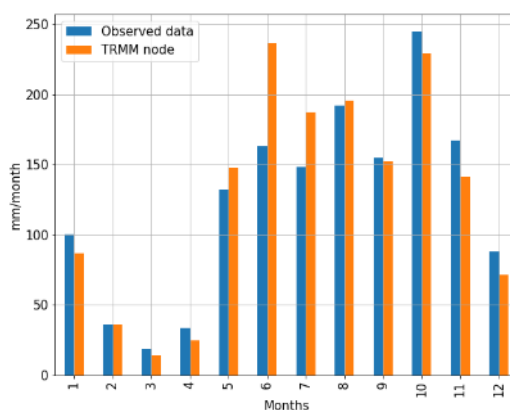


Figure 27. Observed vs TRMM seasonality.

The methodology thus uses the TRMM data to calculate the shape of the IDF curves at a sub-daily resolution. The  $I = \frac{a \cdot T^b}{t^c}$  function is chosen to adjust the shape of the IDF curves and to extrapolate the information to hourly time resolution. Where  $I$  corresponds to the values of rainfall intensity,  $t$  is the duration,  $T$  the return period and  $a$ ,  $b$  and  $c$  are constants that depend exclusively on the characteristics of the study area. Once the shape of the IDF curves are estimated, they are translated by matching with the 24-h return periods calculated for the St. John's College gauge. Figure 28 shows the final result of the methodology.



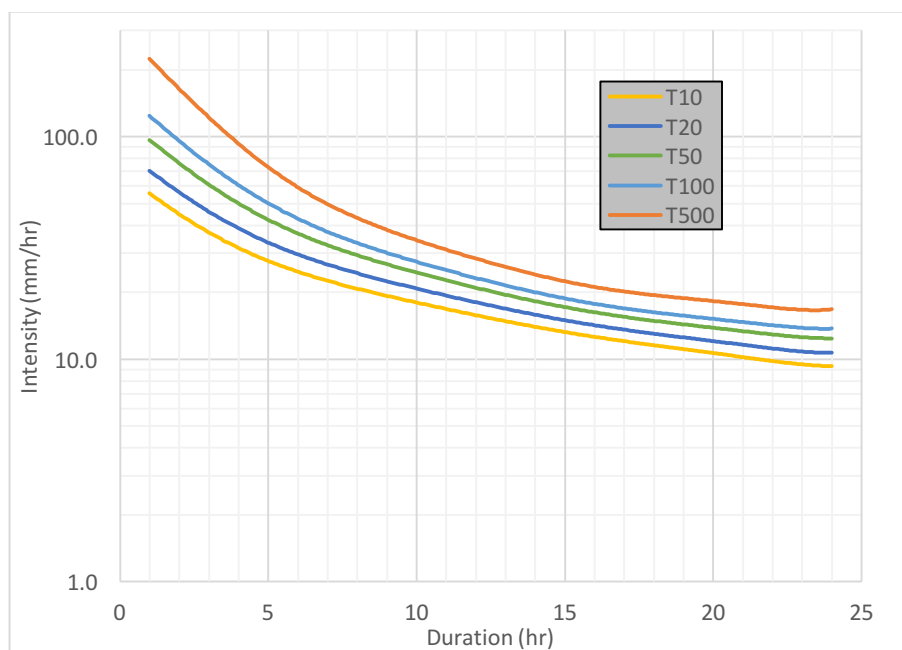


Figure 28. IDF curves in St. John's College meteorological station. Belize City.

In addition, these IDF curves have been compared with the I at Miami Beach station in Florida USA, ID: 08-5658, from the NOAA Atlas 14 volume 9 (Figure 29), with a similar hurricane regime and much longer weather records. The results differ in less than 10% for all the durations and return periods.

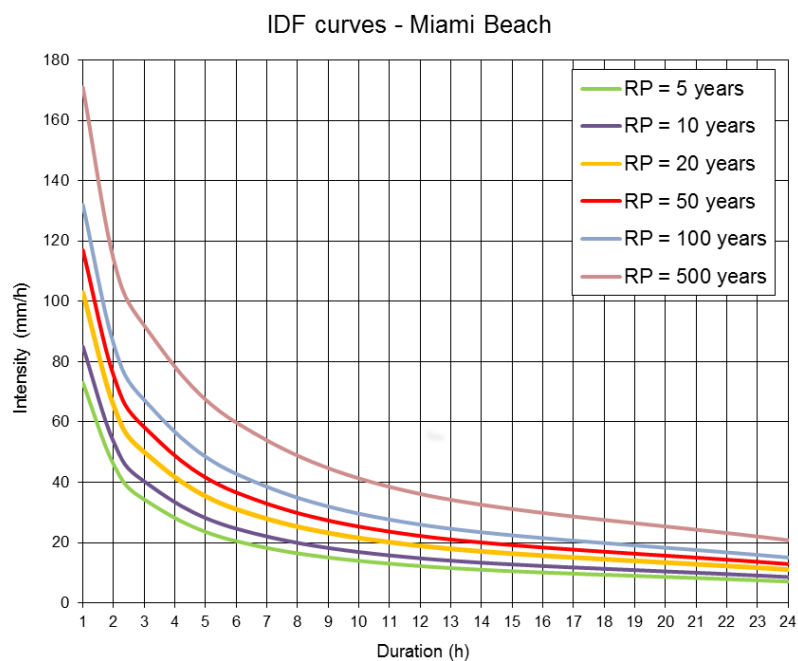


Figure 29. IDF curves in Miami Beach station ID: 08-5658. NOAA.

### 3.4. Climate change analysis and impact on the proposed system

This section presents future climate scenarios for Belize from two sources, namely “the Caribsav Climate Change Risk Atlas (CCCRA)” developed by Caribsav and “Belize’s Third National Communication to the United Nations framework Convention on Climate Change”. The latest is based on two of the three sources of climate scenarios presented in the final report, namely the UNDP Country Profiles and the ECHAM5/A1B and HadCM3Q11/A1B PRECIS-downscaled seasonal data on mean temperature and rainfall.

Climate change will be introduced by means of modifying the statistical distribution of the involved variables. The possible sea level rise scenarios will be also considered in order to capture return period changes due to this phenomenon. Additionally, for hurricanes and extreme short rainfalls, given the great importance they have in the present study, the impact of climate change has been analysed in more detail.

#### 3.4.1. Sea level Rise due to climate change in Belize

Sea-levels in this region are projected by climate models to rise by the following levels (2090-2100), relative to 1980-1999 sea-level (IPCC, 2007):

- 0.18 to 0.43m under SRES B1.
- 0.21 to 0.53m under SRES A1B.
- 0.23 to 0.56m under SRES A2.

However, recent reports have claimed these sea level changes to be rather conservative. Regional variability in sea level change relative to the global average is projected to be higher in the North Atlantic in the region near Belize by the end of this century (Meehl et al., 2007; Gregory et al., 2004). In fact, other recent semi-empirical models estimate that sea level will rise more than 1 meter by 2100, at least double the IPCC (2007) estimates and even more than previously thought, largely due to increased mass loss from the ice sheets mainly in the Arctic regions (Rahmstorf, 2007 and 2010; Horton et al., 2008; Vermeer and Rahmstorf, 2009; Grinsted et al., 2009). Low-lying coastal areas as the coastal zone of Belize would therefore be particularly at risk to these higher projections of sea level rise (Meehl et al., 2007; Jonathan et al., 2004).

In view of this conservativeness, the extreme values of the IPCC (2014) are suggested by Belize’s Third National Communication to the United Nations Framework Convention on Climate Change (2015) for estimating the impact of climate change on the coast.

Following that recommendation, the upper limit of the IPCC (2014) range of sea level rise for the different emission scenarios has been used in this study to estimate future sea levels (see Figure 30).

**Table 5-2** | Projections of global mean sea level rise in meters relative to 1986–2005 are based on ocean thermal expansion calculated from climate models, the contributions from glaciers, Greenland and Antarctica from surface mass balance calculations using climate model temperature projections, the range of the contribution from Greenland and Antarctica due to dynamical processes, and the terrestrial contribution to sea levels, estimated from available studies. For sea levels up to and including 2100, the central values and the 5–95% range are given whereas for projections from 2200 onwards, the range represents the model spread due to the small number of model projections available and the high scenario includes projections based on RCP6.0 and RCP8.5. Source: WGI AR5 Summary for Policymakers and Sections 12.4.1, 13.5.1, and 13.5.4.

Emission scenario	Representative Concentration Pathway (RCP)	2100 CO <sub>2</sub> concentration (ppm)	Mean sea level rise (m)		Emission scenario	Mean sea level rise (m)		
			2046–2065	2100		2200	2300	2500
Low	2.6	421	0.24 [0.17–0.32]	0.44 [0.28–0.61]	Low	0.35–0.72	0.41–0.85	0.50–1.02
Medium low	4.5	538	0.26 [0.19–0.33]	0.53 [0.36–0.71]	Medium	0.26–1.09	0.27–1.51	0.18–2.32
Medium high	6.0	670	0.25 [0.18–0.32]	0.55 [0.38–0.73]	High	0.58–2.03	0.92–3.59	1.51–6.63
High	8.5	936	0.29 [0.22–0.38]	0.74 [0.52–0.98]				

Figure 30. Projections of mean sea level rise in meters relative to 1986-2005. Source: WGI AR5 Summary for Policymakers.

### 3.4.2. Hurricanes and Tropical Storms

Several analyses of global (e.g. Webster et al., 2005) and more specifically North Atlantic (e.g. Holland and Webster, 2007; Kossin et al., 2007; Elsner et al., 2008) hurricanes have indicated increases in the observed record of tropical storms over the last 30 years. It is not yet certain to what degree this trend arises as part of a long-term climate change signal or shorter-term inter-decadal variability. The available longer term records are riddled with in homogeneities (inconsistencies in recording methods through time) - most significantly, the advent of satellite observations, before which storms were only recorded when making landfall or observed by ships (Kossin et al., 2007). Recently, a longer-term study of variations in hurricane frequency in the last 1,500 years based on proxy reconstructions from regional sedimentary evidence indicate recent levels of Atlantic hurricane activity are anomalously high relative to those of the last one- and -a -half millennia (Mann et al., 2009).

Climate models are still relatively primitive with respect to representing tropical storms and this restricts the ability to determine future changes in frequency or intensity. Changes in background conditions that are conducive to storm formation (boundary conditions) can be analysed (e.g. Tapiador, 2008), or applied to embedded high-resolution models which can credibly simulate tropical storms (e.g. Knutson and Tuleya, 2004; Emanuel et al., 2008). Regional Climate Models are able to simulate weak 'cyclone-like' storm systems that are broadly representative of a storm or hurricane system but are still considered coarse in scale with respect to modeling hurricanes.

The IPCC AR4 (Meehl et al., 2007b) concludes that models are broadly consistent in indicating increases in precipitation intensity associated with tropical storms (e.g. Knutson and Tuleya, 2004; Knutson et al., 2008; Chauvin et al., 2006; Hasegawa and Emori, 2005; Tsutsui, 2002). The higher resolution models that simulate storms more credibly are also broadly consistent in indicating increases in associated peak wind intensities and mean rainfall (Knutson and Tuleya, 2004; Oouchi et al., 2006).

With regards to the frequency of tropical storms in future climate, models are strongly divergent. Several recent studies (e.g. Vecchi and Sodon, 2007; Bengtssen et al., 2007; Emanuel et al., 2008, Knutson et al., 2008) have indicated that the frequency of storms may decrease due to decreases in vertical wind shear in a warmer climate. In several of these studies, intensity of hurricanes still increases despite decreases in frequency (Emanuel et al., 2008; Knutson et al., 2008). In a recent study of the PRECIS regional climate model simulations for Central America and the Caribbean, Bezanilla et al., (2009) found that the frequency of 'Tropical -Cyclone-like -Vortices' increases on the Pacific coast of Central America, but decreases on the Atlantic coast and in the Caribbean.

When interpreting the modeling experiments it should be remembered that the models remain relatively primitive with respect to the complex atmospheric processes that are involved in hurricane formation and development. Hurricanes are particularly sensitive to some of the elements of climate physics that these models are weakest at representing and are often only included by statistical parameterizations. Comparison studies have demonstrated that the choice of a parameterization scheme can exert a strong influence on the results of the study (e.g. Yoshimura et al., 2006). It should also be recognised that the El Niño Southern Oscillation (ENSO) is a strong and well established influence on Tropical Storm frequency in the North Atlantic and explains a large proportion of inter-annual variability in hurricane frequency (among other things). This means that the future frequency of hurricanes in the North Atlantic is likely to be strongly dependent on whether the climate state becomes more 'El-Niño-like', or more 'La-Niña-like', an issue upon which models are still strongly divided and suffer from significant deficiencies in simulating the fundamental features of ENSO variability (e.g. Collins et al., 2005).

In order to obtain another estimate of the effect of climate change on extreme precipitations in Belize, for different RCPs, the multi-model, downscaling results presented in Knutson et al. 2013 will be applied to the precipitation regime obtained from the stochastic cyclone model (Najako et al 2014) in this project. The following Figure, extracted from the aforementioned paper, summarizes the main results. For the late-twenty-first century, the precipitation increase amounts to 20% to 30% in the model hurricane's inner core, with a smaller increase (10%) for averaging radii of 200 km or larger.

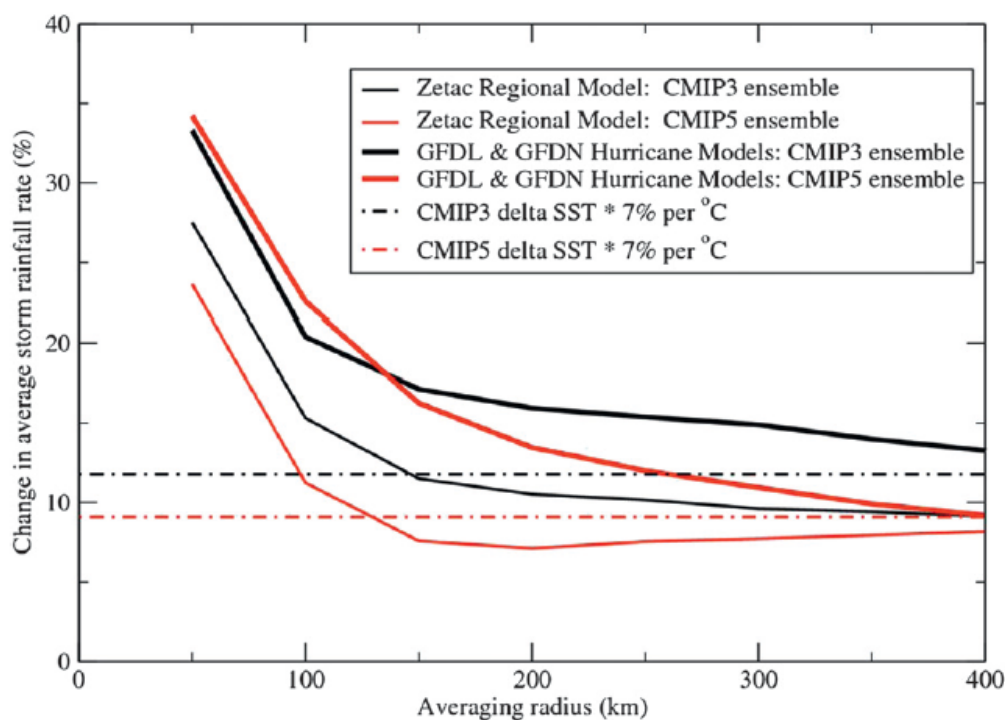


FIG. 11. Change (%) between the control and warm climate in average hurricane rainfall rate for various averaging radii about the storm center (km) for the CMIP3–A1B (black) and CMIP5–RCP4.5 (red) late-twenty-first-century multimodel ensemble climate changes based on the ZETAC regional model (thin solid lines) or the GFDL–GFDN hurricane model ensemble (thick solid lines). The dashed lines illustrate idealized water vapor content scaling, obtained by multiplying the average SST change in the region 10°–25°N, 20°–80°W by 7% °C<sup>-1</sup>.

### 3.4.3. IDF curves for Belize City under Climate Change

The objective of this section is to assess how extreme rainfall events would be affected in a changing climate. In this context a statistical downscaling method based on change factors is used (Akbari, H., Rakhshandehroo 2015 and Graham, L.P 2007) to establish the changes between the future and current return periods from the results of the Coupled Model Intercomparison Project Phase 5 (CMIP5). This changes known as Changes Factors (CF) might be applied to the present IDF curves in order to build the IDF curves from the future.

The methodology makes use of the Earth Exchange Global Daily Downscaled Projections (NEX-GDDP) database to estimate the CFs between the future and the current return periods. NEX-GDDP dataset is comprised of downscaled climate scenarios for the globe that are derived from the General Circulation Model (GCM) runs conducted under the CMIP5 and across two of the four greenhouse gas emissions scenarios known as Representative Concentration Pathways (RCPs). The CMIP5 GCM runs were developed in support of the Fifth Assessment Report of the Intergovernmental Panel on Climate Change (IPCC AR5). The NEX-GDDP dataset includes downscaled projections for RCP 4.5 and RCP 8.5 from the 21 models and scenarios for which daily scenarios were produced and distributed under CMIP5. Each of the climate projections includes daily maximum temperature, minimum temperature, and precipitation for the periods from 1950 through 2100. The spatial resolution of the dataset is 0.25 degrees (~25 km x 25 km).

The methodology starts by selecting the closet NEX-GDPP node to the St. John's College gauge, which is the reference gauge where the CFs will be applied. Figure 31 shows a comparative between the time series of the 21 models from the NEX-GDDP node situated at the location LON, LAT = [-88.375, 17.625] and the St. John's College gauge series (Observed data). As can be seen in Figure 32 the seasonality is well captured by the mean results of the 21 models; however if we compare the values of the return periods from the observed data with the models, the latter are reduced by almost 50% for most of the 21 models. That is why is recommended to apply statistical downscaling techniques instead of using directly the results of the GCMs.

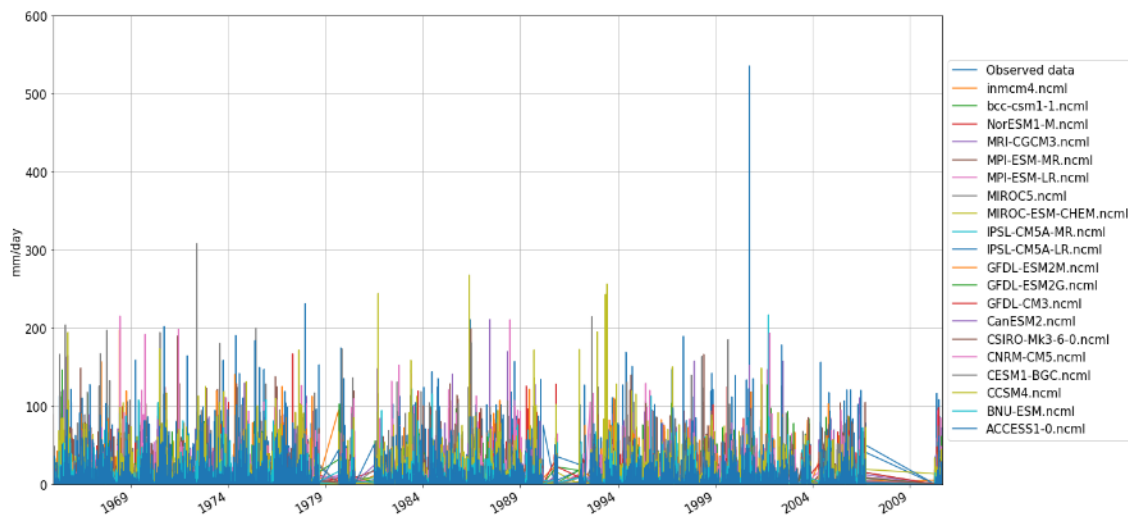


Figure 31. St. John's College gauge (Observed data) vs GCM series.

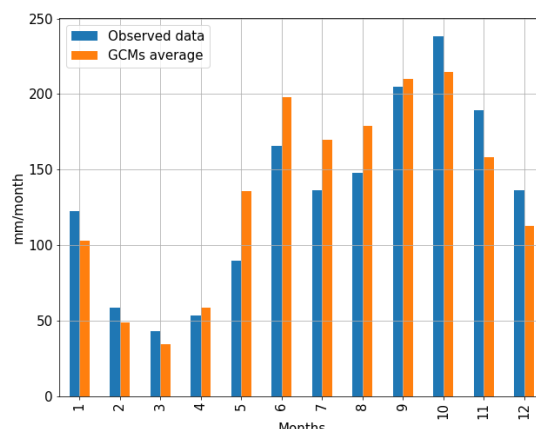


Figure 32. St. John's College gauge (Observed data) vs GCM average seasonality.

In order to estimate the changes in the extreme precipitation regimes, the CFs or “Delta Factors (DF)” are calculated by dividing the ensemble return periods values ( $T = 5, 10, 20, 50, 100$  and  $500$  years) in 2016-2035, 2046-2065 and 2081-2100 by the ensemble return periods values for the reference scenario (1986-2005), both from the NEX-GDDP dataset (Giraldo et al. 2011). The Reliability Ensemble Averaging (REA) method (Tebaldi, C. and Knutti, R., 2007) is applied in order to calculate the return period ensemble for the 21 models by assessing the ability of the GCMs to reproduce the present-day climate while at the same time evaluating the convergence of different GCMs to a given forcing scenario. This procedure is repeated for the RCP 4.5 and RCP 8.5 scenarios. The REA factors were computed using a metric to evaluate the agreement between observed and simulated return periods from each of the 21 models and a convergence criterion based on the future results of the models.

	Periods	T (Years)					
		5	10	20	50	100	500
RCP 4.5	2016-2035	0.997	0.993	0.988	0.980	0.972	0.932
	2046-2065	1.022	0.999	0.971	0.923	0.877	0.715
	2081-2100	1.040	1.026	1.008	0.976	0.943	0.821
RCP 8.5	2016-2035	1.160	1.138	1.108	1.055	1.003	0.822
	2046-2065	1.145	1.162	1.184	1.221	1.258	1.374
	2081-2100	1.066	1.043	1.013	0.965	0.921	0.774

Table 7. Return periods (5, 10, 20, 50, 100 and 500 years) change in 2016-2035, 2046-2065 and 2081-2100 respect to 1986-2005 for the RCP 4.5 and RCP 8.5 scenarios.

As can be seen in Table 7 the CFs are practically negligible for the scenario RCP4.5, excepting those values associated with the return periods of 100 and 500 years where a reduction of more than 20% is expected in some cases. In the case of the RCP 8.5 scenario, an increase in the extreme precipitation regimes between 10 and 20% is expected for the return periods of 5, 10, 20, 50 and 100 years. The results associated with the 500-year return period do not seem consistent since depending on the study period the results increase or decrease sharply. This might be due to the uncertainty associated with the frequency of occurrence of Tropical Cyclones, which cause the most intense events and are poorly captured by the GCMs (Timmermans, B. et al. 2017).



## 4. HYDRAULIC MODELING AND DESIGN FEATURES

### 4.1. Objectives and modelling approach

In this section, the dimensioning of the different elements of the proposed system including the pumping scheme and associated works is presented. The design level for the proposed risk-reduction scheme has been 10-years of return period, and the numerical modeling has been carried out with the EPA Storm Water Management Model (SWMM). This model is the standard tool for the design of urban drainage systems around the world but due to its 1-D nature, is not suitable for calculating the flood extent, once that the design capacity of the different elements has been surpassed. For this reason, the system will also be analyzed using a 2-D model, which will provide flood risk results for events beyond the prescribed design level, including all combinations of sea level and rainfall. This flood risk analysis of the situation after the implementation of the risk reduction scheme will be compared to the situation without works, in order to quantify the benefits (economic and human) of the proposed solution. The 2D analysis has been carried out through the application of the InfoWorks ICM model (Integrated Catchment Modeling) developed by Innovyze in order to obtain the spatial flood maps of 10, 20, 50, 100 and 500 years of return period. Model descriptions are included in Annex III and IV, respectively.

### 4.2. Dimensioning of the pumping scheme and associated works

The present section is focused on dimensioning the pumping scheme and associated works of the proposed system, using the SWMM model of the Environmental Protection Agency of the US as previously mentioned.

#### 4.2.1. Model implementation

##### 4.2.1.1 Geometry model set up

The first step for the implementation of the model is the definition of the different physical elements that make up the conceptual scheme of the system and then introduce all the elements characteristics within each of the corresponding modules. To do this, three different models have been developed: (i) the current situation with the current state of the canals, (ii) an intermediate situation results of the debris removal and (iii) the final proposed geometry of both canals resulting of the bottom regularization. These canals constitute the most of the drainage capacity of the system, being the most important elements in these models, together with the pumping station, as explained in section 2.3).

Based on the field campaigns carried out by Chemtec (see Figure 9 and Table 1 in section 2.3), it has been possible to set up the current geometry of these canals in the three models (Table 2 and Figure 11). It is important to mention that these canals are in a very poor state of conservation, and in the most of the measured sections, the high sedimentation of the canals reduce more than the 50% of their hydraulic capacity.

In addition to the canal geometries, the sub-basins division and the main mesh of the inner streets has been included in the SWMM model based on the map of the canal drainage areas within the study area obtained by Chemtec (Figure 33). The store capacity of street area is actually an important factor in the system, which must be taken into account. In fact, this storage capacity is greater than the main canals actual maximum capacity (Collet and East), almost triplicate it, so it is very important to consider the storing effect of the streets in the numerical model. In order to include the mesh of streets in the model, an average street of 6 m wide and 0.2 meters depth has been used. A 0.2 m depth is considered as an admissible flood during the design events in both cases. Due to the lack of information about the slope of the urban area, a flat urban mesh located at +0.85m above the mean sea water level has been considered with a slight slope in the connection sections with both canals.

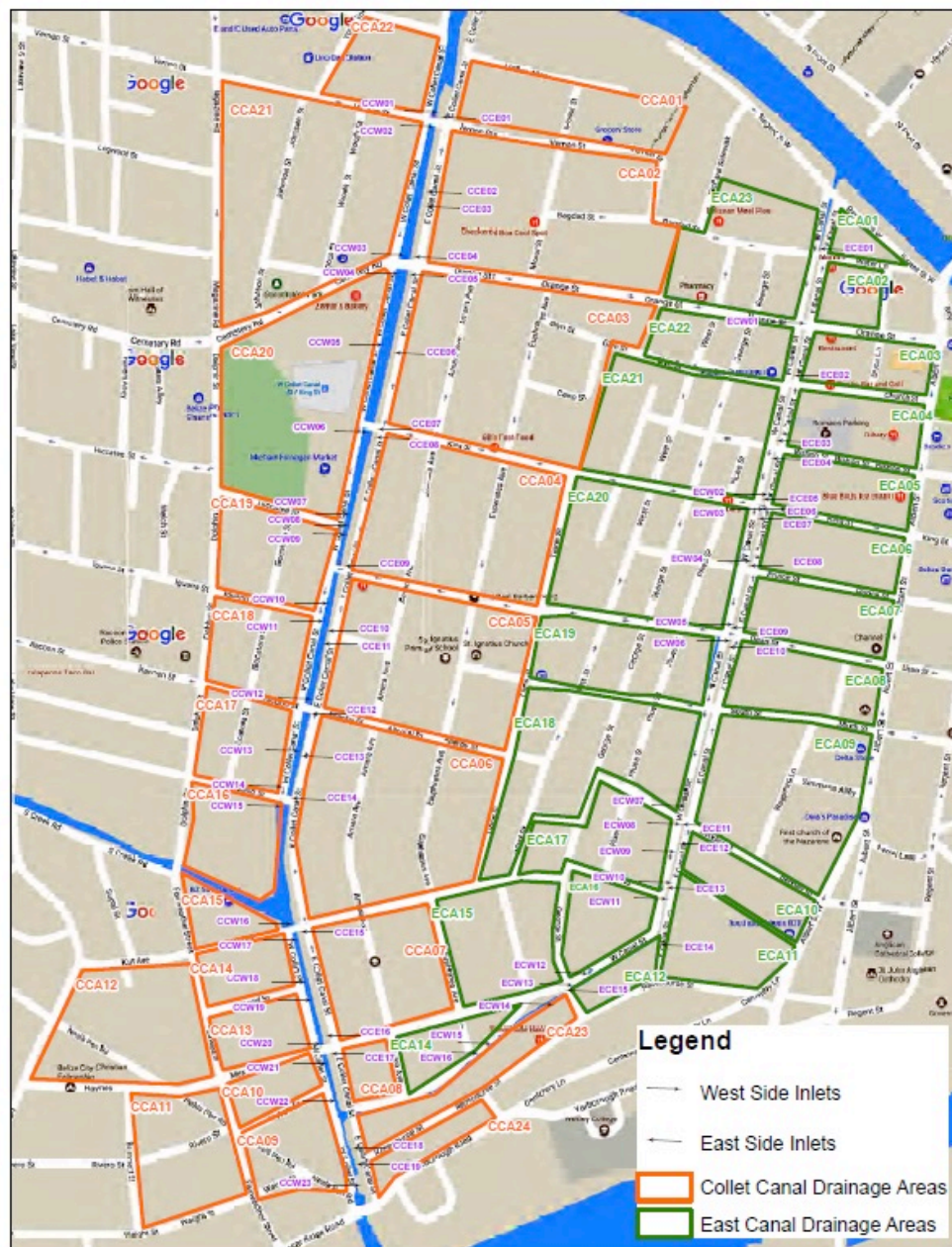


Figure 33. Canal drainage areas within the study area.

As a result, the conceptual scheme is composed of 82 subcatchments, 106 junction nodes, 139 conduct links and the pump scheme for each model.

In the following figures, the conceptual scheme and the longitudinal profiles of the three different stages of the proposed solution obtained as a result of the geometry implementation in the SWMM model are presented:

1. Current geometry: Invert level reference to the local mean sea level (LMSL), current depth and current debris height.
2. Debris removal: Invert level and maximum depth after the cleaning of the canals.
3. Final geometry: Final invert level (reference to the local mean sea level) and dredge height from the clean canal bottom.

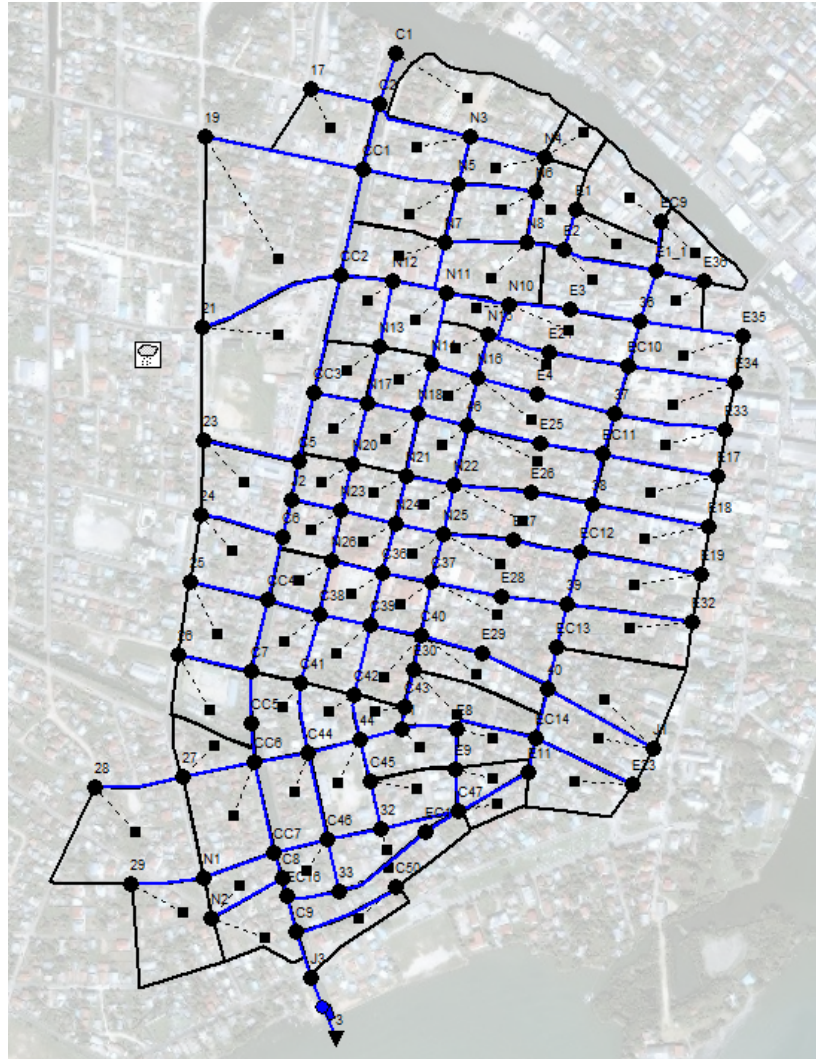


Figure 34. Conceptual scheme of the system implemented in the SWMM model.



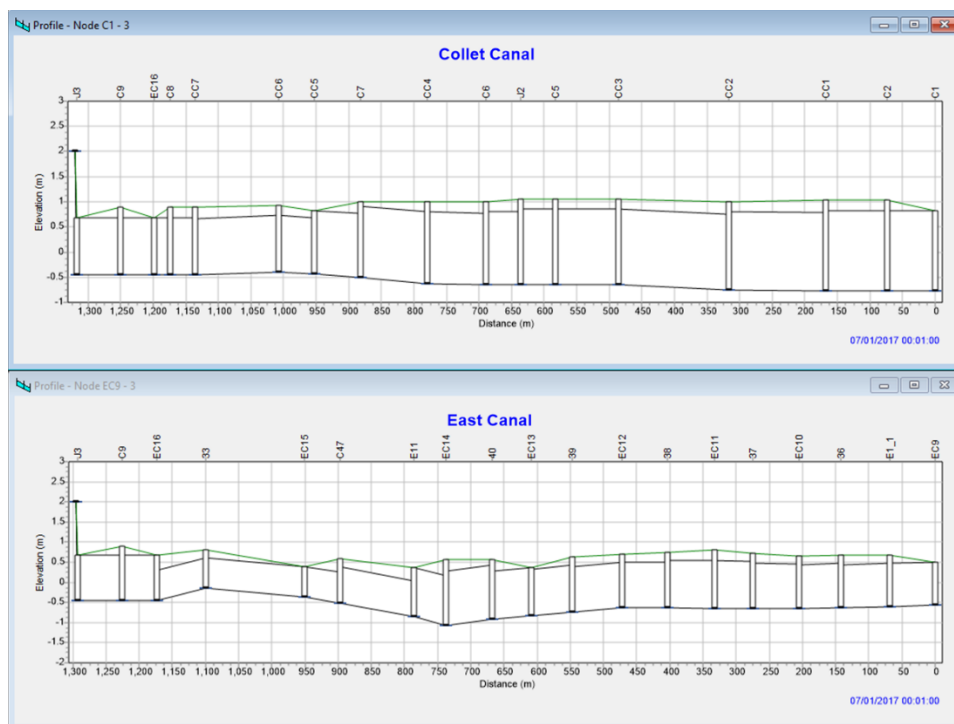


Figure 35. Canal longitudinal profile for the current situation implemented in the SWMM model.

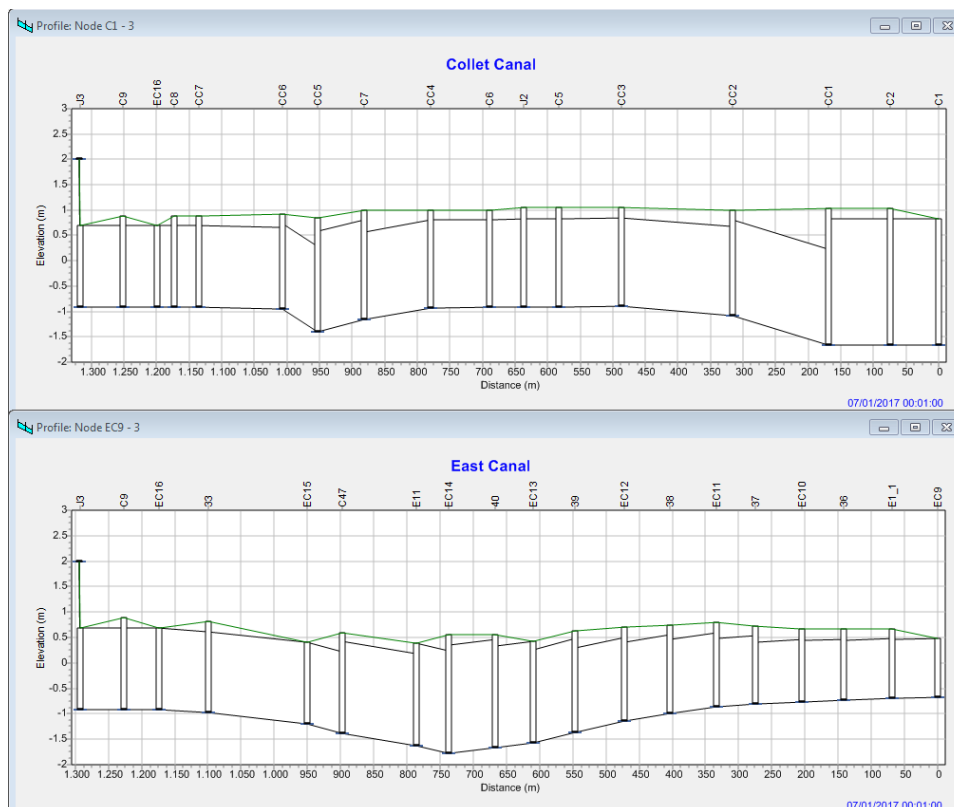


Figure 36. Canal longitudinal profile after debris removal implemented in the SWMM model.

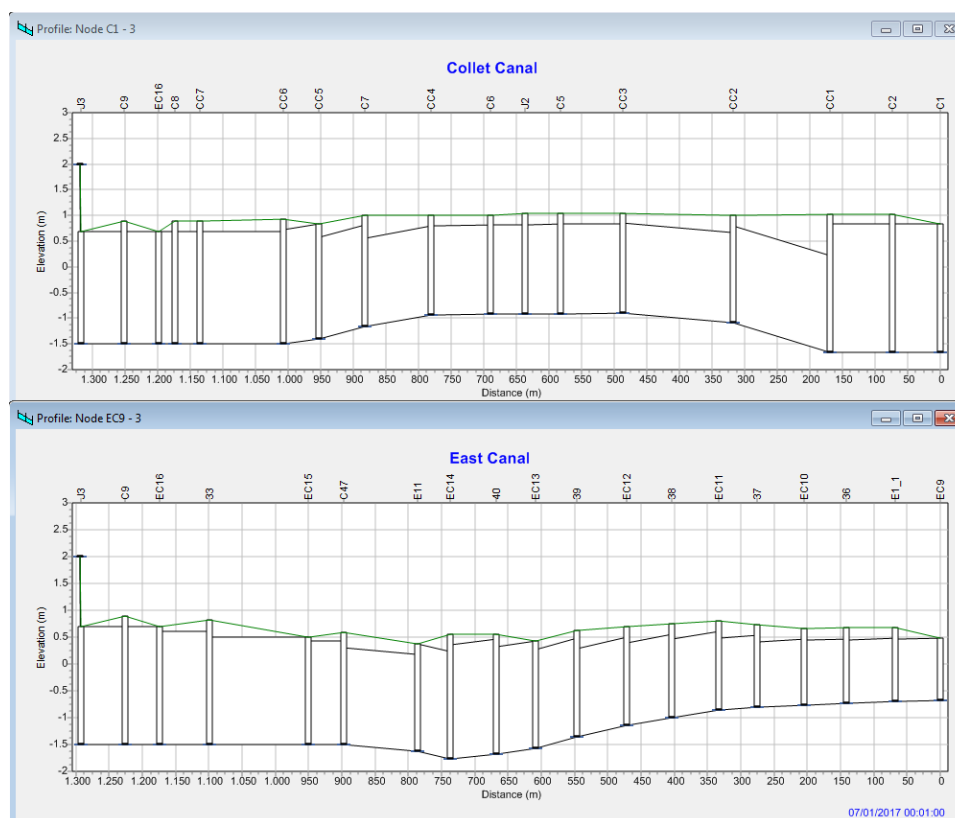


Figure 37. Canal longitudinal profile after bottom regularization implemented in the SWMM model.

#### 4.2.1.2 Design variables and model parameters

In this section, the values used for the different design variables and model parameters are presented. As mentioned in the section 3.3.1 the principal design variables considered for the sizing of the pumping system are duration of the design rainfall spell, amount of precipitation in the total duration of the design spell, distribution of the rainfall and antecedent moisture content.

##### **Design storms: Duration, amount and temporal distribution of rainfall**

For the implementation of the precipitations in the SWMM model, the IDF curves defined in section 3.3.2 have been used, concretely the curve of 10-years return period (selected as the design period) Rainfall events of different durations and shapes have been generated in order to verify the effectiveness of the system in different design situations. Besides, the design events do not correspond to a complete rainfall event that can last several days, but to a spell in the middle of a longer storm.

Specifically, three different design hyetographs (uniform intensity, gamma distribution and alternating block method) for 10-years return period and different durations (1, 1.5, 2 and 3 hours) have been obtained. The choice of these three models is based on the range of standard deviations that they represent within a particular event. The standard deviation of a hyetograph is, after its mean value (related to the total amount of rainfall), the most relevant shape attribute.

The reason to simulate different durations of the hyetographs is to find out the time of concentration of the system, since it is not a system where it is possible to calculate the time of concentration based on the sub-basins



characteristics (length and slope). In this case, the concentration time depends on the velocity induced by the capacity of the pump and the hydraulic slope generated (in opposition to the terrain slope, which governs in classic formulas as Kirpich or California). Table 8 shows the precipitation values (mm) for the selected return periods and event durations.

Return period	Duration			
	1 h	1.5 h	2 h	3 h
<b>T10</b>	80	92	100	115

Table 8. Precipitation (mm) for 10-years return period and different hyetograph durations.

As an example of these results, the design hyetographs corresponding to an event of 10-years return period and a duration of 1 hour, with the three different shapes are presented in Figure 38.

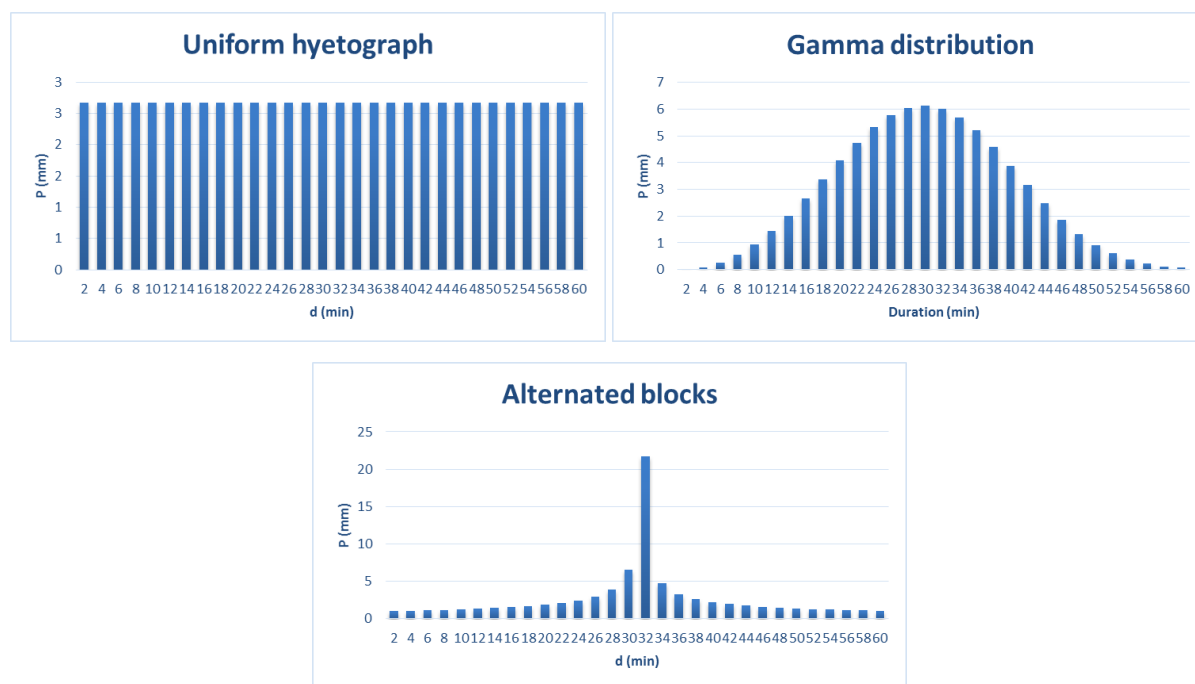


Figure 38. 1-hour design hyetographs for 10 years of return period.

#### **Soil antecedent moisture content: Curve number**

The curve number of normal antecedent conditions (CNII) has been obtained for the area of study that is an urban area giving a value of 90.

Since the design events do not corresponds to a complete rainfall event, but to a gust in the middle of a great storm, it has been considered that the soil at the beginning of the simulation is saturated and there is no runoff threshold. Therefore curve numbers of wet antecedent condition (CNIII) have been used.

The relationships between the curve number for these normal antecedent conditions (CNII) and the saturated soil (CNIII) is presented below and gives a curve number or 95:

$$CNIII = \frac{23 \cdot CNII}{10 + 0.13 \cdot CNII}$$

#### **Canals and streets roughness: Manning coefficient**

Three different roughness values for the canals and the streets, expressed as Manning coefficients, have been used: 0.01, 0.015 and 0.02. These values are based on empirical observations for lined and unlined canals (Ven Te Chow, 1959).

#### **4.2.2. Study cases**

In order to obtain the resilience of the proposed works to different possible situations, a sensitivity analysis of the main variables that govern the inundation in the project area has performed. It has been decided to establish a reference case of study, to be evaluated in the current, intermediate and design situation (Current, Debris removal and Case 0-bottom regularization), which represents the three stages of the proposed solution. From these three base cases, several variants have been tested, based on the perturbation of the expected values of the following design parameters:

- Rain duration.
- Rain distribution.
- Manning coefficient (n).
- Curve number (NC).

Table 9 summarize all the study cases carried out to accomplish the system sensitivity.

Case	P(mm)	Shape	Duration(h)	n	NC
Current	100	cte	2	0.015	95
Debris removal	100	cte	2	0.015	95
0	100	cte	2	0.015	95
1	100	alter	2	0.015	95
2	100	distrib	2	0.015	95
3	80	cte	1	0.015	95
4	92	cte	1.5	0.015	95
5	115	cte	3	0.015	95
6	100	cte	2	0.01	95
7	100	cte	2	0.02	95
8	100	cte	2	0.015	90
9	100	cte	2	0.015	100
10	92	cte	1.5	0.01	95
11	92	cte	1.5	0.02	95
12	92	cte	1.5	0.015	90
13	92	cte	1.5	0.015	100
14	92	alter	1.5	0.015	95
15	92	distrib	1.5	0.015	95

Table 9. Simulation summary table for 10-years return period.

First, the current, debris removal and Case 0-bottom regularization (base cases) have been tested under the same conditions, presented in Table 9. For each case, the necessary pump capacity has been obtained admitting a flooding of less than 100 m<sup>3</sup> (design criteria). The results are shown in the following section where also a sensitivity analysis of the design parameters has been carried out. It has been proved that the necessary capacity of the pump is very sensitive to the storage capacity of the canals.

### 4.2.3. Results

Table 10 and Figure 39 shows the simulation parameter values and the obtained results (pump capacity, flooding volume and number of nodes flooded) for the three base cases: Current, Debris removal and Case 0 – bottom regularization.

Case	Parameter values					Results		
	P(mm)	Shape	Duration(h)	n	NC	Q <sub>pump</sub> (m <sup>3</sup> /s)	Nº nodes flooding	Flooding (m <sup>3</sup> )
Current	100	cte	2	0.015	95	9	4	2816
Debris removal	100	cte	2	0.015	95	6.5	1	71
0	100	cte	2	0.015	95	5.6	2	51

Table 10. Simulation summary results for the three base cases for 10-years return period.

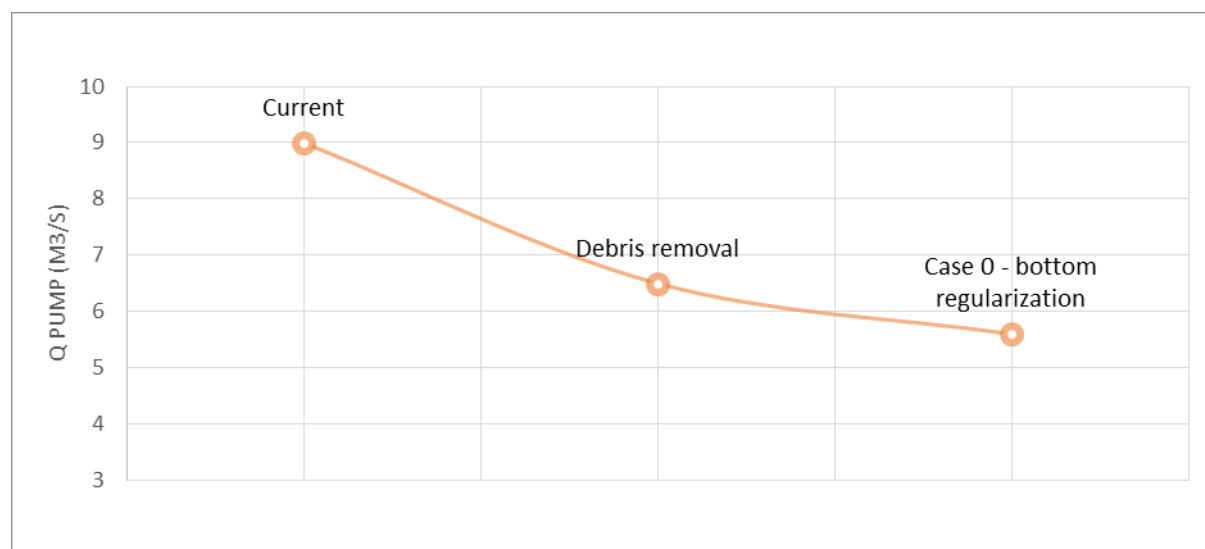


Figure 39. Curve of the three base cases (Current, Debris removal and Case 0- bottom regularization) vs pump capacity.

As seen previously the pump capacity needed to fulfil the design criteria (flooding volume of less than 100 m<sup>3</sup>) as might be expected decreases as the storage capacity of the canals increases reaching a value of 5.6 m<sup>3</sup>/s for the Case 0 with the final geometry. It is also observed that the design criteria is not reached the current case obtaining a flood volume of 2816 m<sup>3</sup> with a pump capacity of 9 m<sup>3</sup>/s which is not acceptable.

Below the results for the three base cases are presented in more detail in order to analyze their differences.

#### 4.2.3.1 Current case

This base case represents a future situation, which includes a system isolation of the seawater level and setting up a pumping station in order to discharge the water outside the system, but without interventions in the Collet and East Canal (existing geometry).

For this case, the design criteria has not been reached obtaining a flood volume of 2816 m<sup>3</sup> with a pump capacity of 9 m<sup>3</sup>/s. In this way, it has been proven that if the system is isolating for the sea and Haulover Creek without intervening in the canals is completely impossible to meet the design criteria being necessary to increase the volume of storage on both canals.

The following figures presents the drainage system map and canals longitudinal profiles at the time step of maximum flooding for a pumping capacity of 9 m<sup>3</sup>/s. Is it observed that the East canal is the critical element of the system, which is overflowed by four nodes, and it is found, along almost all its length, at the limit of its capacity. This is not the case of Collet Canal, which is under the 75% of its capacity. Moreover, the capacity of the streets during the event do not reach the 0.2 m of allowed flooding.

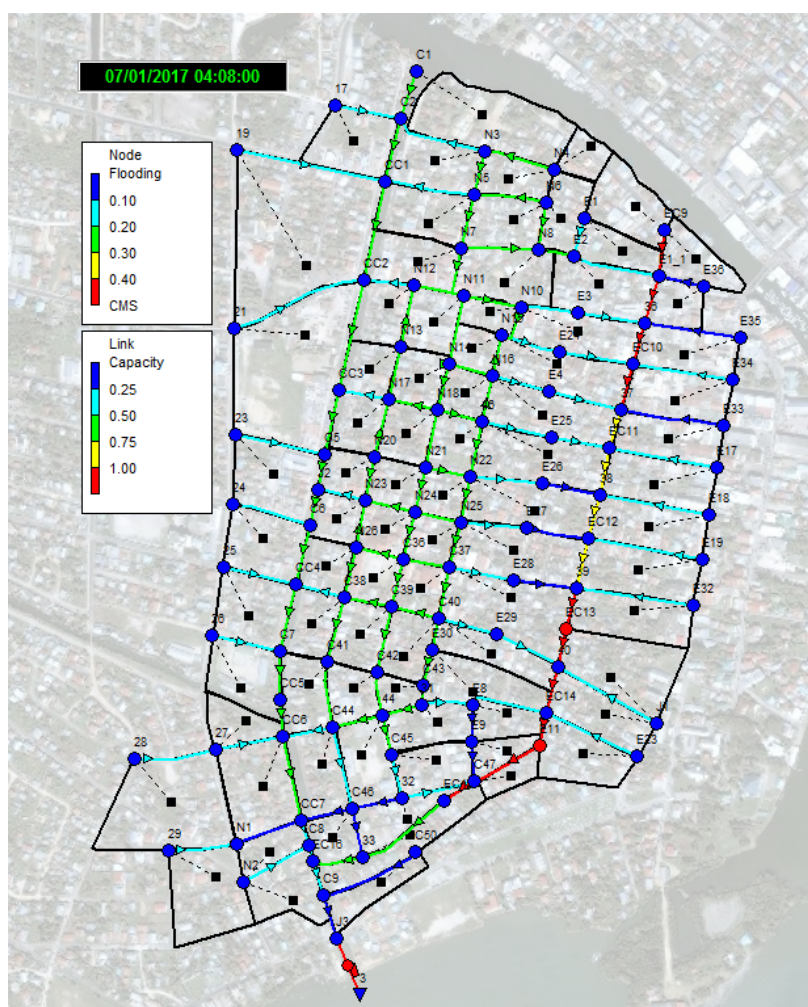


Figure 40. Drainage system map in Current (base case) with a representation of links capacity and nodes flooding.

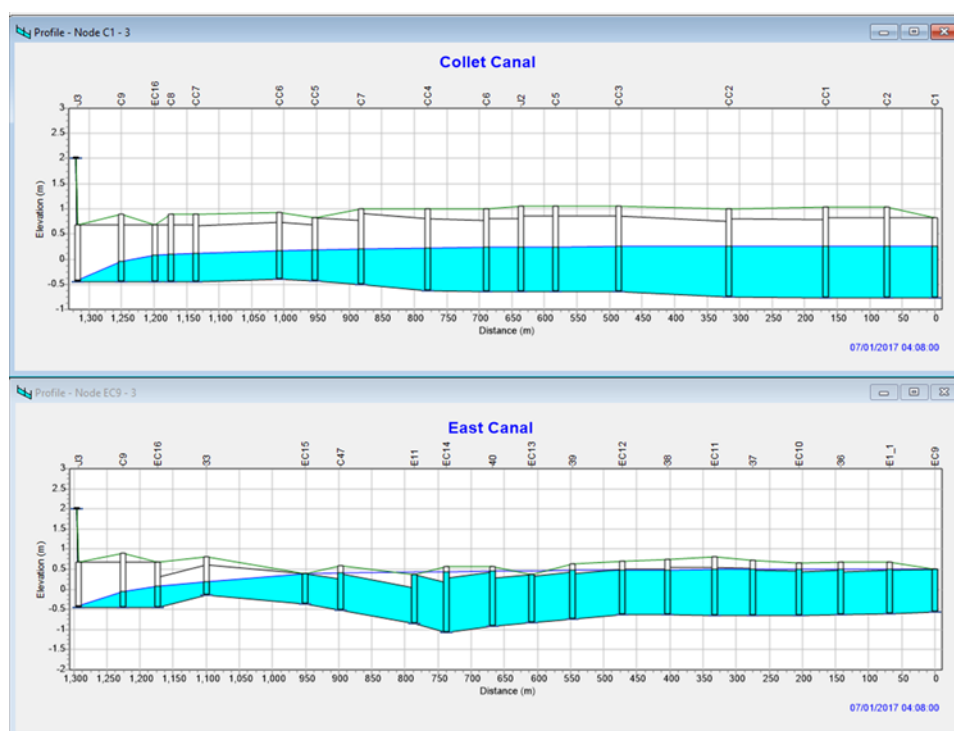


Figure 41. Canals longitudinal profiles in Current (base case) at the time of maximum flooding.

Table 11 shows the characteristics of the four nodes flooding during the simulation period. It can be observed that the fort nodes are EC13 and EC11 with 1302 m<sup>3</sup> and 1083 m<sup>3</sup> respectively.

Node	Hours Flooded	Maximum Rate (m <sup>3</sup> /s)	Hour of Maximum Flooding	Total Flood Volume (m <sup>3</sup> )
EC9	0.65	0.168	4:05	81
EC13	2.09	1.655	3:55	1302
EC15	1.29	0.307	4:16	350
EC11	2.01	1.215	4:01	1083
<b>TOTAL</b>				<b>2816</b>

Table 11. Nodes Flooding. Current (base case).

#### 4.2.3.2 Debris removal case

This base case represents the next step in the system design: a future situation, which includes the sediment removal in the Collet and East Canal in addition to the actions raised in the previous section (system isolation and pumping scheme). This step has been modeled in order to see if it is enough with just dredging the canals.

The following figures presents the drainage system map and canals longitudinal profiles at the time step of maximum flooding for a pumping capacity of 6.5 m<sup>3</sup>/s (necessary capacity of the pump obtained to meet the design criteria) with a flood volume of 71 m<sup>3</sup>.



East canal is again the critical element of the system, although in this case, the overflow volume has been greatly reduced compared with the current base case and only one node is overflow for a briefly time during the simulation (E11). Collet Canal, is under the 100% of its capacity in this case and the capacity of the streets during the event do not reach the 0.2 m of allowed flooding (under 75% of its capacity).

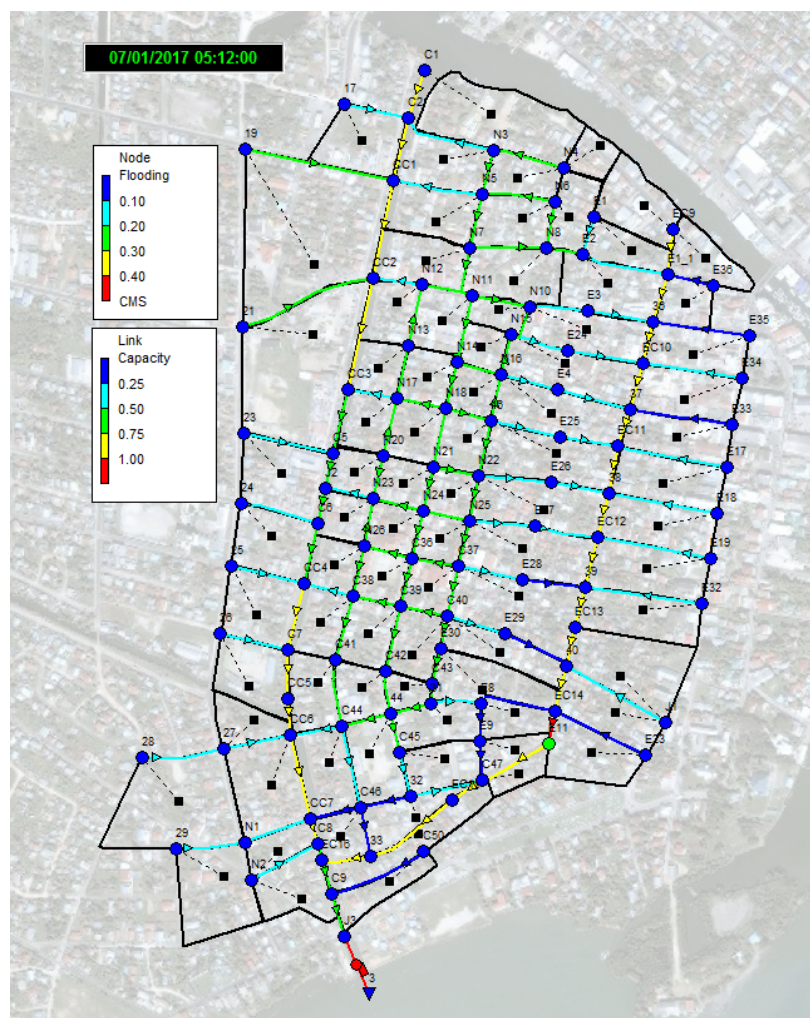


Figure 42. Drainage system map in Debris Removal (base case) with a representation of links capacity and nodes flooding.

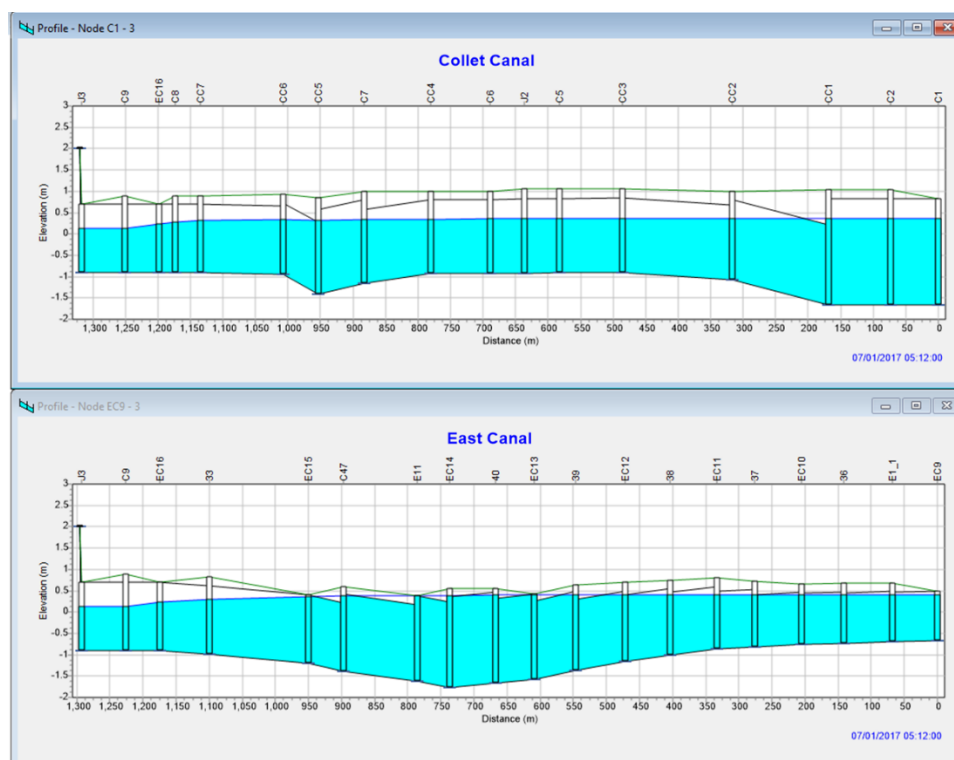


Figure 43. Canals longitudinal profiles in the Debris Removal (base case) at the time of maximum flooding.

Table 12 shows the characteristics of the unique node that overflows during the simulation period.

Node	Hours Flooded	Maximum Rate (m <sup>3</sup> /s)	Hour of Maximum Flooding	Total Flood Volume (m <sup>3</sup> )
<b>E11</b>	0.22	0.309	5:12	71

Table 12. Nodes Flooding. Debris Removal (base case).

#### 4.2.3.3 Case 0 – bottom regularization

This base case represents the final geometry: a future situation, which includes the bottom regularization in the Collet and East Canal, in order to connect their entire profile to the discharge point avoiding low points and stagnant water, in addition to the actions raised in the previous section (sediment removal in both canals, system isolation and pumping scheme).

Figure 44 and Figure 45 shows, the drainage system map and canals longitudinal profiles at the time step of maximum flooding for a pumping capacity of  $5.6 \text{ m}^3/\text{s}$  (necessary capacity of the pump obtained to meet the design criteria) with a flood volume of  $51 \text{ m}^3$ .

The results are similar to the debris removal case but with a minor pumping capacity: East canal is again the critical element of the system, with a similar flooding to the debris removal case and again Collet Canal is under the 100% of its capacity and the capacity of the streets during the event do not reach the 0.2 m of allowed flooding (under 75% of its capacity). As a result, *case 0 - bottom regularization* has been chosen as the design case.

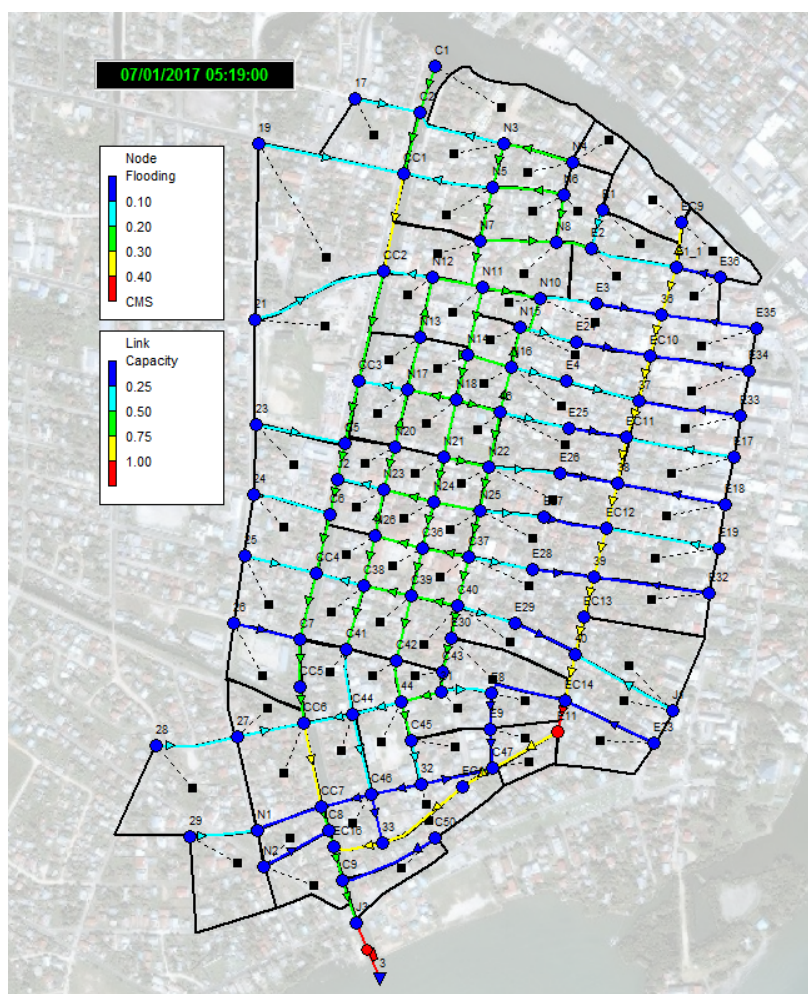


Figure 44. Drainage system map in Case 0- bottom regularization (base case) with a representation of links capacity and nodes flooding.

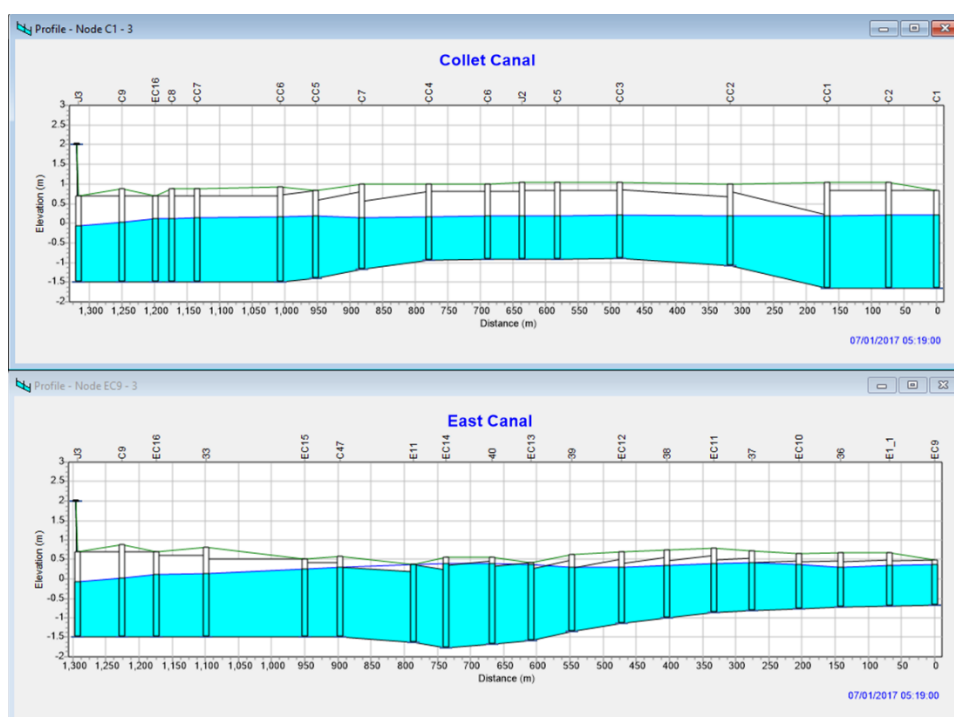


Figure 45. Canals longitudinal profiles in Case 0- bottom regularization (base case) at the time of maximum flooding.

Table 13 shows the characteristics of the two nodes that overflows during the simulation period being E11 the critical node with 50 m<sup>3</sup>.

Node	Hours Flooded	Maximum Rate (m <sup>3</sup> /s)	Hour of Maximum Flooding	Total Flood Volume (m <sup>3</sup> )
EC13	0.01	0.364	5:13	1
E11	0.07	0.915	5:11	50
<b>TOTAL</b>				<b>51</b>

Table 13. Nodes Flooding. Case 0- bottom regularization (base case).

For a more detailed information, the model results of each element of Case 0 (selected as the design case) are included in Annex V.

#### 4.2.3.4 Sensitivity analysis

The results of the runs carried out to determine the performance of the proposed system under other design conditions are now presented. The performance indicator (Y-axis) is the pumping capacity necessary to meet the design criteria, while in the X-axis are considered the following variables:

- Rain distribution.
- Rain duration.
- Manning coefficient (n).

- Curve number (NC).

Table 14 summarize all the study cases carried out. Annex VI includes a results sheet of each case.

Case	Parameter values					Results		
	P(mm)	Shape	Duration(h)	n	NC	Q <sub>pump</sub> (m <sup>3</sup> /s)	Nº nodes flooding	Flooding (m <sup>3</sup> )
0	100	cte	2	0.015	95	5.6	2	51
1	100	alter	2	0.015	95	7.7	3	70
2	100	distrib	2	0.015	95	8.4	3	61
3	80	cte	1	0.015	95	4.8	1	5
4	92	cte	1.5	0.015	95	5.6	3	97
5	115	cte	3	0.015	95	5.3	1	47
6	100	cte	2	0.01	95	5.7	0	0
7	100	cte	2	0.02	95	5.8	2	41
8	100	cte	2	0.015	90	4.7	1	44
9	100	cte	2	0.015	100	6.5	0	0
10	92	cte	1.5	0.01	95	5.7	1	3
11	92	cte	1.5	0.02	95	5.8	2	32
12	92	cte	1.5	0.015	90	4.5	1	39
13	92	cte	1.5	0.015	100	6.7	1	76
14	92	alter	1.5	0.015	95	7	3	74
15	92	distrib	1.5	0.015	95	7.7	3	78

Table 14. Simulation summary results for 10-years return period.

### Rain distribution

Three different distributions have been used: case 0, case 1 and case 2. The results obtained from the simulations shows that the worst distribution is the one in case 2, being the one that needs a greater pumping capacity to fulfill the design criteria. (see Figure 46).

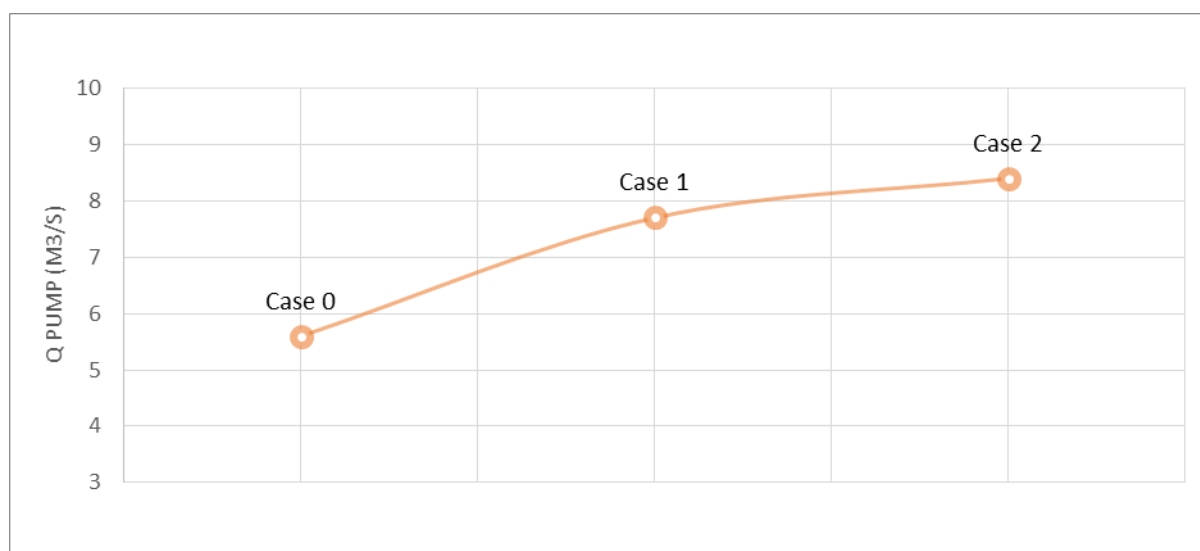


Figure 46. Curve of rain distribution vs pump capacity.



### **Rain duration**

To obtain the critical duration of the storm event 4 different rain event durations have been simulated. Duration events of 1hour, 1.5 hours, 2 hours and 3 hours have been simulated in case 3, case 4, case 0 and case 5, respectively. Figure 47 shows the resulting curve of the four simulations where it is possible to observe that the critical durations are located between 1.5 and 2 hours. The range of pump capacity obtained is significative with a minimum value of 4.8 m<sup>3</sup>/s with a 1-hour event, and a maximum of 5.6 m<sup>3</sup>/s in the 1.5-hours and 2-hours event.

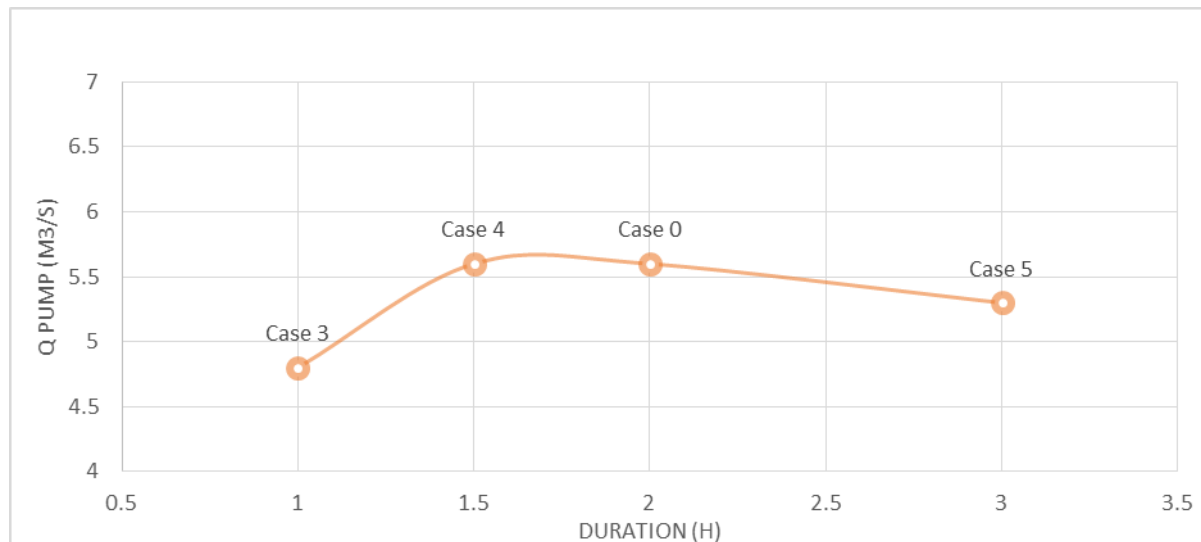


Figure 47. Curve of rain duration vs pump capacity.

### **Manning coefficient**

Three different simulations have been carried out with different manning coefficients: 0.01, 0.015 and 0.02 corresponding with case 6, case 0 and case 7. The results are showed in Figure 48, obtaining the best results in the case 0 with a manning coefficient of 0.015. It is important to mention that the pump capacities differences obtained in the simulations are negligible, (0.2 m3/s difference between the three cases).

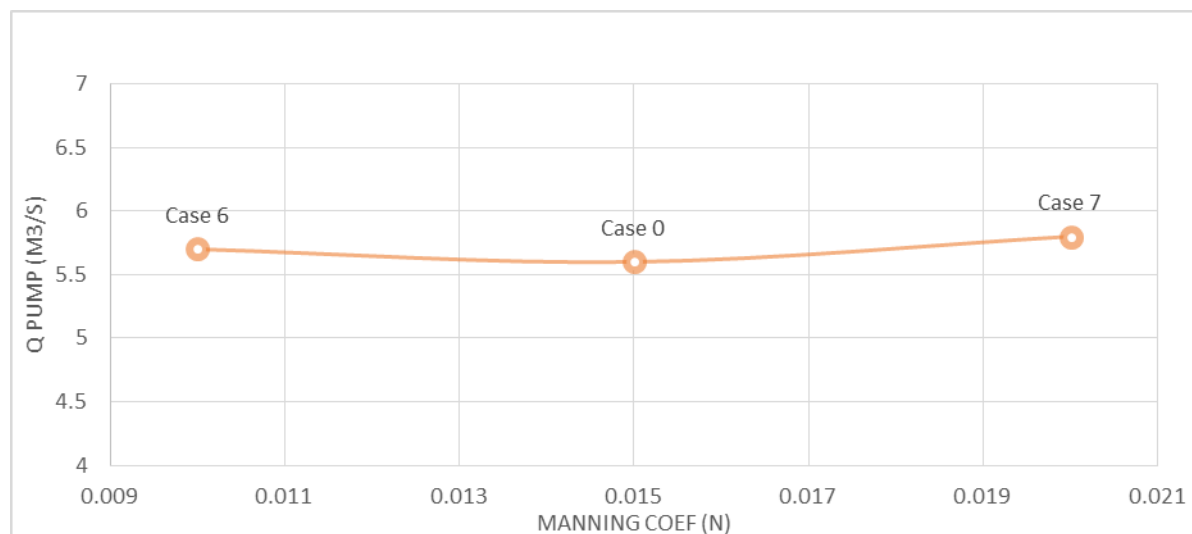


Figure 48. Curve of manning coefficient vs pump capacity.

### Curve number

Due to the location of the pilot area and the situation of the ground water level, a standard curve number of 95 has been selected for set-up the base case (case 0). The variations of this parameter have been carried out in case 8 and case 9 using a curve number of 90 and 100 respectively. The results obtained show a linear dependency of the pump capacity with the different curve numbers (Figure 49). In addition, the range of the capacity of the pump scheme obtained is significant, raising a value of  $6.5 \text{ m}^3/\text{s}$  with a curve number of 100 and a minimum value of  $4.7 \text{ m}^3/\text{s}$  with a curve number of 90.

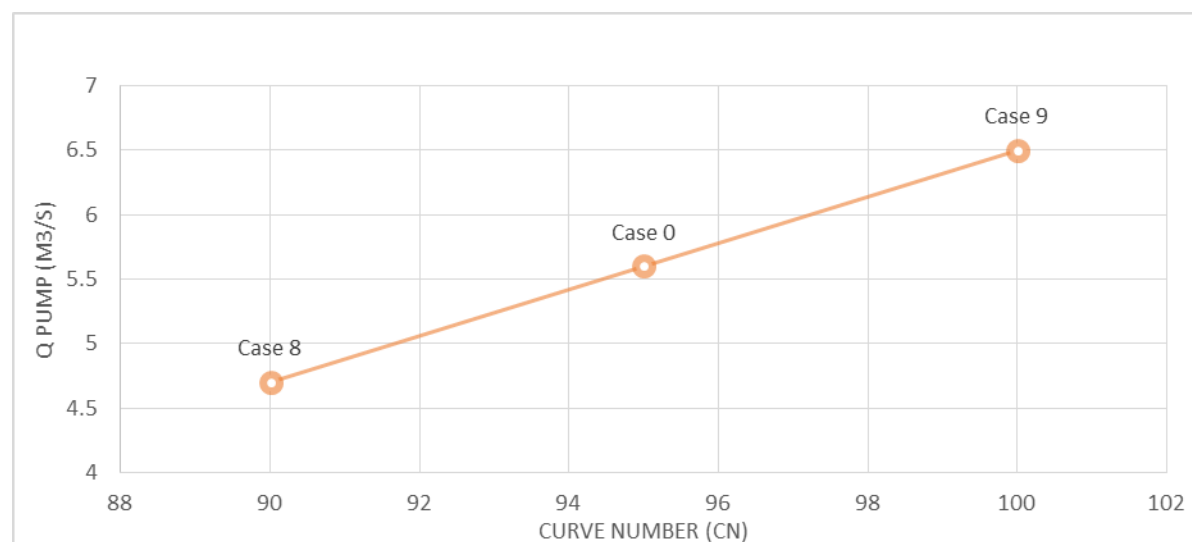


Figure 49. Curve of curve number parameter vs pump capacity.

Finally, Figure 50 shows the comparison between the cases with different parameters for the durations of 1.5 and 2 hours event in order to establish which one of the duration is more restrictive. As a result, it can be seen that the obtained results are very similar and the 2 hours event has been selected as the design event.

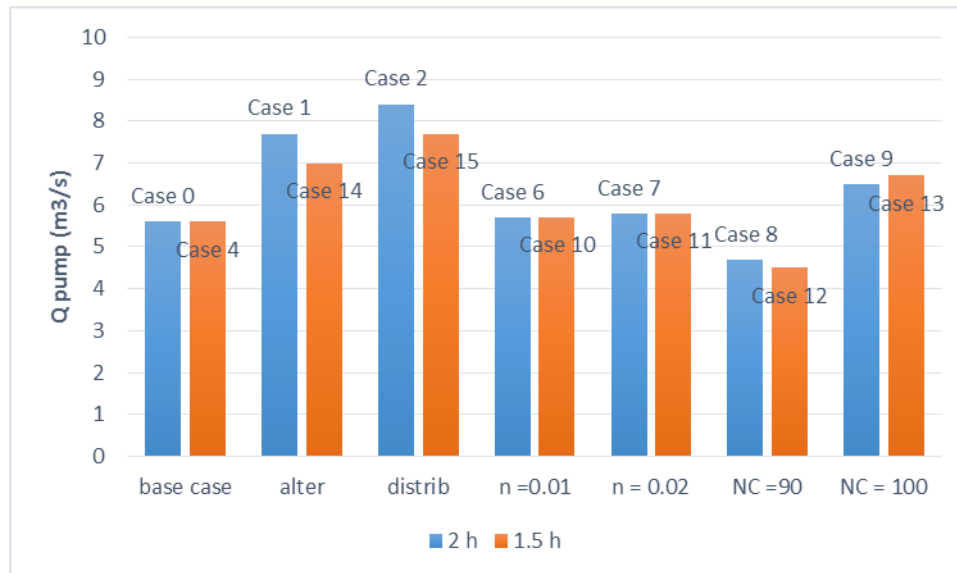


Figure 50. Pump capacity necessary for 1.5-hours and 2-hours event with different parameter values.

### 4.3. Estimation of the probabilistic hazard: 2D hydraulic modeling

In this section, the system will be analyzed using a 2-D model, which will provide flood risk results for events beyond the prescribed design level, including all combinations of sea level and rainfall. This flood risk analysis of the situation after the implementation of the risk reduction scheme will be compared to the situation without works, in order to quantify the benefits (economic and human) of the proposed solution.

#### 4.3.1. Digital elevation Model

For the present study the DEM developed for the Baseline Studies for the ESCI in Belize City. The DTM have is based in a DTM with a spatial resolution of 2m x 2m developed by Telespazio formed from stereopairs has been used to characterise the topography of the study area (Figure 52). The product has a  $\pm 1.5$  m accuracy in the horizontal plane and it is in the UTM WGS84 coordinate system. For the DEM generation aerotriangulation techniques have been applied and field support points have been used to improve the model accuracy. Furthermore, breaklines have been added in order to force the model to adapt to terrain abrupt changes and anomalies.

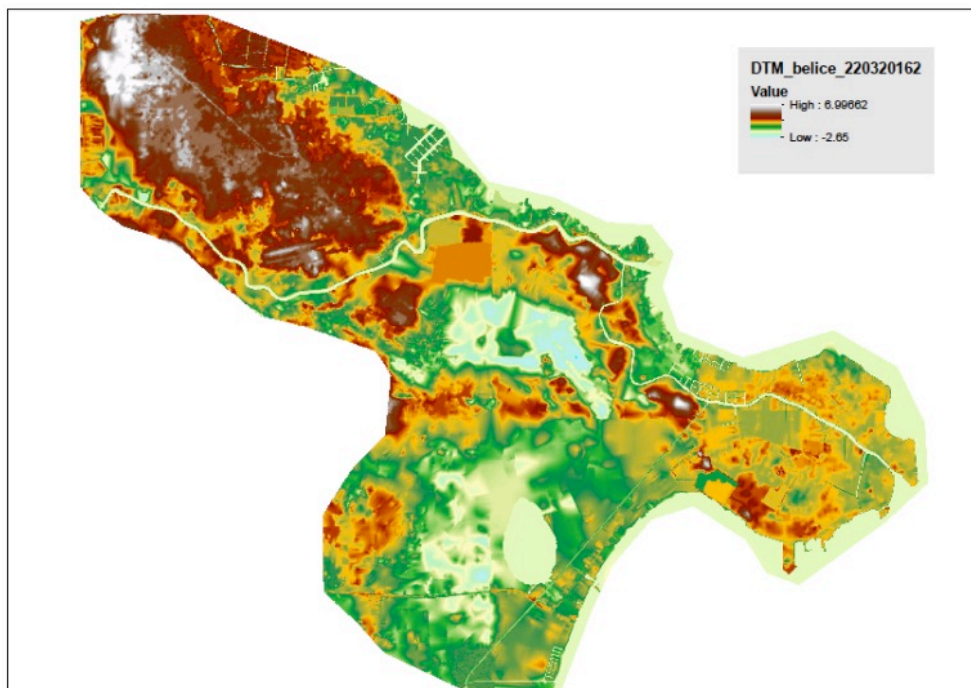


Figure 51. DEM with a spatial resolution of 2x2 m developed by Telespazio.

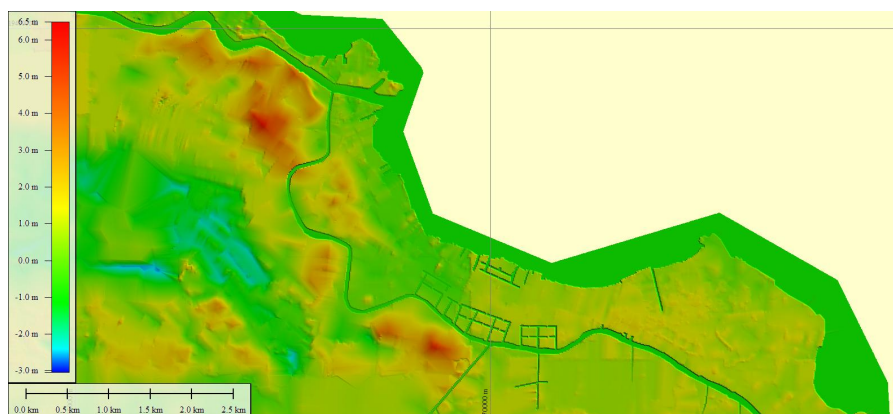


Figure 52. Telespazio DEM zoom.

A series of modifications have been made on the DEM in order to improve the provided depths of the main rivers, canals and lagoons. Moreover, it has been combined with bathymetric information based on Landsat-8 data at 15 m resolution (Satellite Derived Bathymetry, SDB) developed by EOMAP and the country charts digital information outside the coastline (Figure 53).

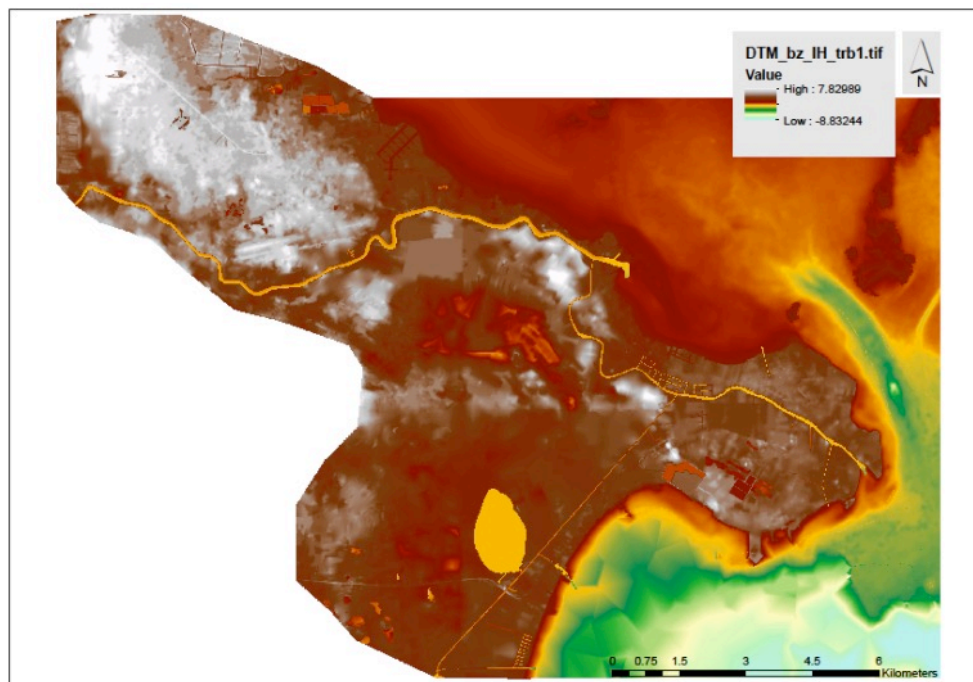


Figure 53. Combined DEM (terrain and bathymetry) with a spatial resolution of 2x2 m.

### Bathymetry

Global and local bathymetry is needed to correctly simulate waves and storm surges at Belize City. In this report a merged bathymetry has been developed combining information from general and detailed bathymetric data (see Figure 56).

The information used includes:

- A general bathymetry extracted from GEBCO database. GEBCO is a continuous terrain model for ocean and land with a spatial resolution of 30 arc-seconds. It was generated by combining quality-controlled ship depth soundings with interpolation between sounding points guided by satellite-derived gravity data. Further information can be found at the web page ([www.gebco.net](http://www.gebco.net)).
- A meso-scale bathymetry obtained from the British Admiralty Nautical Chart 522: Belize City and Approaches (scale 1:40.000), (Figure 54).
- A detailed local bathymetry generated from Landsat-8 data. This bathymetric data was collected at 15m resolution and was processed by the Modular and Inversion System (MIP) by EOMAP GmbH & Co.KG. The data collected provides detailed bathymetric information for an area 1 mile into the sea from both the Haulover Creek and the Belize River mouth, (Figure 55).



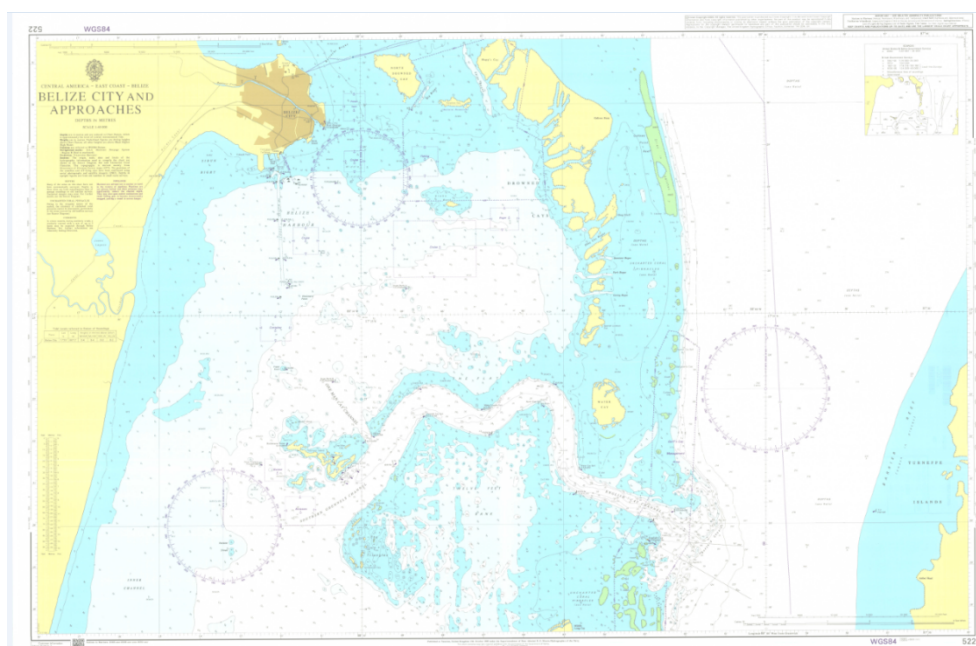


Figure 54. British Admiralty Nautical Chart 522: Belize City and Approaches (scale 1:40.000).

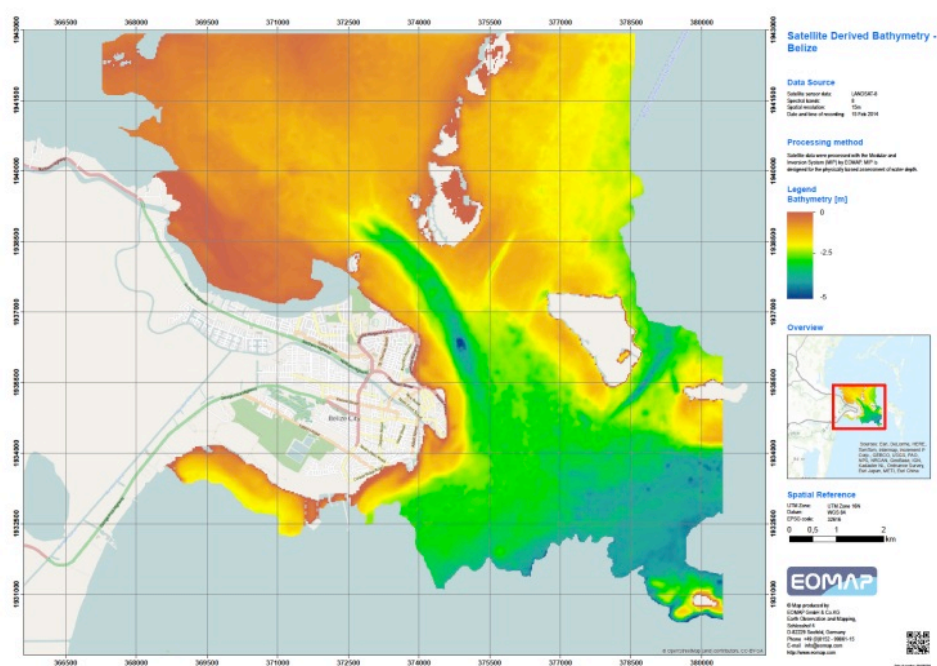


Figure 55. Satellite-Derived Bathymetry Data at 15m resolution.

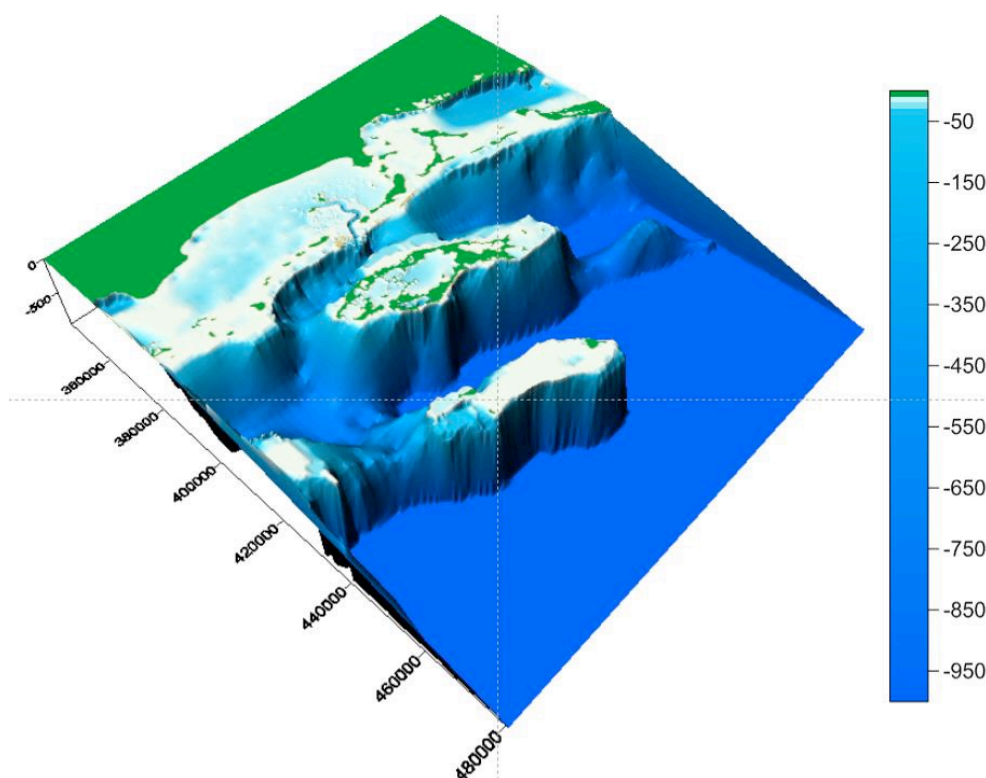


Figure 56. Bathymetry of the study area.

#### **4.3.2. Model description**

InfoWorks ICM (Integrated Catchment Modeling) is an integrated modeling platform to incorporate both urban and river catchments. With full integration of 1D and 2D hydrodynamic simulation techniques, both the above- and below-ground elements of catchments can be modeled to represent all flow paths. InfoWorks ICM enables the hydraulics and hydrology of natural and man-made environments to be incorporated into a single model.

InfoWorks ICM has the ability to create a single model that contains the salient features existing in an environment with a single, unified hydrology. Manholes, pipes, and inlets can be combined with natural and man-made channels to create a model in which the catchment and the floodplain are one. The additional ability to model objects such as bridges, sluices, weirs and pumps allows the creation of accurate models.

#### **4.3.3. Flood hazard maps.**

Rainfall events corresponding to return periods of 2, 5, 10, 20, 50, 100 and 500 years have been simulated numerically, in order to obtain the depth and velocity fields corresponding to each case. These hazard results will be combined with the vulnerability of the exposed elements and population, in order to estimate both economic damages and human losses. Figure 57 and 58 show the effect of the proposed works in the 10-year event, which is practically mitigated, except for a few low-points that require land filling. However, for the 100-year events, although the hazard is widely reduced, there will still be flooded sectors (Figures 59 and 60).



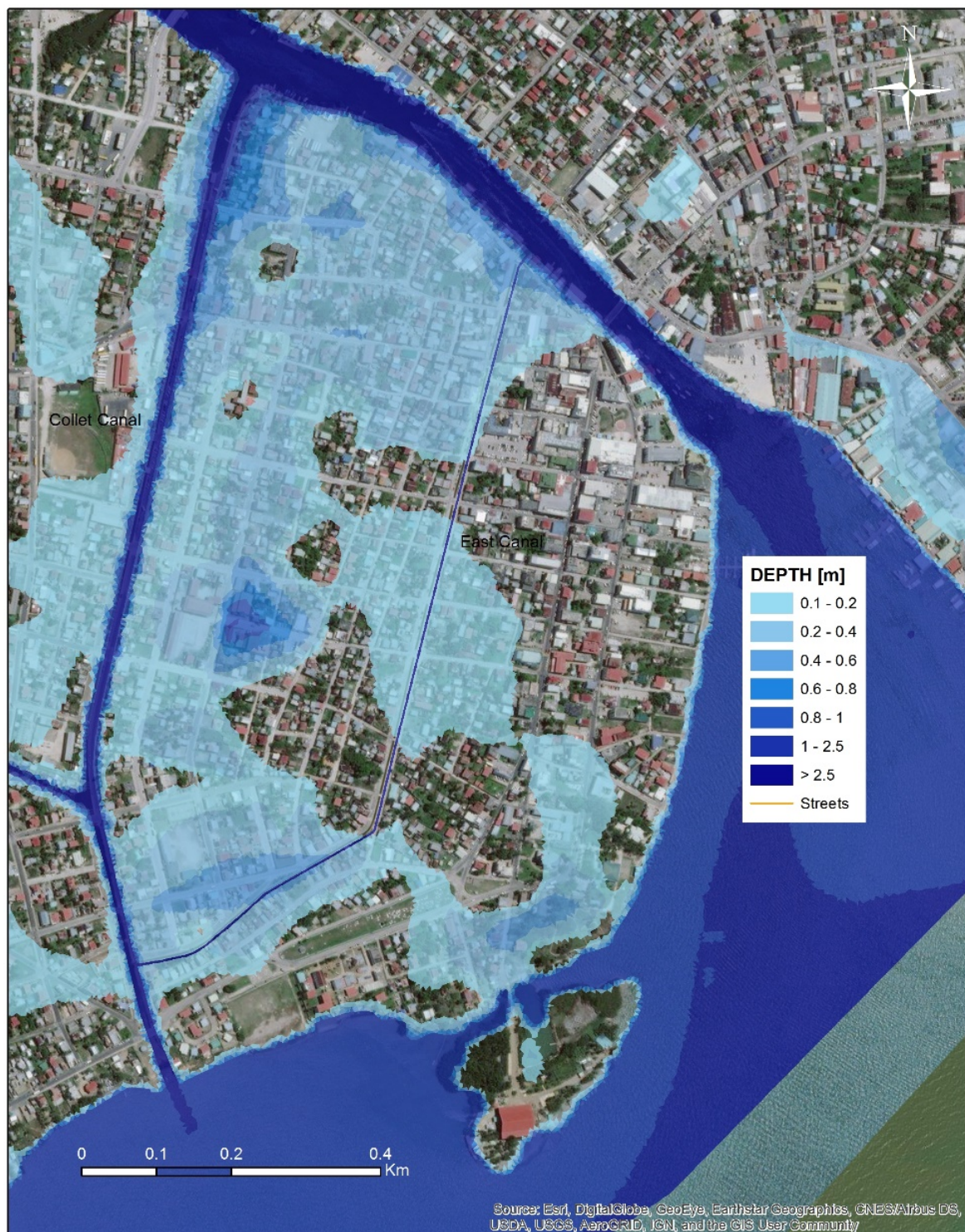


Figure 57. Flood hazard map for the 10-year event, in the present situation, before the implementation of the proposed works.



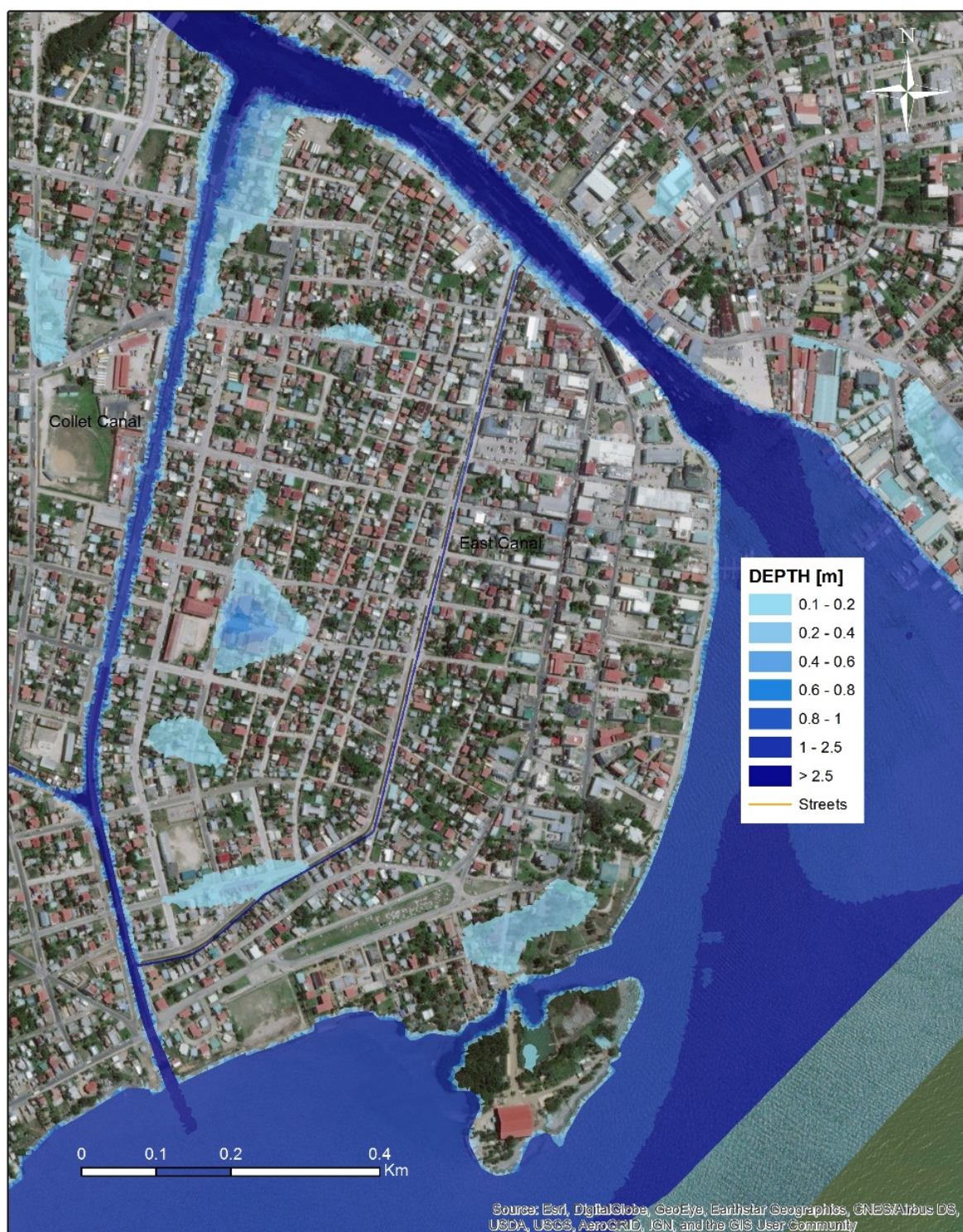


Figure 58. Flood hazard map for the 10-year event, after the implementation of the proposed works.



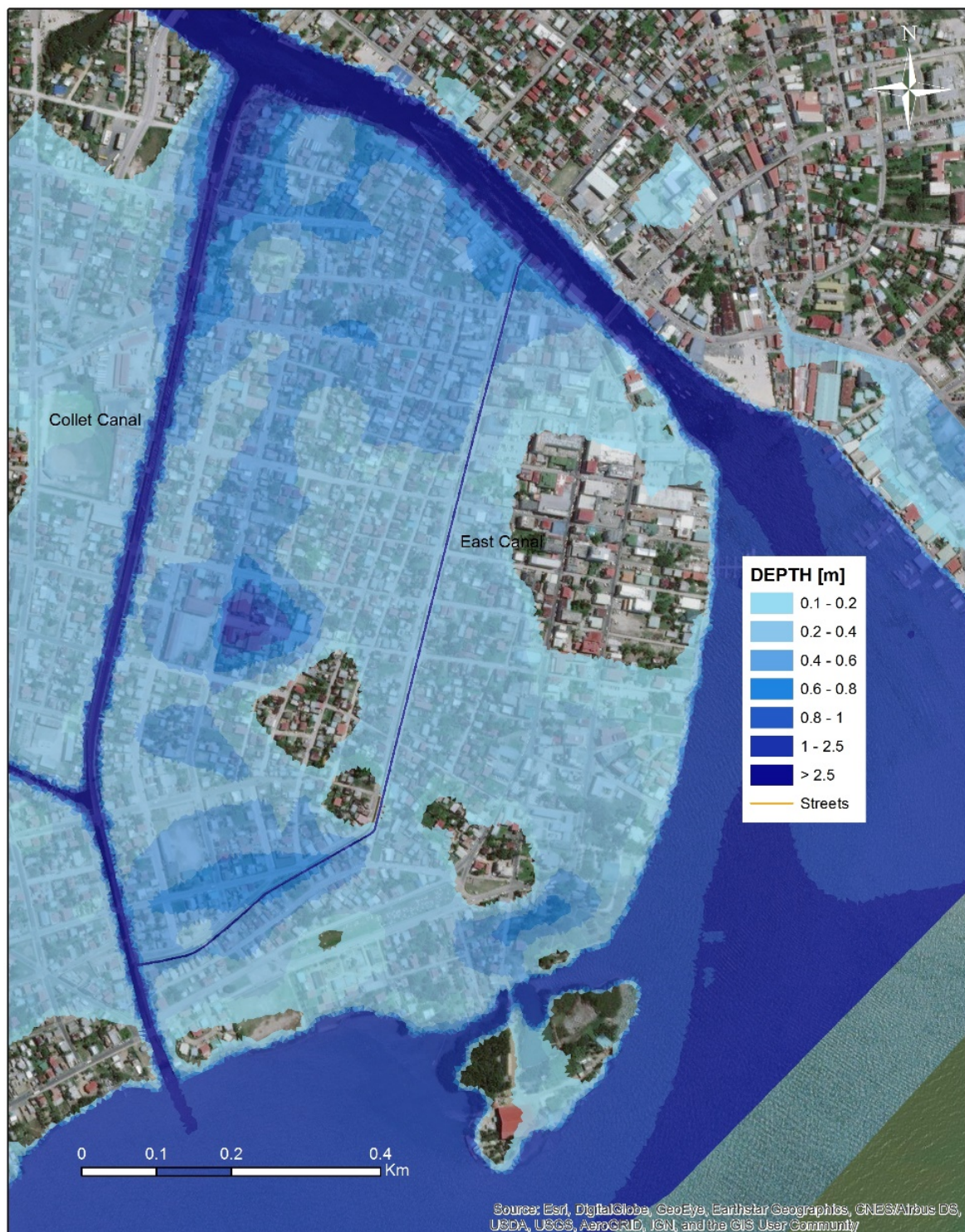


Figure 59. Flood hazard map for the 100-year event in the present situation, before the implementation of the proposed works.



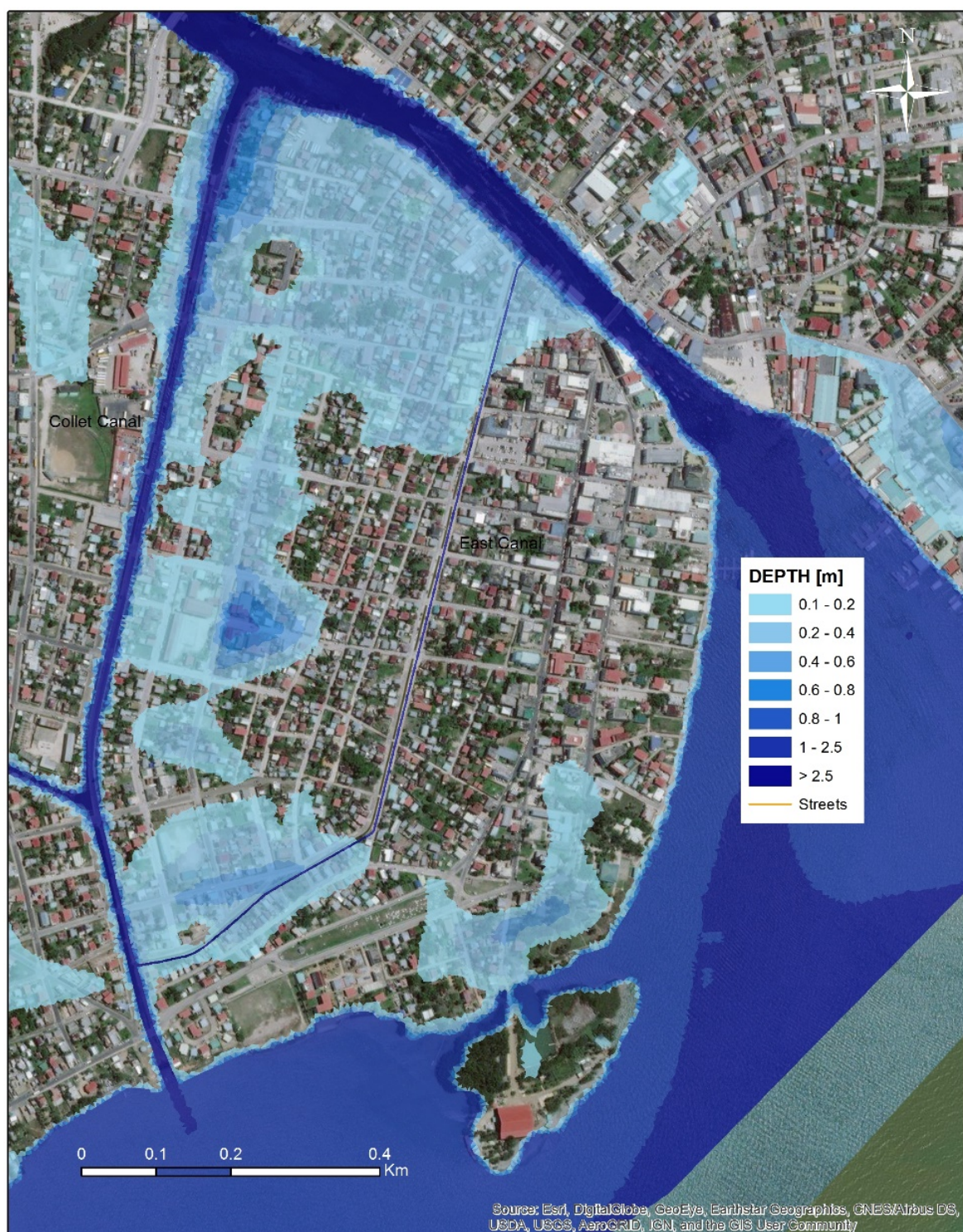


Figure 60. Flood hazard map for the 100-year event, after the implementation of the proposed works.

## 5. COST-BENEFIT ANALYSIS

This section presents a cost-benefit analysis of the proposed works, in order to check if the associated benefits exceed the capital expenditure and operational costs that it entails. The capital expenditure (CAPEX) for the drainage works in Belize Downtown have been estimated by the local firm Chentec<sup>1</sup> in MUSD 5.1, while the operational and maintenance costs have been considered as a 0.5% of the CAPEX, i.e. 25,500 USD/year, not including the SCADA system that will control the pumping scheme and associated elements. The lifetime for all the elements in the proposed facilities is assumed to be at least 30 years. The construction period will be two full years at a constant investment rate (2.55 USD/year); during this period, no risk reduction or land surplus benefits will be considered, but social benefits will be particularly relevant.

### 5.1. Vulnerability functions for economic and human losses.

As expressed in section 3.4, all the buildings included in the project area (approximately 1969 buildings) belong to categories B and C, while only two of them belong to category D. The damage functions used to calculate economic losses for typologies B and C have been chosen from CAPRA database and are shown in Figures 64 and 65, respectively. Category B is assumed to have two stores, and the damage function indicates a 100% damage for a water depth of about 5 m above the ground level, with 50% damage for 2.5 m depth. In case of category C, only one store exists on average, and losses reach 100% for 2.5 m of water, implying the total flooding of the contents and facilities.

These damage functions provide the non-dimensional damage at a particular building, given the water depth as obtained from the flood hazard model (see section 4). To obtain the dimensional economic damage, such percentages are multiplied by the total replacement value of the assets, which in this case has been estimated as follows:

	CAT. B	CAT. C	CAT. B+C
<b>Number of bldgs.</b>	378	1591	1969
<b>Average value per bldg.</b>	150,000	60,000	77,276
<b>Total stock value</b>	56,700,000	95,472,000	152,172,000

According to these figures, the total value at risk of the existing assets, without indirect losses, is around MUSD 152, with an average replacement cost per building of USD 77,276. These values, as correspond to the replacement cost criterion, do not consider the depreciation of existing assets due to its age and potential expiration of its service lifetime.

<sup>1</sup> Updating and Detailed Designs of Flood Control Works in Belize City. Final Report (Draft). Chentec. September 2017.

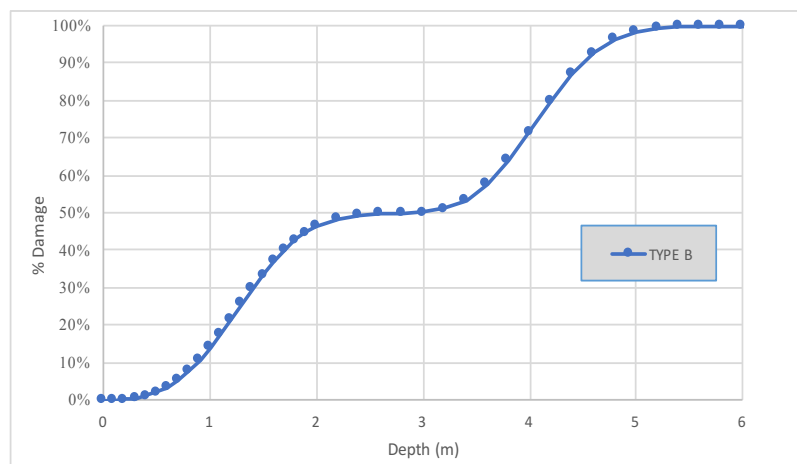


Figure 61. Damage function for type B buildings.

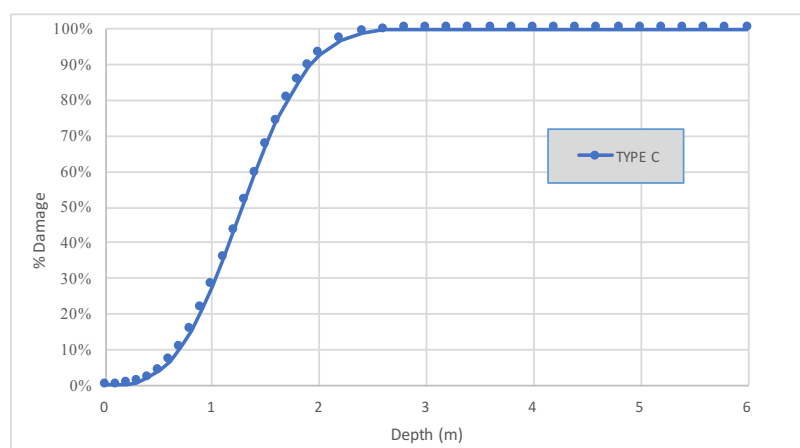


Figure 62. Damage function for type C buildings.

Besides direct economic damages, the project is expected to reduce indirect and human damages. Indirect economic damages were estimated in the Base Studies for Belize City, component 2, based on a comprehensive risk analysis of different classes of critical infrastructures. The reader is referred to the original document for a more detailed description of the methodology used for indirect damages. The final results show that indirect damages amount to approximately 30% of the total direct damages. Since most of the critical infrastructures to be found in the project area are buildings (mainly schools, police stations and shopping areas), this percentage will be considered as a linear factor multiplying to the direct damages.

Finally, human losses will be taken into account in two ways:

- As a resettlement cost, for people whose households have been severely damaged.
- As a cost of the expected fatalities.

The resettlement cost is assumed to be USD 15 per person and per flood event, based on empirical data from other similar places. Miller (2000) estimated the statistical value for the world average life between US\$ 630,000 and US\$ 900,000 of 1995, with the close estimate being 650,000. By adjusting the estimates at current prices and considering per capita income in Belize, the statistical value of life for Belize would be between US\$ 447,068 and US\$ 638,669, with the close estimate of US\$ 461,261.



## 5.2. Risk analysis and avoided losses

Combining the results from the bi-dimensional hydraulic model, as described in section 4, and the vulnerability functions shown previously, the economic damages and human losses for different events can be obtained. Two working alternatives can be defined:

Alternative zero. It assumes that no relevant action is taken to reduce flood risk, neither now nor in the coming decades. All consequences resulting from extreme rainfall events are withstood with the current situation and all the damaged assets are replaced. Future damages increase due to more intense rainfalls, according to climate change predictions.

Alternative one. The proposed works are implemented in two years, after which the damages associated with extreme rainfalls are reduced, but only for events with return period below 10 years. The damages associated with larger events are replaced.

In both alternatives, all cash flows evolve linearly from year zero (present) and year 25 (future scenario horizon), and remain constant beyond that date. The estimated losses for alternative zero in both the present situation and the future scenario are shown in table 15.

PRESENT SITUATION	T2	T5	T10	T20	T50	T100	T500	EAL
Direct damages (USD)	129,180	144,232	183,929	249,648	312,914	473,933	791,049	136,891
Indirect damages (USD)	38,754	43,270	55,179	74,894	93,874	142,180	237,315	41,067
Total econ. damages (USD)	167,934	187,502	239,108	324,543	406,788	616,113	1,028,364	177,959
Refugees (resettlement)	2.59	8.76	20.33	26.59	49.43	61.65	65.96	8.15
Fatalities	0.01	0.02	0.04	0.05	0.10	0.13	0.15	0.02
Affected urban area (ha)			32					

FUTURE SITUATION	T2	T5	T10	T20	T50	T100	T500	EAL
Direct damages (USD)	142,098	158,655	202,322	274,613	344,205	521,326	870,154	150,580
Indirect damages (USD)	42,629	47,597	60,697	82,384	103,262	156,398	261,046	45,174
Total econ. damages (USD)	184,727	206,252	263,019	356,997	447,467	677,724	1,131,200	195,755
Refugees (resettlement)	2.85	9.64	22.36	29.25	54.37	67.81	72.55	8.96
Fatalities	0.01	0.02	0.04	0.06	0.11	0.14	0.16	0.02
Affected urban area (ha)			35.20					

Table 15. Estimated economic damages and human losses for selected events and estimated annual losses (EAL) in alternative zero (present and future situation).

Total economic damages amount to an average of around USD 178,000 per year at present, increasing to USD 196,000 in the future horizon (25 years). The average number of people with temporary resettlement needs are around 9 per year (62 people for a 100-year event), while the fatality rate due to rainfall-only events is very low

(0.02, or 2 fatalities every 100 years on average). The urban area affected by frequent (10-year event) rain floods is estimated in 32 ha (present situation), less than half the total project area.

Table 16 shows the same results for alternative 1, including the proposed flood reduction measures. In this case, all damages and human losses for events below 10-year of return period are mitigated, and also a significant proportion of the 20 and 50-year events. However, the largest possible rainfall still has potential for severe damage, even though less than in alternative zero.

PRESENT SITUATION	T2	T5	T10	T20	T50	T100	T500	EAL
Direct damages (USD)	0	0	0	26,633	61,108	86,941	146,639	3,717
Indirect damages (USD)	0	0	0	7,990	18,332	26,082	43,992	1,115
Total econ. damages (USD)	0	0	0	34,623	79,440	113,024	190,630	4,831
Refugees (resettlement)	0	0	0	2.59	8.76	20.33	26.59	0.56
Fatalities	0	0	0	0.01	0.02	0.04	0.05	0.00
Affected urban area (ha)			0.00					

FUTURE SITUATION	T2	T5	T10	T20	T50	T100	T500	EAL
Direct damages (USD)	0	0	0	29,297	67,218	95,635	161,303	4,088
Indirect damages (USD)	0	0	0	8,789	20,166	28,691	48,391	1,226
Total econ. damages (USD)	0	0	0	38,086	87,384	124,326	209,693	5,315
Refugees (resettlement)	0.00	0.00	0.00	2.85	9.64	22.36	29.25	0.62
Fatalities	0.00	0.00	0.00	0.01	0.02	0.04	0.06	0.00
Affected urban area (ha)			0.00					

Table 16. Estimated economic damages and human losses for selected events and estimated annual losses (EAL) in alternative one (present and future situation).

It must be taken into account that only the losses due to rainfall events have been considered, while other types of losses due to extreme winds and sea level surge are not included, since they are not modified by the proposed works. For these reasons, the total losses for the 100 and 500-year events, even though not negligible, are one order of magnitude lower than the expected losses due to a hurricane of such intensity, which would entail enormous damages due to the sea level surge and extreme winds.

To perform the cost-benefit analysis, the alternative zero will be taken as benchmark (net present value equal to zero), so that the avoided losses induced by alternative one will be considered as benefits. The estimated avoided damages are 173,127 USD/year for the present situation, and increase to 190,440 USD/year for the future horizon.



### 5.3. Land surplus and other benefits associated with the proposed works

In addition to the avoided losses due to the proposed works, two other categories of benefits will be considered in the cost-benefit analysis: the land surplus and the social benefits of the investment.

#### Land surplus.

The proposed works, along with its associated benefits of reduced damages, are expected to bring some indirect benefits in terms of a land value increase in the affected area. To include such effect, several hypotheses regarding key real-state parameters are required:

Land to building value ratio. It reflects the value of the land relative to the value of the building placed on it. A value of one is adopted for Belize Downtown, assuming that it is a well-connected and strategic area for public uses, as long as it is protected.

Property price increase. It is the accrued extra value of the property in percentage, due to the flood reduction effect. Based on a conservative extrapolation from other places, it has been assumed a 5% surplus. This figure applies to the full price in the real-estate market, including the land and the building stock.

Price-to-rent ratio. From a cost-benefit analysis perspective, it is convenient to transform stock variables (like the land surplus) into fluxes, which in this case is equivalent to convert the buy-sell price increase into a renting premium. The coefficient that turns a price into a periodic instalment (usually monthly or annual) is the price-to-rent ratio (PRR). It is often considered that a PRR below 15 is a great opportunity for buying (instead of hiring), while a PRR in excess of 25 would recommend hiring as the most sensible option. An intermediate value of 20 is assumed for Belize Downtown.

With these assumptions, and taking into account the present building stock value for the project area, the following figures can be easily obtained:

<b>TOTAL SURFACE</b>	70	Ha
<b>BUILDING STOCK VALUE</b>	152	MUSD
<b>LAND TO BUILDING VALUE RATIO</b>	1	-
<b>LAND VALUE</b>	152	MUSD
<b>TOTAL VALUE</b>	304	MUSD
<b>PROPERTY PRICE INCREASE %</b>	5%	-
<b>PRICE INCREASE</b>	21.74	USD/m <sup>2</sup>
<b>PRICE-TO-RENT RATIO</b>	20.00	-
<b>ANNUALIZED PRICE INCREASE</b>	10,869	USD/ha·year

Therefore, an annual benefit of 10,869 USD/ha·year can be reasonably expected from the project. This surplus will be applied only to the land surface that is effectively relieved from frequent floods, which is not the full project area (some places are not frequently flooded in the current situations, and some others are affected and will still be in the future. With an urban surface relieved from frequent floods of around 32 ha (see the last row

of Tables 15 and 16), the total land surplus benefits for the present situation amount to USD 347,822, reaching USD 382,604 for the future scenario.

#### **Social benefit of the investment.**

A reversion to the local community of a fraction of the total investment is also considered as a benefit of the proposed investment, mainly through the hiring of local work force to perform some of the tasks involved. For this payback of the investment to the local communities, based on the experience gained by the Inter-American Development Bank in similar projects, it has been considered that 20% of the budget is equivalent to social benefit, channelled to the population through the creation of direct and indirect employment.

### **5.4. Cost-benefit analysis of Belize Downtown flood reduction scheme.**

Combining the figures of costs and benefits, an internal rate of return of 12.15% is achieved (Table 17). Above this discount rate, the projected investments would not be profitable. For a discount rate of 12%, as required by IDB for an investable program, the return on investment is 1.01 and the payback period is 38 years. Figure 66 shows the cumulative cash flows (evolution of the net present value), where the equilibrium time can be appreciated.

<b>Discount rate</b>	<b>12%</b>
<b>Discounted total investment (US\$):</b>	<b>5,015,694</b>
<b>Total discounted benefits (US\$):</b>	<b>5,065,986</b>
<b>Net present value (US\$)</b>	<b>50,291</b>
<b>Internal rate of return (IRR)</b>	<b>12.15%</b>
<b>Return on investment (Benefits/Investment)</b>	<b>1.01</b>
<b>Payback period (years)</b>	<b>38</b>

Table 17. Profitability indicators of the projected investments.

The total benefits generated by the proposed project, expressed as net present value after discounting, can be broken down into the following components:

	<b>USD</b>	<b>%</b>
<b>Total discounted social benefits</b>	<b>1,003,139</b>	<b>19.8%</b>
<b>Total discounted land surplus</b>	<b>2,672,993</b>	<b>52.8%</b>
<b>Total discounted avoided losses</b>	<b>1,389,854</b>	<b>27.4%</b>
<b>TOTAL DISCOUNTED BENEFITS</b>	<b>5,065,986</b>	<b>100.0%</b>

Roughly a half of the total benefits stems from the land value increase, followed in similar proportions by the avoided losses (27%) and the social benefits (20%) resulting from the local impact of the investment.

This analysis is based solely on costs and benefits of an economic nature, and cannot reflect the full benefits derived from the proposed works in the city. Some of the non-monetary benefits that have not been considered in the CBA, but nonetheless would clearly improve the local living conditions, are:

- Improvements in terms of public health and aesthetics (odors, water-borne diseases, etc.)
- Less frequent and lighter traffic interruptions due to flooding.
- Commercial, industrial and touristic activities will clearly be enhanced due to flood reduction, probably beyond the land surplus that has been assumed. For instance, the arrival of international retail shops or hotels could happen as a result of the proposed works.

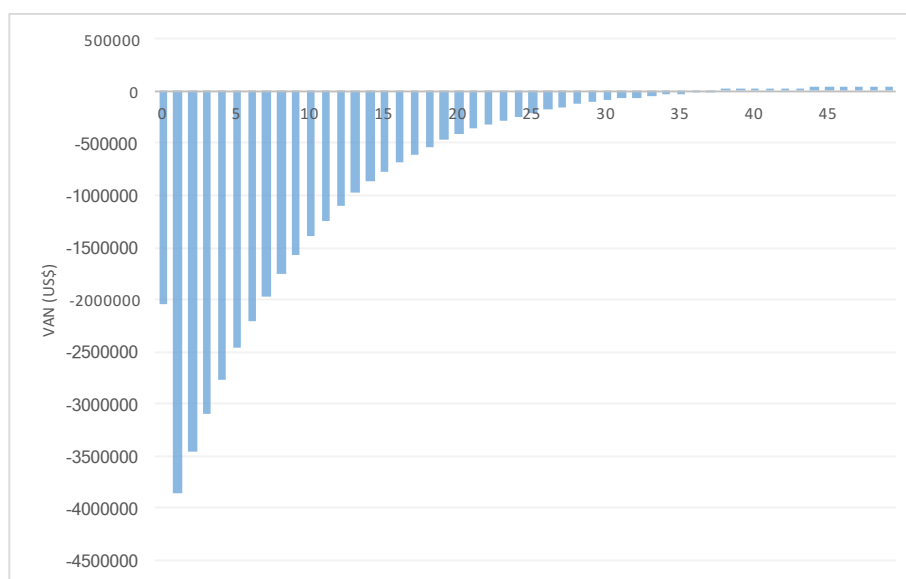


Figure 63. Evolution of the net current value over time for a discount rate of 12%

## 6. REFERENCES

- Abascal, A. J., Castanedo, S., Cid, A., Medina, R., 2012. A high resolution storm surge hindcast in southern Europe: a useful database for coastal applications. Proceedings 33rd International Conference on Coastal Engineering.
- Akbari, H., Rakhshandehroo, G.R., Afrooz, A.H., Pourtouserkani, A. Climate Change Impact on Intensity-Duration-Frequency Curves in Chenar-Rahdar River Basin (2015) Proceedings of the Watershed Management Symposium, 2015-January, pp. 48-61.
- Ayman G. Awadallah, Nabil A. Awadallah. "A Novel Approach for the Joint Use of Rainfall Monthly and Daily Ground Station Data with TRMM Data to Generate IDF Estimates in a Poorly Gauged Arid Region". Open Journal of Modern Hydrology, 2013, 3. 1-7.
- Centella A, A. Bezanilla and K. Leslie, 2008: A Study of the Uncertainty in Future Caribbean Climate Using the PRECIS Regional Climate Model. Technical Report, Community Caribbean Climate Change Center, Belmopan, 16pp.
- Chow, V. T. (1959). Open-channel hydraulics. McGraw-Hill, New York.
- Climate scenarios used were from the NEX-GDDP dataset, prepared by the Climate Analytics Group and NASA Ames Research Center using the NASA Earth Exchange, and distributed by the NASA Center for Climate Simulation (NCCS).
- Collins, M. (2005). El Niño-or La Niña-like climate change?. Climate Dynamics, 24(1), 89-104.
- D. M. Hershfield, "Rainfall Frequency Atlas of the United States for Durations from 30 Minutes to 24 Hours and Return Periods from 1 to 100 Years," Weather Bureau Technical Paper, No. 40, 1961, p. 115.
- Efron, B., Tibshirani, R. Bootstrap methods for standard errors, confidence intervals, and other measures of statistical accuracy (1986) Statistical Science, 1 (1), pp. 54-75.
- Egbert G.D., Erofeeva, S.Y., 2002. Efficient inverse modeling of barotropic ocean tides. Journal of Atmospheric and Oceanic Technology, 19, 183-204.
- Elsner, J. B., Kossin, J. P., & Jagger, T. H. (2008). The increasing intensity of the strongest tropical cyclones. Nature, 455(7209), 92.
- Emanuel, K., Sundararajan, R., & Williams, J. (2008). Hurricanes and global warming: Results from downscaling IPCC AR4 simulations. Bulletin of the American Meteorological Society, 89(3), 347-367.
- F. C. Bell, "Generalized Rainfall-Duration-Frequency Relationship," Journal of Hydraulic Division, Vol. 95, No. 1, 1969, pp. 311-327.
- Giraldo Osorio, J.D., García Galiano, S.G. Building hazard maps of extreme daily rainy events from PDF ensemble, via REA method, on Senegal River Basin (2011) Hydrology and Earth System Sciences, 15 (11), pp. 3605-3615.
- Graham, L.P., Andréasson, J., Carlsson, B. Assessing climate change impacts on hydrology from an ensemble of regional climate models, model scales and linking methods - A case study on the Lule River basin (2007) Climatic Change, 81 (SUPPL. 1), pp. 293-307.
- Gregory, J.M., et al., 2005: A model intercomparison of changes in the Atlantic thermohaline circulation in response to increasing atmospheric CO<sub>2</sub> concentration. Geophys. Res. Lett., 32, L12703, doi: 10.1029/2005GL023209.

- Holland, G. J., & Webster, P. J. (2007). Heightened tropical cyclone activity in the North Atlantic: natural variability or climate trend?. *Philosophical Transactions of the Royal Society of London A: Mathematical, Physical and Engineering Sciences*, 365(1860), 2695-2716.
- IHCantabria and IDOM Consulting, Engineering & Architecture, (2016). Baseline studies for Belize City: Climate change and urban development studies. Emerging and Sustainable Cities Initiative (ESCI). Inter-American Development Bank, IDB.
- IHCantabria and M&K, (2016). Natural disaster risk assessment study of Belize City design. Inter-American Development Bank, IDB.
- IPCC. 2007. The Physical Science Basis. Contribution of Working Group I to the Fourth Assessment Report of the IPCC. Solomon, S., Qin, D., Manning, M., Chen, Z., Marquis, M., Averyt, K.B., Tignor, M. and Miller, H. L. Eds.). Cambridge University Press, Cambridge, UK and New York, NY, USA. 996pp. (available at <http://www.ipcc.ch/pdf/assessment-report/ar4/wg1/ar4-wg1-spm.pdf>).
- IPCC, 2013: Climate Change 2013: The Physical Science Basis. Contribution of Working Group I to the Fifth Assessment Report of the Intergovernmental Panel on Climate Change [Stocker, T.F., D. Qin, G.-K. Plattner, M. Tignor, S.K. Allen, J. Boschung, A. Nauels, Y. Xia, V. Bex and P.M. Midgley (eds.)]. Cambridge University Press, Cambridge, United Kingdom and New York, NY, USA, 1535 pp, doi: 10.1017/CBO9781107415324.
- IPCC. 2014. "Climate Change 2014 Synthesis Report Summary Chapter for Policymakers." Ipcc, 31. doi:10.1017/CBO9781107415324.
- Kossin, J. P., Knapp, K. R., Vimont, D. J., Murnane, R. J., & Harper, B. A. (2007). A globally consistent reanalysis of hurricane variability and trends. *Geophysical Research Letters*, 34(4).
- Knutson, Thomas R., et al. "Dynamical downscaling projections of twenty-first-century Atlantic hurricane activity: CMIP3 and CMIP5 model-based scenarios." *Journal of Climate* 26.17 (2013): 6591-6617.
- Lewis A. Rossman Environmental Scientist, Emeritus U.S. Environmental Protection Agency, 2015. Storm Water Management Model User's Manual Version 5.1. National Risk Management Laboratory Office of Research and Development U.S. Environmental Protection Agency 26 Martin Luther King Drive Cincinnati, OH 45268.
- Libertino, A., Sharma, A., Lakshmi, V., Claps, P. A global assessment of the timing of extreme rainfall from TRMM and GPM for improving hydrologic design (2016) *Environmental Research Letters*, 11 (5), art. no. 054003 .
- Mann, M. E., Woodruff, J. D., Donnelly, J. P., & Zhang, Z. (2009). Atlantic hurricanes and climate over the past 1,500 years. *Nature*, 460(7257), 880.
- McSweeney, C., New, M. and Lizcano, G. 2008. UNDP Climate Change Country Profiles: Uganda, Available at <http://countryprofiles.geog.ox.ac.uk/index.html?country=Uganda&d1=Reports> Accessed 15th/10/2011.
- McSweeney, C., Lizcano, G, New, M. and Lu, X. 2010. The UNDP Climate Change Country Profiles: Improving the accessibility of observed and projected climate information for studies of climate change in developing countries, *Bulletin of the American Meteorological Society*, 91(2): 157-166
- Meehl, G. A., Tebaldi, C., Teng, H., & Peterson, T. C. (2007). Current and future US weather extremes and El Niño. *Geophysical Research Letters*, 34(20).
- Nakajo, S., Mori, N., Yasuda, T. & Mase, H., 2014: Global stochastic tropical cyclone model based on principal component analysis with cluster analysis *J. Applied Meteorol. Climatol. Am. Meteorol. Soc.* 53, 1547–1577.
- NHC-NOAA Website: National Hurricane Center, National Oceanic and Atmospheric Administration <http://www.nhc.noaa.gov/>



- Reguero, B. G., Menéndez, M., Méndez, F. J., Mínguez, R., & Losada, I. J. (2012). A Global Ocean Wave (GOW) calibrated reanalysis from 1948 onwards. *Coastal Engineering*, 65, 38-55.
- Tapiador, F. J., & Sánchez, E. (2008). Changes in the European precipitation climatologies as derived by an ensemble of regional models. *Journal of Climate*, 21(11), 2540-2557.
- Tebaldi, C., Knutti, R. The use of the multi-model ensemble in probabilistic climate projections (2007) *Philosophical Transactions of the Royal Society A: Mathematical, Physical and Engineering Sciences*, 365 (1857), pp. 2053-2075.
- Timmermans, B., Stone, D., Wehner, M., Krishnan, H. Impact of tropical cyclones on modeled extreme wind-wave climate (2017) *Geophysical Research Letters*, 44 (3), pp. 1393-1401.
- Knapp, K. R., Kruk, M. C., Levinson, D. H., Diamond, H. J., & Neumann, C. J. (2010). The international best track archive for climate stewardship (IBTrACS) unifying tropical cyclone data. *Bulletin of the American Meteorological Society*, 91(3), 363–376.
- Knutson, T. R., & Tuleya, R. E. (2004). Impact of CO<sub>2</sub>-induced warming on simulated hurricane intensity and precipitation: Sensitivity to the choice of climate model and convective parameterization. *Journal of climate*, 17(18), 3477-3495.
- UN/ISDR, 2009; Terminology on disaster risk reduction (<http://www.unisdr.org/we/inform/publications/7817>).
- USDA Soil Conservation Service. (1971). Classification system for varied flow in prismatic channels. Technical Release No. 47 (TR-47), Washington, D.C.
- Vecchi, G. A., and B. J. Soden, 2007: Increased tropical. Atlantic wind shear in model projections of global warming. *Geophys. Res. Lett.*, 34, L08702, doi:10.1029/2006GL028905.
- Webster, P. J., Holland, G. J., Curry, J. A., & Chang, H. R. (2005). Changes in tropical cyclone number, duration, and intensity in a warming environment. *Science*, 309(5742), 1844-1846.
- Yoshimura, J., Sugi, M., & Noda, A. (2006). Influence of greenhouse warming on tropical cyclone frequency. *Journal of the Meteorological Society of Japan. Ser. II*, 84(2), 405-428.